Power flow modeling in a substation of a wind- and solar farm

BSc. Graduation Thesis

Group D.3

F.G.N. Rimon, 4652827
M. Mastouri, 4599470

TUDelft

Power flow modeling in a substation of a wind- and solar farm

BSc. Graduation Thesis

by

Group D.3

F.G.N. Rimon, 4652827
M. Mastouri, 4599470

to obtain the degree of Bachelor of Science
at the Delft University of Technology,
to be defended publicly on 01-07-2020.

Student number: 4652827   4599470
Project duration: April 2020– July 2020
Thesis committee: Prof. dr. ir. J. Rueda Torres,   TU Delft, supervisor

This thesis is confidential and cannot be made public until 2025

TUDelft

Abstract

Renewable energy generation is nowadays increasing around the world, especially wind- and solar power generation. However, increasing wind and solar power integration into the grid have a significant effect on the power system. The variability and uncertainty of these energy sources propose new challenges for companies involved in grid management. To face these challenges, advanced control schemes and optimization algorithms were implemented to ensure the stability and efficiency of the power flow [1] [2]. But these algorithms can only be implemented if the power flow in the system is modeled accurately. This thesis explains how the power flow in a substation of wind- and solar farm in ████████████████ is modeled to guarantee efficiency and acceptable steady-state performance. Firstly, a model of the system configuration was designed with the implementation of each component's data. To fulfill the system configuration design, a solar farm was designed. This solar farm would not provoke violations of the system's physical constraints. Secondly, the aggregated model for the Wind Turbine Generator (WTG) was converted to a model on the string level, i.e. with implemented data of each WTG configuration. Lastly, test models were designed to determine the transmission system's behaviour under normal and extreme operating conditions. These operating conditions involved a variety of power generation from the wind- and solar farm, as well as requested reactive load demand at the Point of Common Coupling (PCC).

Preface

The scope of this thesis is to ▮rovide an accurate model of the power flow in a substation with renewable energy sources, the ▮▮▮▮▮ wind-and solar park. The thesis is part of a project given by ▮▮▮▮▮ aims to use this model as a complementary solution to satisfy TSO requirements at the Point of Common Coupling with minimal losses in power and maximal steady state stability.

We would like to thank our supervisor dr. ir. José Rueda Torres for his exceptional guidance throughout the project. In cooperation with José, we were able to iteratively formulate requirements that would satisfy a realistic representation of the substation. Especially, dr. ir. José made an effort in providing the best quality of guidance under the COVID-19 circumstances. Furthermore, our gratitude is expressed for Dennis Groenenberg and ▮▮▮▮▮ ho constantly provided us with the information of the ▮▮▮▮▮▮▮ eeded for fulfillment of the scope of the project. Lastly, the complete project would not have been possible without the help of our colleagues, Alexandru Neagu, Dennis Groenenberg, Jin Han Bai and Laurens Beijnen. Because of you, the motivation stayed high while being in an enjoyable online atmosphere.

Group D.3

F.G.N. Rimon, 4652827
M. Mastouri, 4599470

Delft, May 2020

Contents

1

Introduction

In the past decade, the renewable energy market has increased significantly [1]. Equivalently, the current methods for energy provision such as coal, are becoming less popular. Ongoing research has the aim to make the transition to renewable energy as safe, e.g. no overloading, and efficient, e.g. no transmission losses, as possible [2].

1.1. Project objective

Ideally, once the substation is connected to the grid, the substation provides its full capacity at all times. However due to fluctuations in wind- and solar profiles, the Transmission System Operator (TSO) requirements can not always be satisfied at the Point of Common Coupling (PCC) [3]. There is also loss in several of the components that form the subsystem such as power loss in the transmission lines, bus bars, transformers and even in the Wind Turbine Generators (WTGs) and PV panels. Since these losses will affect the power generated and the power delivered at the Point of Common Coupling, they have to be taken into account in order to implement an accurate model for the system. Besides, advanced control schemes [4] are designed to find the optimal setpoints in the substation that satisfy TSO requirements. The setpoints indicate the power flow through each generation string. The optimisation is based on the system's configuration and non-idealities, but also the grid code requirements [1]. This mathematical scheme cannot determine the feasibility of the given setpoint in reality. It needs information of the substation's power flows. Through communication between the modeling and optimization entity [6], the scheme can make its search space smaller and find a global optimum.

The project aims to use the case study, shown in Fig. 1.1, to design an accurate model of the power flows that shows the effects of fluctuating wind/solar profiles and components' non-idealities. When the optimization algorithm sends setpoints to the model, the model returns the actual feasibility by providing the power flows in each of the branches in the system configuration. Dependent of the development status of a project, this model can indicate if the system configuration is to be improved/changed. Additionally, it provides the feasibility for future expansion of the substation without violating any physical constraints. Steadily, increasing the RES generation for the growing energy demand worldwide.

For the scope of this project, a realistic model of the system behavior shall be designed and tested. The models for the PV- and WTG farm of the case study are combined and tested under critical conditions, such as low wind speed, low solar irradiance, or both for high reactive power requests from the TSO. The problem formulates: "How does the system react to normal and critical operating conditions, i.e. too low or too high, generation of power from the renewable energy systems or high load demands?". The research question is therefore divided into the following questions:

1. How are the system components modeled correctly?

2. What is the relation held between voltage magnitudes, power losses and load demands in the system?

---

[1] "Grid codes specify the electrical performance that generation assets must comply with in order to obtain the required approval for its connection to a grid."[5]

1

3. What are the effects on the aforementioned parameters and mutual relation for a variation in dispatch profiles, i.e. wind speed profiles and solar irradiance profiles?

4. What are the effects on the aforementioned parameters and mutual relation for a change in the system topology, i.e. aggregated model of the WTG farm, PV farm or a combination of both for the Hybrid farm?

5. What are the effects on the aforementioned parameters and mutual relation for an improved model of the system configuration, i.e. modeling the WTG farm on string level (individual WTG level)?

In the stator, rotational energy of the blades of the wind turbines is converted into electrical energy. Since the conversion is made with magnets, AC current production occurs. This gives rise to different AC voltages on the nodes of the power system of the wind modules. These voltages can be lagging or leading to the current in the power system, which gives rise to either absorbing or generating reactive power by the wind turbines. However, at the nominal value of 1 p.u, the voltages will not be lagging or leading, but in phase with the current, which will result in no reactive power. One of the requirements of the Transmission System Operator is to control the reactive power and assure that, when needed, the reactive power at the Point of Common Coupling is brought to zero.

The power in the PV module is generated in DC conditions. Hence, the solar modules do not generate any reactive power. Since the transmission grid operates in AC conditions, the DC power has firstly to be converted to AC in order to be fed back into the grid. For this conversion process, DC/AC inverters are used. These inverters will either generate or absorb reactive power [7]. This reactive power has to be taken into account in order to design an accurate solar farm.

1.2. Test models and state-of-art

In order to perform several power system analysis, information about the power system is needed, which consists of the system topology and nodal power injections. The nodal power injections consist of active- and reactive power, which are either measured or determined by power flow solving methods. In Fig. 1.2 the input and output data of an iterative power flow calculation is shown.

Furthermore, in the iterative power flow calculation block certain equations are applied. The generic equation, as shown in Eq. 1.1, will be used in order to generate the voltage magnitude p.u and angle of all nodes iteratively. However, there is one bus, frequently allocated to the bus at the PCC, for which the voltage magnitude p.u. and angle are known. This bus is called the slack bus. In this bus the active and reactive power injections are determined with the known voltage magnitude p.u and angle in order to check whether certain requirements at the PCC are fulfilled. In the remaining nodes the voltage magnitude p.u. and angles of the busses will be determined with the known values of the active and reactive power injections. These busses are called PQ-busses and are used since they give rise to a set of finite equations, which will result in a finite number of solutions for the magnitudes and angles. For the PQ-busses, there are in principle two equations generated, one for the active power and one for the reactive power, as shown in Eq. 1.2 and 1.3. Since the unknown variables in all PQ-busses are the voltage magnitudes p.u and angles, a state variable matrix **x** can be constructed, as shown in Eq. 1.4, from which all the PQ-busses can be solved iteratively by solving Eq. 1.5.

$$I_{[Nx1]} = Y_{bus_{[NxN]}} \cdot U_{[Nx1]} \tag{1.1}$$

$$P_i = f_p(U_1, U_2, ..., U_N, \delta_1, \delta_2, ..., \delta_N) \tag{1.2}$$

$$Q_i = f_q(U_1, U_2, ..., U_N, \delta_1, \delta_2, ..., \delta_N) \tag{1.3}$$

$$\mathbf{x} = [\delta \, U]^T \tag{1.4}$$

$$f(\mathbf{x}) = 0 \tag{1.5}$$
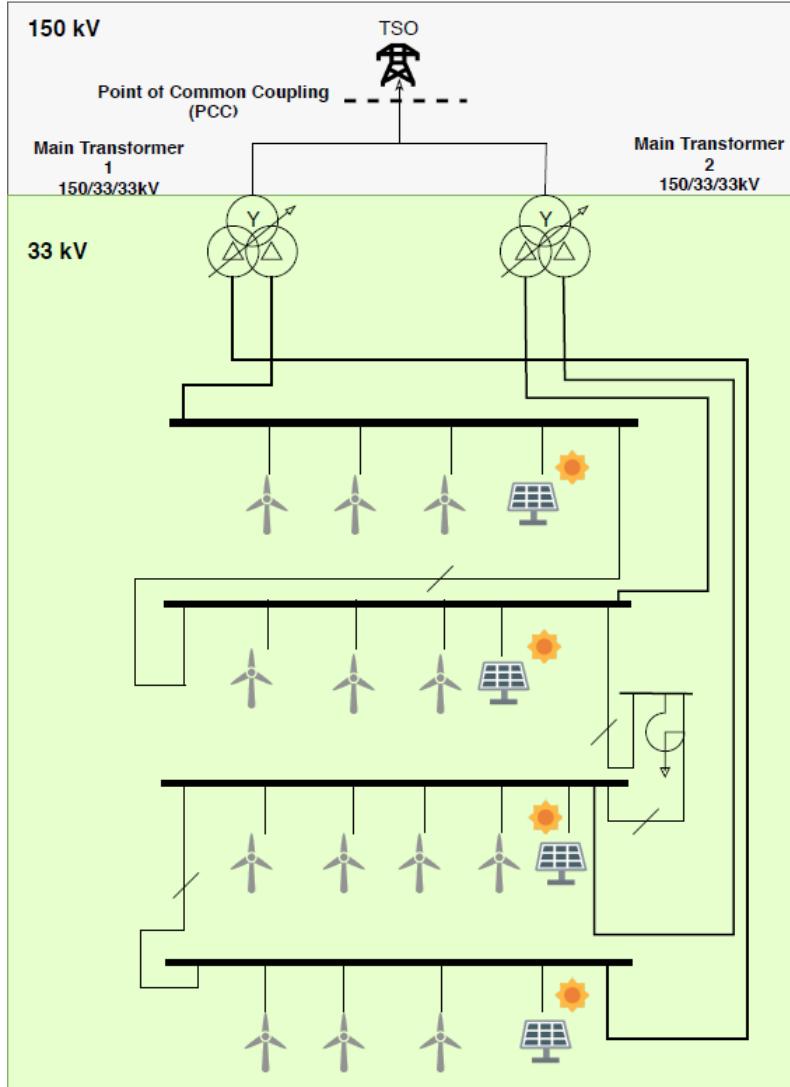
Figure 1.1: Simplified schematic of case system. This system configuration will be modelled and tested for nominal and extreme operating conditions.

Different algorithms have been designed to solve **x** in Eq. 1.5 in an iterative manner. Reason for more algorithms are its solving (or convergence) time and accuracy for specific networks. These modern algorithms still make use of the two conventional approximation methods, Gauss-Seidel method [8] and Newton Raphson method [9]. Gauss-Seidel is a simpler technique requiring less computation per iteration. The computation time is sensitive to the system parameters. Therefore, the majority bases the algorithm on Newton-Raphson, since the system converges in less iterations, which gives smaller computation time, more accuracy and makes it less sensitive to other system parameters. This makes it suitable for a complex system, as shown in Fig. 1.1. A more precise schematic is visible in App. A.2.

A fluctuation in wind/solar profile, causes a fluctuation in the power generated. Current methodology takes this fluctuation in wind/solar profiles by designing algorithms that describe a probabilistic behavior of wind speed and solar irradiance [10] [11] [12]. This probabilistic behavior is to test the system under the most common operating situations, i.e. common wind/solar profiles, since little variation from the rated wind speed is included to the model. Additionally, the probabilistic model offers the possibility to create both random load demands and generation capabilities in the system at random dispatches. Therefore occasionally violating physical constraints of the system. This offers a test model for alert operating conditions [2]. Hence, the proba-

---

[2] alert operating conditions in which physical constraints are violated or there is a high vulnerability to disturbances
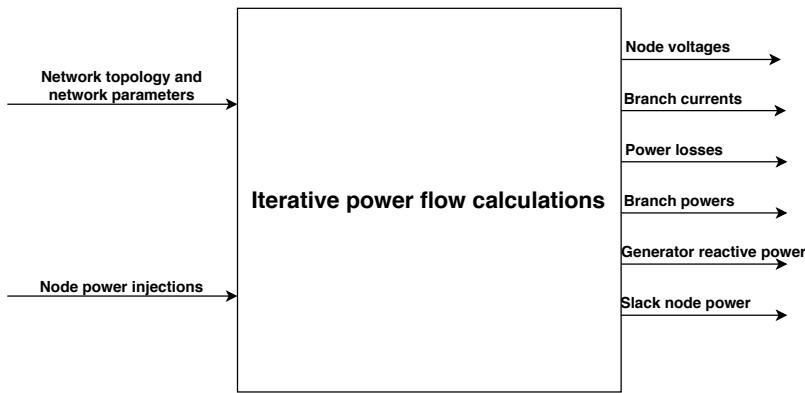
Figure 1.2: Block diagram with the input and output data in order to perform power flow calculations. The input data are known parameters for the system. The output data is needed for analysis of the system behavior in Chap. 4.

bilistic model offers a suitable test model under different operating conditions. Compared to use of historical data, which can vary throughout time periods (per season or year), this test model runs more situations.

To model daily wind profiles, research makes use of, a Weibull distribution, historical data or a versatile distribution that combines Beta, Cauchy and Gaussian to model a daily wind profile [13] [14]. However the majority makes use of Weibull PDF, since it was determined that the distribution resembles real life situations the most [15] [16] [14].

For solar irradiance, each research makes use of an own model. These models can be divided into: Design based on historical data and chosen PDF [17], Beta distribution [18] [14] or Weibull distribution [18], design based on spatio-temporal stochastic model with each spatio (or season such as sunny, cloudy, etc.) having own stochastic parameters [19].

Out of these models, the probability for output power is determined. This offers a solution in case of insufficient or inaccurate wind-and profile data. Other research, suggest a π- model of the individual WTGs and PV panels to determine the output active- and reactive power. It makes use of properties of the system. This provides an accurate solution if all data is known, i.e. datasheet of the WTG as well as the profile data [20] [21] [7]. For the probabilistic model of the RES, the reactive power output is unknown in case of insufficient data about the system itself.

Due to its maturity and proven performance as open source tool, Matpower was selected for the design of a model in steady state and AC conditions. Furthermore, MatPower has no bugs, due to contiguous revisions of the functions and has been widespread used in research projects. Matpower is a MATLAB package aiming to solve steady-state power simulations [22]. For this model the basic Newton-Raphson method is used. More sophisticated methods would be possible if the system was a radial network, where each load has its own generator. The system configuration in Fig. 1.1 analyses a network system, which has multiple generating sources for a single load. Also, the sophisticated methods, are focused on reducing computation time, which is not part of the scope for this project.

The challenge for this project is to have a trustworthy model of the steady state AC power flow for a substation that combines both wind-and solar generation under normal and extreme weather conditions. The state of art does not seem to analyse such a case study. Research does address the effects of such a substation on the transmission grid, but not on the substation. In addition, there will be looked at the effective replacement of the loss effects for the 3-winding transformers. These will be approximated with an equivalent 2-winding transformer model. The sub group responsible for optimisation shall find the optimal tap position and send it to the modeling subgroup. This interaction is visible in Figs. 2.1, A.1.

Due to insufficient data of both wind profile and WTG's components for the specific case study, using only one model will yield inaccurate results of the power flow. To model such WTGs under fluctuating wind profile conditions, the best model is achieved by combining both methods. The different operating conditions is

tested with the probabilistic behavior, while the PQ/RX model determines the exact output of wind modules after internal losses. Therefore, a correct estimate of the active, reactive power generation and voltage profile is formulated for each dispatch profile.

Next, the same can be done for the PV modules. The models for reactive power capability and probabilistic solar irradiance are combined. In reality, most of the time, both PV- and WTG farm will be active. All generating strings, Fig. 1.1, influence the system simultaneously in normal-and critical operating conditions. With the farm being fully active, voltage profiles can deviate a lot from the ideal 1 p.u., leading to violation of technical constraints.

1.3. Thesis outline

To formulate a correct answer for the project objective, the thesis will delve into the necessary requirements to determine what it means to have an accurate power flow model. Once requirements are determined (Chap. 2), a procedure will be followed on the model of the system (Chap. 3) and subsequently, the behavior of the system model is determined under different operating conditions (Chap. 4). Then, results are assembled and analysed (Chap. 5). Out of the results, a conclusion is made (Chap. 6) Additionally, recommendations are made for future research related to this project subject and a discussion about the results can be formulated. This discussion offers room for improvement and recommendations for future researchers modeling power flows for similar case studies.

2

Programme of Requirements

2.1. Functional requirements

As mentioned in Chap. 1, to formulate a correct research, the problem shall be divided into smaller subproblems. The model should be able to:

1. Update the components' parameters in the system topology after every setpoint iteration.

2. Indicate when constraint limits of voltage and/or current are violated in each branch or bus of the substation.

3. Indicate losses and injections of each branch and bus of the system for given setpoints.

4. Take influences into account for power generation due to fluctuating wind speed and solar irradiance profiles.

To determine how the model will indicate if requirements are satisfied, one needs a correct definition of setpoints received from the optimisation scheme [6]. The interaction of the subgroups is specified in Fig. 2.1. The interaction between the three components of the optimisation unit is found in App. A.1. For the case study, the setpoints will be given in the form a dispatch vector, which indicates the required reactive power from the generating strings, 13 WTG strings, and 4 PV strings, shown in App. A.2. Additionally, the connection status for the reactor is required. Usually the reactor is disconnected, but if the optimisation scheme [6] requires this to satisfy reactive power at the PCC, the reactor will absorb reactive power (-12 MVAr).

2.2. Model requirements

The sub problems are formulated in Mandatory requirements, Trade-off requirements and optional requirements. Mandatory requirements are:

1. To take the influence of each component in the system into account:

   (a) Formulate a system topology which connects each node of App. A.2. Hereby, all information of the system is implemented. This includes the PCC, wind- and solar PV strings, transformer- and cable data.

   (b) The design of the solar farm. This overview consists of the interconnection of the solar modules, the cable types and the type of DC/AC converters used.

   (c) To determine the reliability of the implemented case system, power flows are compared to own hand calculations that apply the theoretic approach [9].

   (d) After completion of the first two requirements, the system topology is formulated on string level. Hereby, the system topology is updated with the subdivision of individual WTGs at each string. Each WTG has its rated power output, cable and inverter type connection. More will be explained in Subsec. 3.2.1.
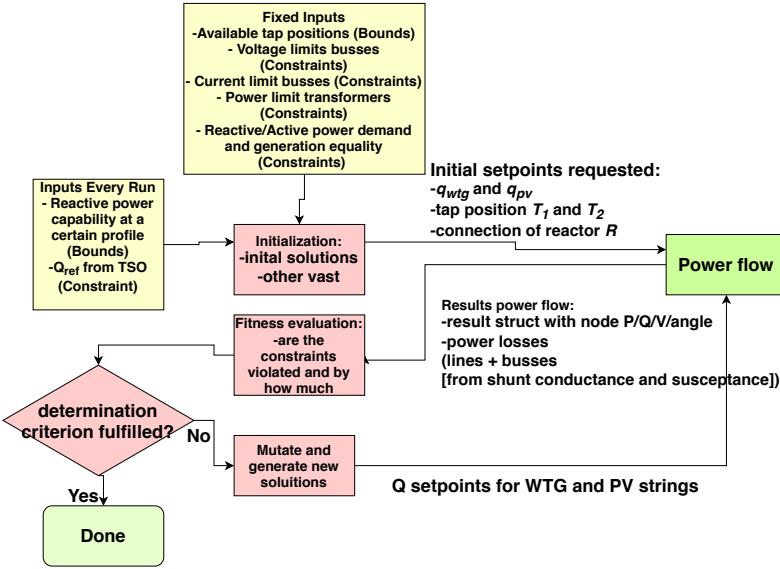
Figure 2.1: Interaction between optimisation and modeling of the power flows. By running several power flows in the system model, the optimal solution for setpoints is found.

2. To determine the system behavior for every possible operating condition:

   (a) An analysis of the system behavior for different operating conditions. From this, the relation is determined between total losses, injections, and voltage profiles for each combination of generation and demand. This includes extreme combinations for which the power demand will not only come close to generated power, but also exceed generation of the strings.

   (b) An analysis of the behavior of components that cause most voltage physical violations and losses.

3. For proper communication between the requests of the optimisation controller and the model:

   (a) The system topology has to be updated twice after each given setpoint. The first update is to change the active and reactive power generation according to the wind and solar dispatch. The second update is to change the reactive power of the generation strings.

   (b) Before receiving setpoints from the optimisation scheme [6], the available active and reactive power, with tap positions from each transformer is sent to the optimisation scheme [6]. With this information and system, the optimisation scheme [6] can determine the initial vector of string setpoints.

The satisfaction of mandatory requirements can be tested once the system converges on MatPower for a Newton Raphson power flow [22], after the system parameters are updated or sent to the optimisation scheme [6].

Trade-off requirements are necessary to improve the research in a stepwise manner. This results in conclusions that can be used for future expansion of the case study used, since its behavior is modelled for every possible condition. Therefore, trade-off requirements are:

1. Include losses generated by changing the tap position of the equivalent model of the 3-winding transformers. This tap position is updated in the system topology according to the procedure in Fig. 2.1.

2. Include losses generated by the equivalent model of the 3-winding transformers' inner-and outer winding in the transmission lines.

Furthermore, there are also optional requirements, which are not needed to design, implement and test the model, but can be implemented in the future in order to add new insights to the research, namely:

1. Design the PQ and RX models used in state of the art research to model the PQ-capability curves of the wind turbines [20]. However, for this research the PQ-capability curves of the WTG's were available [23] and no data is supplied about the impedances of the rotor and stator of the WTG's. This resulted in considering the implementation of the PQ and RX models as an additional requirement. In a later phase, the PQ and RX models could be designed using data from other researches to give an as accurate as possible estimation of the PQ-capability curves. Eventually, these estimations can be used to give a comparison between two different modeling methods.

Additional requirements are needed for the proof of concept. Hereby, the design of a visualization model for the Single Line Diagram of the case study, with the power flow and losses indicated after every system update [23]. Note: For the prototype, it is not of importance which component, i.e. cable or transformer, generates the loss.

Concluding, once mandatory requirements are satisfied, the model will prove to be accurate for power control at the PCC, because it includes transmission losses and most importantly, the behavior of the wind-and PV modules for rated power output. In addition, trade-off requirements will supplement the model by testing the system configuration under different situations determined by the probabilistic behavior. Furthermore, optional requirements firstly add a new level of accuracy to the model, since additional losses in the farms are accounted for. Secondly, they could give new insights to research, since results of state of the art models are compared with the results of the models used in this research. Additionally, losses of previously ideally assumed components are included, providing actual power flow in the system topology.

3

Model of the system configuration

For the design of the model, the data in [23] [24] was used. This offers the configuration with assigned bus numbers, cables', transformers' type and length shown in App. A.3. Here, the rightmost generating strings of bus bar 7,12,16,23 are the PV strings. In App. A.2, the system configuration is shown with maximum voltages for bus bars and maximum current for branches. On the left, the base voltage is indicated for each section of the substation.

Since [23] offered insufficient data of capability curves of the WTG and PV- farm, certain assumptions were made. Firstly, it was decided to make the slack node the PCC, i.e. bus bar 1. The voltage magnitudes and angles of each bus were compared to the PCC node, with a magnitude of 1 p.u. and 0 degrees. To implement the constraints for the voltage profile, it was decided to determine this from the main transformer data. The transformer data indicates the maximum input/output voltage and current. These values are shown in Tab. 3.1. Although the cable type can handle more, the main transformers set the power flow limits for the system configuration.

3.1. Component modeling

3.1.1. Cable modeling

Different branches in the system topology had different three-phase configurations. It was decided to model this configuration, using an equivalent π transmission line model. In Fig. 3.1, each branch will have a starting node, i.e."Bus from", and ending node, i.e."Bus to". The branch between these nodes has a series impedance, Z_s, consisting of a real and imaginary impedance. The injection charge of busses is modeled with a parallel charging susceptance, b_c. Some of the branches are transformers. To specify this systematically, each branch has a transformer with a tap ratio, i.e. **N**. For most branches this ratio is equal to 1. The phase shift, θ between nodes is unknown and therefore considered to be its ideal value of 0.

To calculate the π model values for each branch of the system in App. A.3, the cable type and configuration were determined. The DC resistance value for a nominal temperature of 20 degrees Celsius was assumed. The configuration is specified with AxBxCCxD mm2 "material". **A** specifies the amount of cables per single phase. **B** specifies the amount of phases, i.e. in this system it is a three-phase system for each node. **C** specifies the amount of parallel cables in one single phase cable. The extra C stands for "cable", indicating where the single phase specification commences. **D** specifies the cross-section area of the cable in mm2. An example of the configuration is shown in Fig. 3.2. Diagrams of other configurations are found in App. A.4.1.

Table 3.1: System's voltage magnitude constraints based on transformer data for the input region of the transformer (primary side) and output region of the transformer (secondary side). Voltages higher than these values will result in non-convergence of the power flow.

	V_{max} (kv)	I_{max} (A)
primary side	33	735
secondary side	171.316	808.6

Table 3.2: Absolute impedance and capacitance values per km of cable types. Data acquired from [23]. This data is used for the branches modeling of the system configuration.

Cable	Resistance (Ohm/km)	Reactance (Ohm/km)	Capacitance (e-6 F/km)	Apparent power rate (MVA)
3x1Cx2500mm2 XLPE Al	0.0119	0.06788	0.3	400
1x800mm2 AAC Conductor	0.0356	0.101	0.366	400
2-winding transformer	0	0	0.2025	240
3x1Cx1000mm2 XLPE Al	0.0291	0.1666	0.38	46.2977
4x3x1Cx1000mm2 XLPE Al	0.007275	0.0415	1.52	185.19
3x630mm2 Cu	0.0283	0.163	0.35	36.86
3x630mm2 Al	0.0469	0.177	0.32	36.86
3x400mm2 Al	0.0778	0.19	0.26	28.29
3x240mm2 Cu	0.125	0.196	0.22	20.86
3x150mm2 Al	0.206	0.208	0.19	16.28
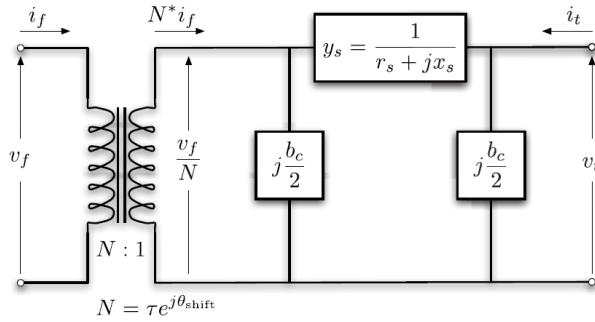
Figure 3.1: Equivalent π transmission line model for the branches of the system topology, Fig. taken from [22].

After the specification of the cable configuration, the parameter values are calculated to per-unit to have a more uniform definition of the differences in absolute values. Tab. 3.2 specifies the parameter values of the branches per km. Multiplying it with the distance of the specified branch, the absolute value is obtained. Eq. 3.2 describes the calculation of the base impedance. The base voltage is dependent on the region where the branch is, i.e. two regions. The first region is the secondary side of the transformer with a 150 kV output voltage. The second region is the primary side of the transformer with a 33 kV input voltage. For the sake of simplicity, a base power of 100 MVA is chosen for the entire transmission system. After the base impedance is calculated for the specified region using Eq. 3.2, Eq. 3.3 calculates the per-unit values for each branch. Similarly, the susceptance is calculated. Additionally, the apparent power rates of the branches have to be determined in order to satisfy the power limits of the system. The rated apparent power is determined using Eq. 3.1.

$$S_{Rated} = \sqrt{3} \cdot I_{Rated} \cdot V_{Base} \tag{3.1}$$

$$Z_{base} = \frac{V_{base}^2}{S_{base}} \tag{3.2}$$

$$Z_{per-unit} = \frac{Z_{absolute}}{Z_{base}} \tag{3.3}$$

All branches are modeled, but there are specific branches that are considered to be disconnected unless stated otherwise by the optimisation setpoints received. Firstly, **The shunt reactor** is assumed to be disconnected. Therefore, branch 12-28 and 17-28 are disconnected. Ideally, this is connected only in the case that the generating strings are unable to satisfy a specific amount of reactive power demand from the TSO. Additionally, if negative reactive power is needed in the system to prevent violations of constraints. The influence of the shunt reactor is analysed in Chap. 4. **Branch 7-12** and **17-23** are disconnected. These branches are safety branches in case of faulty conditions, i.e. overcurrent or overvoltage at the bus bars. The current will in such case be higher than 2500 A, or higher voltage than 36 kV, shown in App. A.2.
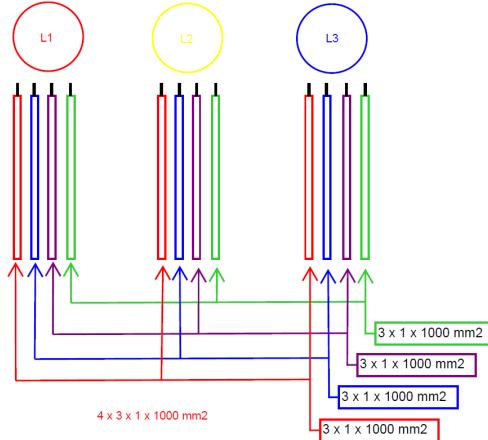
Figure 3.2: Configuration of a branch with XLPE 4x3x1Cx1000mm2 Al cable. Data from [23].

3.1.2. Transformer modeling

In order to model the main 3-winding transformers shown in App. A.2, a 2-winding approximation is implemented as shown in Fig. 3.3. Eq. 3.2 is used in order to calculate the Z_{base}, in which the base voltage of the low voltage side is used. Furthermore, the leakage reactance of the main transformers is used to calculate the impedance of the inductors shown in Fig. 3.3 according to Eq. 3.4. Afterwards, this value is converted to per-unit values using Eq. 3.3. With a leakage reactance of 15% this resulted in a impedance value of j0.680625 Ω, which is equal to j0.0625 Ω p.u..

$$Z_{Im} = \frac{Z_\%}{100} \cdot Z_{base} \tag{3.4}$$
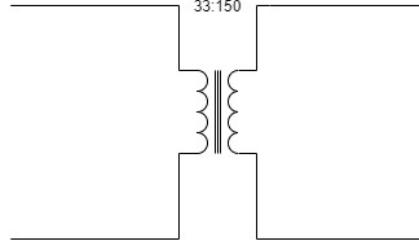
Figure 3.3: 2-winding model for the 3-winding transformers.

3.2. Modeling the WTG farm

In the WTG farm of App. A.2, it can be seen that the WTG strings are modeled as an aggregated model of individual WTGs [25]. Here, the WTG strings generate apparent power equivalent to the summation of the WTGs of Apps. A.4, A.5 connected to these strings. For the scope of this project, this model is satisfactory and used until the effects of the non-aggregated models are analysed.

$$P_{output} = P_{rated} \cdot \frac{v_{wind}^3 - v_{cutin}}{v_{rated}^3 - v_{cutin}} \quad \text{for} \quad v_{cutin} < v_{wind} <= v_{rated} \tag{3.5}$$

$$P_{output} = P_{rated} \quad \text{for} \quad v_{rated} < v_{wind} <= v_{cutoff} \tag{3.6}$$

$$P_{output} = 0 \quad \text{elsewhere} \tag{3.7}$$

To calculate the output power of the aggregated model for the WTG, Eqs. 3.5, 3.6, 3.7, were used. The Eqs. calculate this output power with the wind speed velocity (m/s) as the input parameter. Once this wind speed

reaches a minimum or maximum threshold, Eq. 3.7 indicates that the WTG string output will be equal to 0 MW. Using Eq. 3.6, it can be found that there is also a threshold for the wind speed as input parameter. Once this threshold is reached, the output power is constant and maximal. The thresholds used to calculate the output power of the WTG strings is specified in Tab. 3.3

Table 3.3: Threshold wind speeds to calculate the output power of the WTGs.

	Wind speed (m/s)
Cut-in	3
Rated	14
Cut-off	25

3.2.1. Design of WTG on string level

To improve the model accuracy, it was decided to model the WTG strings on individual level. It is expected that the modeling of individual WTGs will have a significant effect on the accuracy of the modeling. Mainly, because several components that initially were assumed ideal, are now modeled according to its realistic values. Components that are now taken into account are:

1. The cable lengths and type from WTG to string. Initially, this was the distance from bus bar to string. Now, the distances among the WTGs on one string is considered.

2. The rated apparent power of the cables connected to the individual WTGs.

3. The leakage reactance of the WTG transformers. Each WTG operates at a base voltage of 0.4/0.63 kV. Therefore, a step-up conversion is needed for this base voltage from 0.4/0.63 kV to the base voltage of the bus bar its connected to, i.e. 33 kV.

4. The capability curves of each WTG. This is briefly explained in Sec. 3.2.2.

App. A.19 shows the string level modeling of main bus bar 7 as an example. The configuration is different for each string, but the same principle is held throughout the modeling. The WTGs are modeled as a generator. The last generator is connected to the main bus bar by the branch that was previously used to model the distance from WTG string to bus bar, e.g. branch 7-36 has the same length as branch 7-8 from App. A.3. However, in some cases there will be a joint terminal, which are highlighted in green in App. A.19, between the last generator and main string. If connected, it will have a length of 37 m and of cable type 3x1x630 mm2 AL XLPE. This joint terminal is needed to connect two types of cables without adding an active component to the system configuration.

The WTGs are modeled by a generator with horizontal terminals, which are highlighted in yellow as shown in Fig, A.19. The length specified between two WTGs, is the mutual distances between the two. To determine the parameters for these branches, Tab. 3.2 and [23] were accessed to determine the resistance in p.u., reactance in p.u. and power limit for each of the branches. The transformers to which the output of the WTGs are connected, are modeled as a bus with losses. In this case with horizontal terminals as well, which are highlighted in light blue as shown in App. A.19. To determine the losses caused by the transformers, the leakage reactance was calculated and the impedance of the cable type its connected to. This cable is located in the WTGs and connects the generator with the transformers. Since no data was made available about this cable, a research is done in order to find the best suitable cable for this system. Firstly, this cable type is assumed to be 3x1x150 mm2 AL XLPE. However, when running the test models with this cable type, the results showed that the system is unstable in the strings. This is mainly caused by a high voltage magnitude, e.g. in the range of 1.2 p.u. - 1.4 p.u. From the tests it became clear that this is caused by the high impedance of the cables. So it was decided to implement a cable with lower impedances in order to have a stable system, from which useful conclusions could be derived, which will be further elaborated in Subsec. 5.2.5. Eventually, the cable type is assumed to be 3x1x630 mm2 Cu NYY [26].

Subsequently, this leakage reactance of the transformer was added in series to the reactance of the cable 3x1x630 mm2 Cu NYY from the transformer to WTG connection. The transformers are solely seen as a series leakage reactance specified by Eq. 3.4. Since the inductances in series can be added, it is concluded that

the series approximation can be considered to be correct. At last, the photovoltaic strings are highlighted in salmon pink as shown in App. A.19. The design of the photovoltaic strings will be further elaborated in Sec. 3.3.

This procedure is implemented for each generating string of App. A.2. The purpose of this model is to improve the system configuration. Additionally, the configuration serves as a comparison to the previous aggregated model. From this, it can be concluded what the difference is in the analysis of the system behavior for the two system models. This conclusion will serve as a recommendation to future research concerning the negligence of the string level components or not.

3.2.2. Design of the WTG capability curve

For the WTG, there is a relation between the active output power and reactive output power. In most WTG modeling, the relation is straightforward. The WTG will provide maximum reactive power at all times. With the Enercon Type C used as example [23], this relation is shown in App. A.17 for a voltage magnitude of 1 p.u. When the voltage is unequal to 1, the P-Q relation changes. In addition, some WTGs will produce maximum reactive power, once a certain active power threshold is reached. This condition is shown in App. A.18.

Both cases make the modeling of the output reactive power for the WTG complex. Ideally, from the PQ/RX model, the function for the P-Q relation dependent of the voltage magnitude is calculated [20]. From this derivation the exact output and P-Q relation are determined. However, due to insufficient given data from the case study, the implementation for a PQ/RX model is not feasible. For this reason, the P-Q relation is derived from the Enercon P-Q diagrams of Apps. A.4, A.5, [23].

The procedure to implement the non-ideality of the P-Q relation will consist of determining the equivalent P-Q relation for each WTG generating string in Apps. A.4, A.5. An approximation of this P-Q relation is made by dividing the capability curve into three sections. The first section models the linear slope for a voltage of 0.9 p.u., to reach maximum reactive power at the threshold for the active power. The second section approximates the common case of maximum reactive power. The third section will approximate the decrease of reactive power specified with the slope of a voltage of 0.9 p.u., shown in App. A.18. This slope is considered to be a reliable approximation, since it is the closest to the minimum physically allowed voltage of 0.8576 p.u. This prevents a complex implementation of the P-Q relation as a function of varying voltages for each WTG string. Out of this approximation, the wind speed and Q relation is determined and plotted for each generating string in Fig. 3.4. This capability curve will be implemented for every wind speed test model designed in Chap. 4.

Design of the WTG capability curve on string level   For the design of the P-Q relation on string level, the same procedure, as described in Subsec. 3.2.2, is followed. The P-Q relation is also approximated by dividing the capability curves in three sections. Instead of summing the capability curves of every WTG in order to model the string as one generator, the three sections are implemented for every type of WTG in the string. In total four types of turbines are modeled. Out of this procedure, the wind speed and Q relation is determined for every WTG and plotted as shown in Fig. 3.5.

3.3. Design of the solar farm

3.3.1. Determination of solar farm parameters

For the design of the solar farm, there was no data supplied. This offered a degree of freedom in the design. A rule-based approach is used for the design of the farm.

Firstly, the active power generation of the solar farm is determined. The generation is determined by analysing the weak components of the system. Weak components are considered to be the components, which will have apparent power overloading when running the power flow. In this case study, the weak components are considered to be the transformers and the cable to the PCC. In order to prove this, these components are analysed with the WTG farm generating active power at rated wind speed. The results of this analysis are shown in App. A.37, A.36, and A.38.

In App. A.37, A.36, and A.38, it can be seen that for the case study used, the branch to the PCC is the weakest component. As can be seen in Fig. A.38 a capacity of 38.2 MW can be added before reaching the branch limit
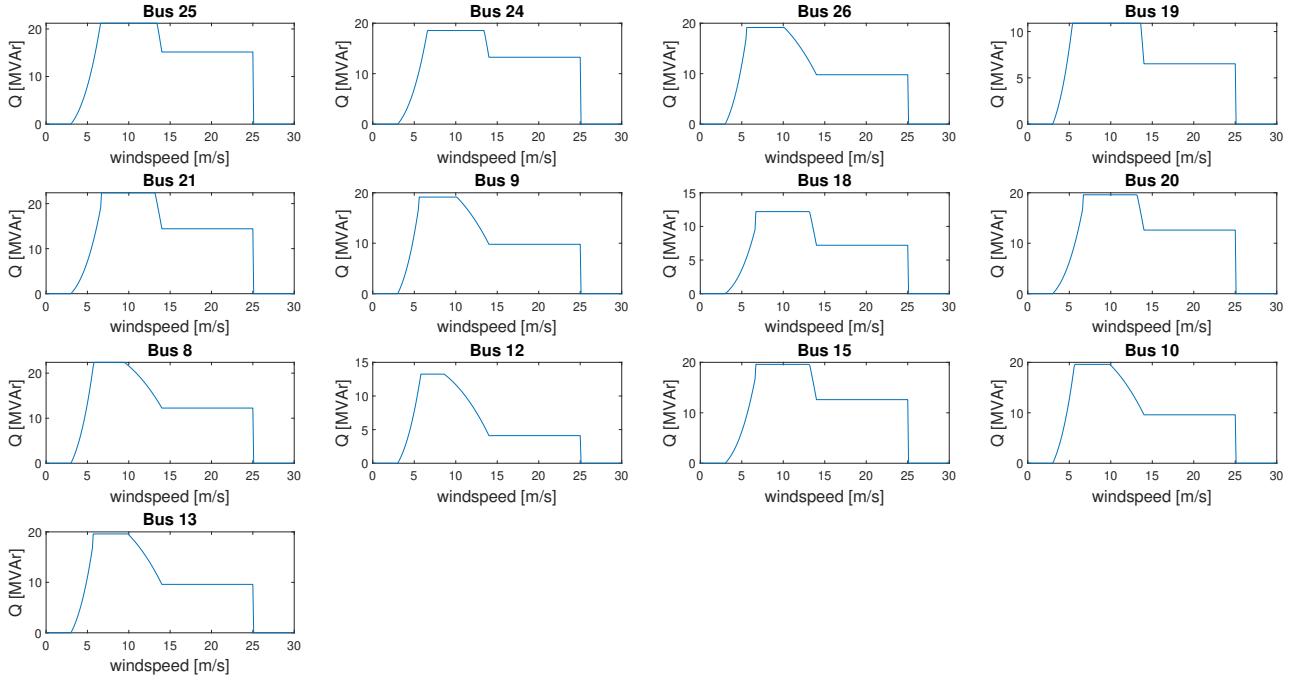
Figure 3.4: The model designed for reactive power output for different wind speeds for each bus connected in App. A.3. The busses correspond to the WTG power generating strings. For a wind speed of 7.5 m/s the reactive power output achieves its maximum. At a wind speed of 14 m/s the reactive power output decreases until it achieves its minimum at the cut off speed.

of the cable. Thus, for each solar farm string, and rated power generation of 12 MW is chosen. Therefore, some parts of the day the cable to the PCC will be overloaded with 8 MW. This overloading is needed to give power flow control scheme [4], the opportunity to come up with solutions in order to guarantee stability and reliability of apparent power at the PCC.

Additionally, the type of solar modules has to be chosen. It was decided to implement the Sunpower X-Series solar modules, because these modules have a high efficiency of 22.2%, in comparison to the average solar modules efficiency of 18%, and a sufficient amount of data about the modules is available online [27].

Secondly, because of the AC powerflow in the case system shown in App. A.2, the DC power generated by the solar modules has to be converted into AC power. [7]. Thus, in each photovoltaic string, DC/AC inverters are implemented in order to apply this conversion. However, during this conversion, reactive power is generated by the DC/AC inverters [7]. As shown in [28], the efficiency of this conversion is 98,7%, which will be taken into account when calculating the maximum output power. Since no data of the P-Q capability curves for these solar modules is available, a popular approximation used in research was used for Q, as shown in Eq. 3.8 [29].

$$Q_{gen} = \frac{1}{3} \cdot P_{gen} \tag{3.8}$$

Afterwards, the irradiance in W/m^2 of the location is examined using [30]. When implementing the irradiance profile, a summer model is chosen. This choice is made, since in the summer the irradiance has less fluctuations due to less uncloudy and the highest in comparison to the other seasons. This research resulted in a rated irradiance of 800 W/m^2. This value is used in order to calculate the number of modules needed for each solar farm. As can be seen in [27], the output power of each module at Standard Test Conditions (temperature of 25°C, irradiance of 1000 W/m^2 and an air mass of 1.5 (AM 1.5) is 360W. For the sake of simplicity, the output power is considered to be linearly dependent with the irradiance. Thus, the other two variables, temperature and air mass, are not considered to be of influence in this model. With this assumption, the output power of each module is calculated by Eq. 3.9.

$$P_{module-location} = \frac{I_{location}}{I_{STC}} \cdot P_{module-STC} \tag{3.9}$$
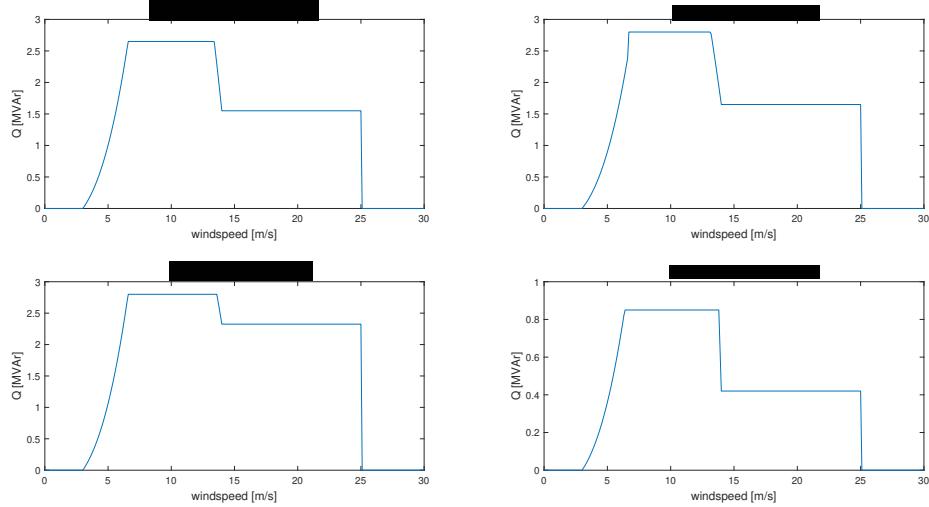
Figure 3.5: The capability curve for the reactive power output as a function of wind speed in m/s for each type of WTG connected in the aggregated model of App. A.3. App. A.19 is an example for the configuration of a bus, but the types are not specified in the Fig. At a wind speed of 7.5 each WTG achieves its maximum reactive power output and stays on that level until cut off wind speed. The letters in parentheses indicate of the type of the WTGs.

$$N_{modules} = \frac{12 \cdot 10^6}{P_{module-location}} \tag{3.10}$$

In addition, the amount of solar modules needed is calculated by Eq. 3.10. These calculations resulted in 41667 solar modules for each photovoltaic string.

Table 3.4: Maximum output current and voltage of one solar module [27] and the bus and branch limits of the case system shown in App. A.3.

Maximum Output voltage	69.5 V
Maximum Output current	6.48 A
Bus limit	36kV
Branch limit	1402.96 A

3.3.2. Solar farm overview

Additionally, the interconnection of the solar modules is determined by considering the capacity limits of the bus bars to which these photovoltaic strings are connected . An interconnection as shown in Fig. 3.6 is chosen, since this interconnection will not violate any voltage or current bus/branch limits [31]. In Fig. 3.6, 204 solar modules are connected in series per array, which results, using Kirchhoff's voltage law and Tab. 3.4, in a maximum output voltage of 14,178 V for each array. This voltage has to be transformed to the base voltage of the bus bar in order to connect to the grid. Therefore, a 14 kV/33kV transformer is connected as shown in Fig. 3.6. On the other hand, 205 arrays are connected in parallel, which results, using Kirchhoff's current law and Tab. 3.4, in a total maximum current of 1328 A for each photovoltaic string. The last consideration that had to be made is that the inverter has a limited number of inputs, i.e. three inputs. Therefore, sub array connectors are used in order to connect the arrays with the inverter.

Eventually, the cable length from the interconnection point to bus bars is approximated by examining the data of the location and the cable lengths of the WTG strings. This resulted in the approximated length shown in Apps. A.2, A.3.

3.4. Method to determine model accuracy

MatPower solves the power flows, voltage/current profiles, and power losses of nodes in the system, using the Newton Raphson method [9]. To determine if the model was implemented correctly and MatPower is a
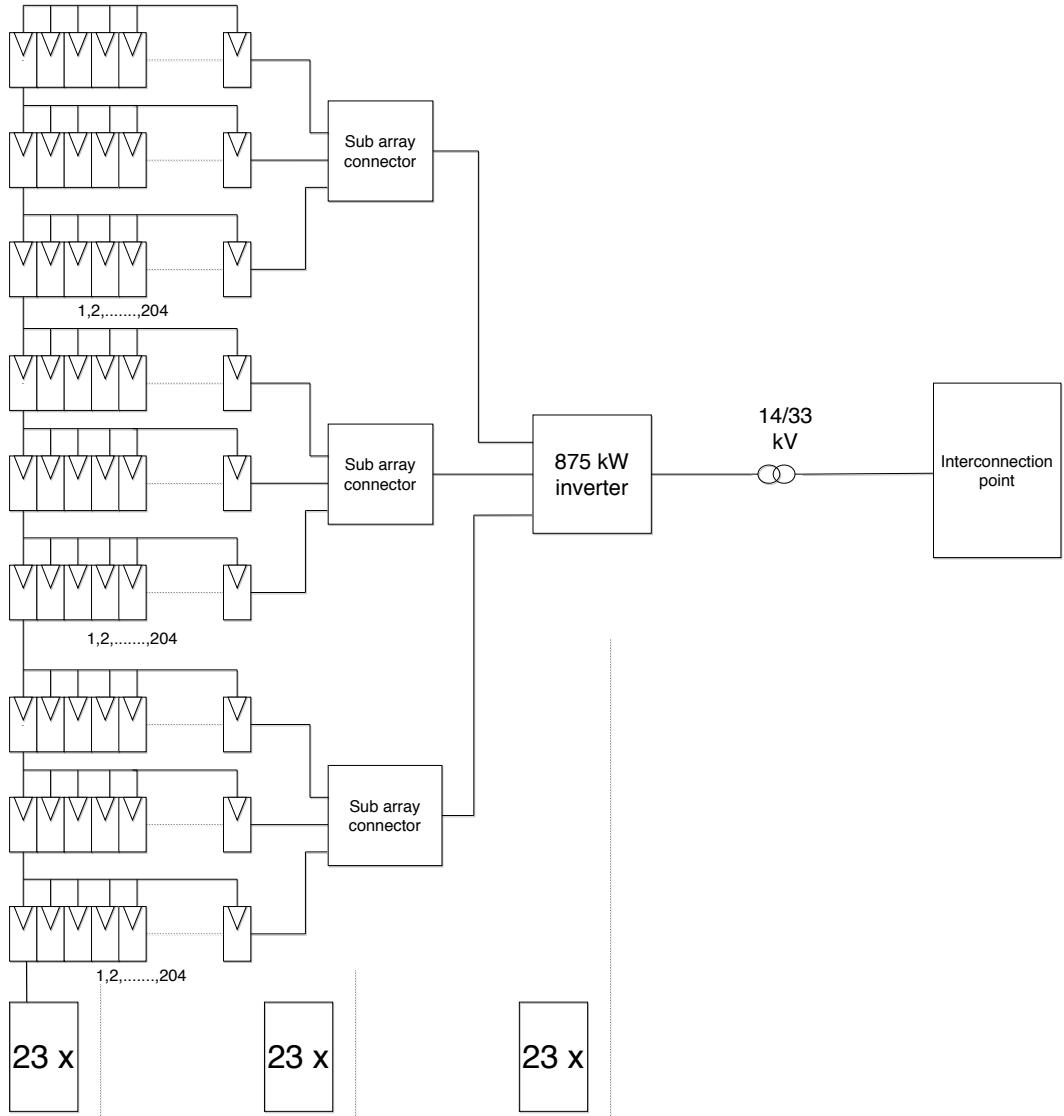
Figure 3.6: Overview of a part of the solar farm, in which the sub array connector, inverter and transformer are shown. For each photovoltaic string this part is implemented 23 times in order to have an active power generation of 12 MW.

reliable source tool, the same method was applied with hand calculations. Hereby, the same setpoints for generating strings used for the MatPower code were used to solve the iterative power flow.

Since the system configuration consists of 28 bus bars and 17 generating strings, it could be concluded that performing hand calculations on the entire system would be too intensive for the purpose of this project. Therefore, it was decided to perform the calculations for one string. This comparison is done for two different reactive power setpoints. The strings chosen were based on the known parameters of the system. When there is a PCC request, reactive power setpoints are sent to the generating strings from the slack node top to the strings down. Based on this, the voltage profile and current is best known between the WTG and connected bus, e.g. the power flow of branch 7-8 with bus 8 being the WTG, is known after the reactive power demand is known at bus 7. To choose which branch is most relevant to model, the longest branch was chosen since this will cause a higher voltage difference and power loss in the string. With a length of 7561 m, branch 23-24 is tested.

Firstly, an equivalent test model is made for the branch, shown in Fig. 3.7. After, an equation is formulated for the active and reactive power through branches Eq. 3.11 and Eq. 3.12. In these equations, i will be the node

for which the power is unknown and n will be the node with known magnitude and angle values. Y_{in} is the admittance value in the admittance matrix for the branch between node i and n. With the Jacobian of Eq. 3.13, Eq. 1.4 is solved. From Eq. 1.4, the power flow is determined. If the mismatch between the calculated power flow and the desired power flow is below a certain threshold, the vector of Eq. 1.4 yields the final solution.
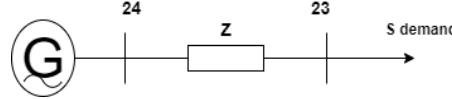
Figure 3.7: Equivalent test model of branch 23-24 used to perform the hand calculations to determine the model accuracy.

$$P_i = \sum_{n=1}^{N} U_i \cdot U_n \cdot Y_{in} \cdot cos(\delta_i - \delta_n - \theta_{in}) \tag{3.11}$$

$$Q_i = \sum_{n=1}^{N} U_i \cdot U_n \cdot Y_{in} \cdot sin(\delta_i - \delta_n - \theta_{in}) \tag{3.12}$$

$$\begin{vmatrix} \frac{\partial P_i}{\partial \delta_i} & \frac{\partial P_i}{\partial U_i} \\ \frac{\partial Q_i}{\partial \delta_i} & \frac{\partial Q_i}{\partial U_i} \end{vmatrix} \tag{3.13}$$

To solve the equations, all values will be in per-unit. To arrive at the known parameter values, the Mat-Power code shown in App. A.9.1 is ran with random setpoints centered around 0 and maximum active power generation for each string. From this test, the values in Tab. 3.5 are determined. Using Fig. 3.7, in the first test it is assumed that the generation is known, i.e. at bus 24, and the voltage profile on bus 23. In the second test the apparent power demand is known, i.e. at bus 23, and the voltage profile on bus 24. In this manner, the Newton Raphson method is applied for both sides of the model, yielding a more reliable hand calculations result.

Table 3.5: MatPower known parameters for the model of branch 23-24. Bus # is the bus number. Voltage magnitude and angle are specified for the busses. The admittance (Y) value of the cable connecting the busses. Power flows from bus 24 to 23. Therefore, P and Q are the power injection of bus 24 and the power absorption for bus 23.

Bus #	Voltage (p.u.)	V $\angle$ (degrees)	Y admittance (p.u.)	P (p.u.)	Q (p.u.)	P loss (MW)	Q loss (MVAr)
23	0.9801	18.5814	1.265 - j 7.216158756	0.294	0.000169	0.0607	0.3465
24	0.9776	19.2510	1.265 - j 7.216158756	0.294	0.00023	0.0607	0.3465

For the purpose of this project, a threshold of 0.0001 p.u. for the power flow mismatch is chosen, which is recommended in the lectures of the supervisor for the project. After the final solution is found from Eq. 1.4, the current magnitude and angle are determined. Using Ohm's law, the active and reactive power losses are calculated. Then, the mismatch between the MatPower and hand calculations is analysed to determine if this mismatch can be neglected for the purpose of this project. Based on the total active power, 400 MVA, that theoretically could be provided at the PCC (Bus 1), a maximal mismatch of 1 MW for active power and 1 MVAr for reactive power is chosen. The relative mismatch is 0.25 % which is considered to be a negligible inaccuracy. Furthermore, this mismatch is well within the allowable deviation of the PCC request [23]. The hypotheses is that if the MatPower results are sufficiently close to the hand calculations, MatPower modeling proves to be accurate.

4

Test models for operating conditions

To determine the system behavior after each system update, different Operating Conditions (o.c.) were designed. System updates occur when the dispatch profile is known, i.e. wind speed (m/s) and solar irradiance (W/m^2). Furthermore, the system is updated after receiving setpoints for generating strings. The setpoints indicate if a certain string is required to be connected and deliver apparent power and what the amount is that shall be delivered, this relation is shown in Fig. 2.1. The results of these test models yield the relation between dispatch profiles, losses in the system, and setpoints received from the PCC.

After defining what parameters shall be tested, the relevant o.c. should be determined for the transmission system. This can be divided into normal o.c. and extreme o.c. Normal o.c. is defined by the most frequent PCC setpoint request at a nominal dispatch profile. Following [23], normal setpoints are defined by the request of maximum active power output (MW) and zero reactive power (MVAr). Consequently, in most cases the power factor requested at the PCC is equal to 1. Furthermore, nominal dispatch profiles are defined by $v_{wind} = 7.5 m/s$ and $I = 500 W/m^2$. Using Eqs. 3.5, 3.6, 3.7 and Eq. 3.9 the active power output is computed for WTG and photovoltaic strings. Using Fig. 3.4 and Eq. 3.8, the reactive power output is computed. It can be seen from Eq. 3.5, that nominal wind speed will not give maximum active power output. However, from Fig. 3.4 every WTG string will generate maximum reactive power. The rated power for each string is found in App. A.4, and A.5.

Therefore, extreme o.c. are defined for setpoints of which the power factor is lowest for a specific dispatch. The power factor is given by Eq. 4.1.

$$pf = \frac{P}{\sqrt{P^2 + Q^2}} = \frac{P}{|S|} \tag{4.1}$$

Eq. 4.1 derives that the lowest power factor is reached when the maximum positive or negative reactive power that the string can deliver, is requested from the PCC. For the extreme test models, this behavior is analysed for a very low P generation and a very high P generation of the connected strings. To determine the dispatches corresponding to realistic low P generation and high P generation, the probabilistic distribution for wind profiles is run with parameters from the case study [23]. For the solar profiles, it is based on the historical data of the case study [30].

There might be concerns about the Q requests made by the PCC to the WTG and PV strings, leading to a violation of the rated apparent power of the branches, explained in Sec. 3.1. Therefore, a quick calculation was made to determine the maximum apparent power flow through these branches. $P_{max} = 33 MW$ and $Q_{max} = 22.4 MVAr$, therefore $S_{max} = \sqrt{(33)^2 + (22.4)^2} = 39.9 MVA$. This is below the rated apparent power limit, i.e. $46.2977 MVA$, of the branches and shall therefore not need consideration for the design of the test models.

Since the load demand is unpredictable in a realistic situation, it was decided to apply a normal distribution with a standard deviation of 8 % from the maximum reactive power output [10]. The mean of the distribution is calculated by dividing the reactive power at the PCC by the amount of connected generating string. This reactive power mean is swept from the maximum negative reactive power to maximum positive reactive power

in certain steps. It is believed that by doing this sweep, it will be able to derive relations between the voltage magnitude and active/reactive power losses or reactive power injections in the system.

It should be noted that for each wind/solar dispatch design, it is assumed that the noncorresponding renewable energy system is inactive. For example, when the photovoltaic power generation is modeled with the designed solar irradiance daily dispatch, the WTGs are considered to be disconnected. The same counts for the wind daily dispatch design and the disconnected PV module. Once each design is tested individually, the dispatches can be combined in a normal random distribution function for wind-and solar power connected simultaneously.

To test the system behavior, the model is tested under different operating conditions. A total of 300 dispatches are made, i.e. 300 of 15 minute dispatches [10]. More dispatches will be confusing to analyse and less will be insufficient data. For the correctness of the tests, it is important to disconnect or neglect components that are not part of the components of interest.

For each test model the procedure explained in Fig. 4.1 will be followed. It is divided in different sections that make it possible to derive conclusions in a stepwise manner. Firstly every relevant system and test parameters are calculated and implemented to run power flows.

Out of the power flows the data is processed to make relation plots and data vectors indicating violation of voltage magnitudes constraints. The voltage limitations are shown in Tab. 4.1. The constraints are based on the voltage limitations of the transformer inputs, i.e. bus 4 and 6 of Fig. A.3. Lastly, these plots are used again to compare it to other test models results.
Especially, the 3-D plots make data analysis more manageable. For each dispatch, the total system behavior is plotted for different dispatches. Out of this comparison it can be concluded if expectations are satisfied.

Table 4.1: Voltage constraints for the transmission system based on the voltage limitations of the transformer inputs.

Minimum allowed voltage (p.u.)	Maximum allowed voltage (p.u.)
0.8576	1.1424

4.1. Hypotheses on results

4.1.1. Active and reactive power losses

As is already known, the PCC receives reactive power demand from the generating strings. This situation can be reformulated by a simplified AC model shown in Fig. 4.2 and Fig. 4.3. When the demand at the PCC is positive, the PCC behaves as an inductive element, for which $X = j\omega Ł$. Fig. 4.2 shows that when this is the case, the voltage at bus bar 1, i.e. the PCC, is the negative terminal of the reactance. Therefore, the average voltage magnitude of the transmission system, i.e. the positive terminal, must be higher than bus bar 1 to satisfy this behavior. For a capacitive element, for which $X = \frac{-j}{\omega C}$, the opposite relation applies. The average voltage magnitude, i.e. the negative terminal, must be lower than bus bar 1. The PCC was considered to be the slack node with 1 p.u. and 0 angle degrees, explained in Chap. 3. Reactive power is calculated from multiplying the impedance with the current squared, as shown in Eq. 4.5 for losses. For a higher positive or negative reactive power, the system voltage must deviate more from the PCC voltage to increase the reactive behavior from the element model. From this relation it can be concluded, the more positive the reactive power demand, the higher, above 1 p.u. the average voltage will be. The more negative the reactive power demand, the lower, below 1 p.u. the average voltage.

Out of the relations described by Figs. 4.2 4.3, also the voltage-loss relation of the system could be derived. Eqs. 4.3, 4.4 describe a parabolic relation between the parameters, mirrored in the x-axis around the voltage of the slack node. One should notice that the Eqs. 4.3 4.4 are multiplied with the voltage base squared, otherwise the losses were in per-unit values.

Although, a parabolic relation is described, the reactive power demand strongly influences which part of
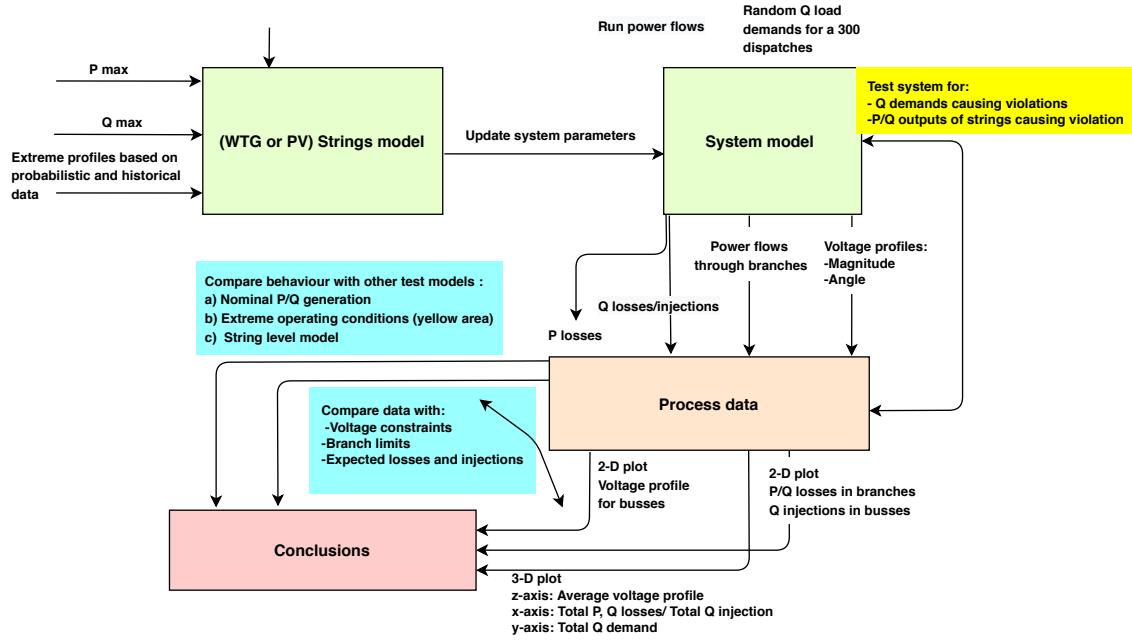
Figure 4.1: Overview of procedure followed to analyse the power flows in the case system shown in App. A.3. The green blocks indicate the design process of the system and testing of it. Orange indicates the data gathering to arrive at conclusions, the red block. Blue blocks are the data of previous models that serve as a reference to the data gathered for the current model. Yellow block indicate the extreme test operating conditions. The mentioned violations are for the boundary voltage magnitudes of the system, since it is expected some busses will violate these boundaries after power flows are ran.

the graph is extended in losses. The same demands, but of the opposite sign have other effects on the losses. Using the simple Eq. 4.2 from Ohm's Law, it is expected that negative demands of equal magnitude to its positive demands, will cause higher losses in the system. Since Ohm's Law must be satisfied for all circumstances, when $\Delta V = V - V_{slack}$ is higher for negative demands, the current through the branches of the system becomes higher to still satisfy the power flow through the system. Because of this higher current, there will be more dissipation through the impedances of the branches in the system, leading to higher losses.

Ideally the slack voltage is 1 p.u., but this value inserted can slightly deviate if the Newton Raphson solves the power flow with a different vector solution in Eq. 1.1. This is caused by a small power mismatch.

$$V = I \cdot Z \tag{4.2}$$

$$P_{loss} = \frac{(V - V_{slack})^2}{R} \cdot (V_{base}^2) \tag{4.3}$$

$$Q_{loss} = \frac{(V - V_{slack})^2}{X} \cdot (V_{base}^2) \tag{4.4}$$

Eventually, when comparing the P_{loss} and Q_{loss} results, it is expected that the Q_{loss} will be significantly higher than P_{loss}. Matpower implements Eqs. 4.5 in order to calculate the power losses in the branches. As shown in Tab. 3.2, the reactance values are almost 5 times higher than the resistance values. So with Eq. 4.5, it can be concluded that the dissipation in the reactances will be higher than the dissipation in the resistances, which will result in higher reactive power losses than active power losses.

$$Losses = I^2 \cdot (R + jX) \tag{4.5}$$
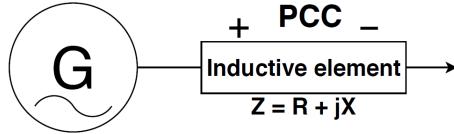
Figure 4.2: Visualization of the PCC behaving as an inductive element.
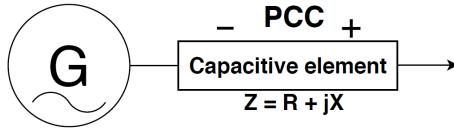
Figure 4.3: Visualization of the PCC behaving as a capacitive element.

4.1.2. Reactive injection losses

The expected relation for the average voltage and losses due to injections in the bus bars, is explained by Eq. 4.6, with Q reference = 0 MVAr. This was relation was derived from [32] and shall be consulted for further explanation. Here, it was assumed that the injection losses are equivalent to the reactive power present by droop losses. Eq. 4.6 describes a linearly increasing reactive injection for decreasing voltage transmitted to the PCC. This relation is expected for every test condition. Furthermore, it will not change for different generations of the same system model, since the droop coefficient does not change. It stays constant and therefore the same relation holds.

$$Q_{injected} - Q_{reference} = -\frac{1}{R_u} \cdot (V_{transmitted} - V_{slack}) \tag{4.6}$$

4.1.3. Reactive power demand

To derive the exact relation between total reactive power demand by the PCC and the average voltage of the system, [33] suggested an analysis of an exponential load model. The exact parameter values that describe the relation described by this load model is yet unknown. This will be derived from the results in Chap. 5. However, it is expected that the same relation is held for every test model analysed.

$$Q = Q_n \cdot (\frac{V}{V_n})^{k_{qu}} \tag{4.7}$$

4.1.4. Expected system behavior

Following the relations described above, it was concluded that the power flows through the system directly influence the voltage magnitude and losses. Therefore, the higher the total active power generation, the higher the active power losses. The order of available generation for the farms is from solar farm (40 MW), to wind farm (363 MW), to hybrid farm (403 MW). Concluding, in the same order the active power losses will increase. Furthermore, active losses and reactive losses have a linear relation if plotted against each other. Active and reactive losses will simultaneously linearly increase or decrease, but not with the same magnitude.

However, using Eqs. 3.5, 3.6, notice that for higher active power generation of the system for wind farm, the reactive power generation becomes lower because of the decrease in the capability curve shown Fig. 3.4. Hence, using Eq. 4.1, the apparent power is decreased. If the total apparent power for higher active power generation becomes lower than that of nominal active power generation, the reactive losses in the system will be higher for nominal active power generation. This is because the apparent power flow becomes higher with increasing availability in reactive power from the generating string. However, it is yet unknown if this will be the case. Therefore, the results will be analysed and discussed in Chap. 5, from which it can be concluded whether the apparent power is indeed lower for higher active power generation from the WTG strings.

4.2. Wind farm procedure

For the wind farm, the solar farm will be disconnected. The procedure of Fig. 4.1 is followed for three different wind speeds, one of them being the nominal wind speed, i.e. 7.5 m/s.

The choice of the wind profiles was based on a Weibull PDF. Out of data for the case study, the scale parameter, 2.54 p.u. and shape parameter, 7.86 m/s was found [23]. With these parameter, the probability for extreme wind speeds were determined. By running 1000 samples of the Weibull PDF, the probability of the chosen wind speeds is analysed. This believed to be a correct approximation. [14] makes use of 135 wind speed data points for the research and [15] uses 4096 samples to run the Weibull distribution. Hence, the amount of samples ran is arbitrary, as long enough samples are created, the approximation proves to be correct. In the proposed model, the data processing is based on three years of historical hourly data to forecast the random behavior of wind speeds and solar irradiance at different times of the year. of 135 irradiance and wind speed data points with the assumption that one month is made up of 30 days [14] In Tab. 4.2, it is found that the probability to be at extreme wind speeds is relatively high, namely approx. 10 % of the time. This probability is higher for windy seasons, making its inspection relevant. The wind speeds chosen were close to the cut in and cut off speed boundaries. For extreme low generation it was decided to choose 4 m/s. For extreme high generation this was 14 m/s. From Eq. 3.6, will generate maximum at this chosen wind speed.

Table 4.2: Probability of extreme wind speeds for the location of the case study. This probability is based on the Weibull parameters for a yearly wind dispatch of the location [23].

V low (m/s)	Probability of exceeding V	V cut in (m/s)	V rated (m/s)
4	0.135	3	14
V high (m/s)	Probability	V cut off (m/s)	V rated (m/s)
13	0.016	25	14
14	0.07	25	14

As explained in the Sec. 4.1, the mean of the normal distribution for load demands will be swept from maximum negative reactive power to maximum positive reactive power. The average maximum of the WTG strings is calculated by summing the reactive power at nominal wind speed(7.5 m/s) using Fig. 3.4, yielding 18.46 MVAr. For a correct behavior analysis from different sample points as means, it was decided to sweep this mean in 20 steps, from 18.46 to -18.46 MVAr. 20 steps is considered an estimate for sufficient means to yield plots that show a relation between the 3-D plots. Since the generation of reactive power is lower for extreme wind speeds, the means and subsequently, the sample points in the 3-D plots will be closer to each other, making the plots unreadable if a higher amount of dispatches is used, strengthening the argument of using 300 dispatches for analysis [18].

To test the effect the shunt reactor component has on the system behavior, a test will be run for which the shunt reactor is connected at nominal wind speed. Although the shunt reactor is connected, the same reactive power setpoints are sent by the PCC to the WTG strings, as done for the test models with shunt reactor disconnected. By doing this, the difference between the results of the test models, will solely indicate the effect of the shunt reactor.

4.3. Solar farm procedure

In order to test the behavior of the solar farm solely, the wind farm is disconnected before running the test models. The procedure shown in Fig. 4.1 is executed for three different solar irradiances.

As described in Subsec. 3.3.2, the solar profile is implemented for summer days and is based on historical data. Additionally, the normal and extreme o.c of the photovoltaic strings have to be determined. This done by examining the solar irradiance of the location assigned for this project. Furthermore, the irradiance is modeled discretely, meaning that a certain irradiance is modeled for the whole day. This is not an optimal modeling of the reality because the solar irradiance increases in a stepwise manner during the day. However, this can be justified, since the emphasis of these tests is on testing the capability of the system in dealing with extreme conditions.

For the extremely low o.c the minimum irradiance of the location is taken. The same is done for extremely

high o.c. For the normal operating condition, the average and most common irradiance is taken [30]. The results are shown in Tab. 4.3. In order to determine and implement the random load demands the same procedure is used as for the wind farm as described in Sec. 4. The same procedure as described in Sec. 4.2 is used in order to determine the average maximum of the Q demands of the photovoltaic strings. This resulted in an average of 10 MVAr. For a correct behavior analysis from different sample points as means, it was decided to sweep this mean in 10 steps, from 10 to -10 MVAr. For the photovoltaic strings 10 steps are considered to be sufficient menas to yield plots that show a relation in 3-D plots. The same reasoning as for the windfarm tests is used in order to justify the amount of steps. The complete elaboration can be found in Sec. 4.2.

Table 4.3: Low, normal, and extreme o.c. of the photovoltaic strings in terms of the solar irradiance in W/m^2. These values are needed for the test models designed. [30].

Category of operating condition	Irradiance [W/m^2]
Extremely Low	100
Normal	500
Extremely High	800

4.4. Hybrid farm procedure

Eventually, the wind farm, and solar farm are both connected to the system configuration in App. A.2. The procedure described in Secs. 4.2, 4.3 were combined in order to test the behavior of the hybrid farm. The extreme conditions of wind as described in Sec. 4.2 are combined with those of solar, which were elaborated in Sec. 4.3. For normal operating conditions the same procedure is implemented. This total of three operating conditions with subsequent dispatch profiles are shown in Tab. 4.4. The results of these test models will be further elaborated in Subsec. 5.2.4.

Table 4.4: Overview of the o.c. implemented for the test models in terms of the wind speed in m/s and irradiance in W/m^2.

	Wind speed (m/s)	Solar irradiance (W/m2)
Low generation	4	100
Nominal generation	7.5	500
High generation	14	800

4.4.1. Prototype hybrid farm

The prototype to show the system model fulfills requirements specified in Chap. 2, will be a simple visualizable diagram. This diagram is a snapshot of the power flows and voltages in the system, after four different dispatches and setpoints are received. The setpoints to the WTG and PV strings in order to satisfy load demands are not designed according to procedures described above. Rather for the prototype, the final setpoints are received from the optimisation scheme [6], after several power flows were run with the system model designed by this project according to the procedure in Chap. 3. After a discussion with the three subgroups, Tab. 4.5 is the desired test profile. These values were chosen such that the system behavior is known for the system components around nominal operating conditions. The +-50 MVAr are considered unfrequent load demands if the grid code is followed [34]. To show the power flows in the system, App. A.3 will be used as the visualizable diagram. In addition, the voltages will be shown on every bus number of the system.

Table 4.5: Test profile values for the prototype model. Each profile indicates a varying apparent power PCC request and apparent power generation based on the dispatch profile for the WTGs and PVs.

Profile #	PCC request (MW)	PCC request (MVAr)	Wind speed (m/s)	Solar irradiance (W/m2)
1	70	0	6.5	650
2	70	-50	7.5	600
3	110	0	8.5	800
4	155	50	10	450

5

Results

5.1. Determination of model accuracy

After the Newton Raphson method was applied to the test model of Fig. 3.7, interesting observations were made. Firstly, it was found that unless the first initial guess of the unknown voltage magnitude and angle is close to the final values for Vector 1.1, the Newton Raphson method would not converge in less than 10 iterations. This behavior is shown for the first test in Tab. 5.1 for which the voltage at bus 24 and the power demand of bus 23 are unknown. The power mismatches between the previous iteration and current iteration were increasing, which is an indication that the NR is working. However, the higher the number of iterations to solve the power flow, the more the voltage magnitude and degrees would differ from the final answer. An alternative had to be searched to prevent complex hand calculations for a calculation that can be simplified.

Any power flow calculation that requires more than 10 iterations, is considered to be too complex to solve with the hand [9]. Moreover, the calculations were performed for solely one branch. If the power flow was tried to solve for a test model of a greater section of the system in App. A.3, the complexity would increase and therefore the required time to solve. Because of this complexity, it was decided to make an own MatLab code for the hand calculations of NR-method found in App. A.9.1. This code will yield the final answer and the amount of iterations immediately. Secondly, it was found that the threshold of 0.0001 p.u. for the power mismatch was not feasible for hand calculations. In most cases, the system would not converge. It was decided to increase the allowable power mismatch to 0.1. After this was done, the NR would converge in some cases. In Tab. 5.2 the results are shown and the indication of the initial guess. It can be seen that the power mismatch between the first iteration and the current iteration is high compared to when the initial guess is closer to the final solution Vector of Eq. 1.1. The reason for not showing the mismatch between the previous iteration and the current iteration as explained in Sec. 3.4, is because of convergence issues. After each iteration, the mismatch is added to the power flow of the previous iteration. When the system does not converge, this would mean a significant amount of intermediate steps have to be noted. Therefore, it was decided to analyse solely the mismatch between first and last iteration and subsequently inspect if the solution Vector of Eq. 1.1 is approaching the final answer, since its approximate value was already calculated by MatPower. One could doubt this approach, but since MatPower is trusted to an extent that the solution at minimum approaches correctness, the values indicated by Tab. 3.5 are used as a reference.

The smallest power mismatch is found when the first initial guess is $\mathbf{V} = 1\angle 20$. A similar test was performed to determine if the voltage at bus 23 could be calculated, as well as the power generation of bus 24. Using the results of Tab. 5.3, the smallest mismatch is when the initial guess is $\mathbf{V} = 0.97\angle 20$.

The results are compared to the results of MatPower, having a noticeable margin of error in either the Mat-Power or the hand calculations results. For the voltage magnitude and angle the difference seems to be minimal. However, in Tab. 5.4 it can be seen that the hand calculations give higher P and Q losses in the branch. Several explanations were found to explain this difference for $\Delta P = 0.1318 MW$ and $\Delta Q = 0.7513 MVAr$. It should be noted that these values are within the maximum allowed power difference of 1 MW and 1 MVAr, explained in Sec. 3.4. Since MatPower also makes use of the NR-method to solve the power flows, it was decided to analyse how MatPower applies this method [22]. The threshold MatPower uses by default is sig-

Table 5.1: Hand calculations for test 1; voltage profile at bus 24 is solved. Voltage of bus 23 and power generation at bus 24 are known parameters. V guess and $\angle$ are the initial guesses for the solution vector. $\Delta P/Q$ is the difference between power flow of first iteration and current iteration. V result and $\angle$ result are the Vector solution of Eq. 1.1.

Iter.	V guess (p.u.)	$\angle$ guess (degrees)	V result (p.u.)	$\angle$ result (degrees)	ΔP (p.u.)	ΔQ (p.u.)
1	1	0	0.9465	-22.7570	N.A.	N.A.
2	1	0	0.3053	-110.6236	N.A.	N.A.

Table 5.2: Hand calculations with code of App. A.9.1 for test 1; voltage profile at bus 24 is solved. Voltage of bus 23 and power generation at bus 24 are known parameters. The iterations indicate iterations run by MatLab. If the system does not converge, the code is stopped manually. The calculations by MatLab are done so fast during this manual action, a significant amount of iterations are formed. V guess and $\angle$ are the initial guesses for the solution vector. $\Delta P/Q$ is the difference between power flow of first iteration and current iteration. V result and $\angle$ result are the Vector solution of Eq. 1.1.

Iter.	V guess (p.u.)	$\angle$ guess (degr.)	V results (p.u.)	$\angle$ results (degr.)	ΔP (p.u.)	ΔQ (p.u.)	Conv.
256944	1	0	0.9465	-22.7570	2.4503	-0.9096	No
294631	1	10	0.9983	-1.0222	1.3063	-0.4098	Yes
1	1	20	1.0157	19.0616	0.0928	-0.1162	Yes
1645122	0.99	20	0.9959	19.0518	0.1074	N.A.	No
1	0.996	20	1.0078	19.0577	0.0987	N.A.	Yes

Table 5.3: Hand calculations with code of App. A.9.1 for test 2; voltage profile at bus 23 is solved. Voltage of bus 24 and power demand at bus 23 are known parameters. The iterations indicate iterations run by MatLab. If the system does not converge, the code is stopped manually. The calculations by MatLab are done so fast during this manual action, a significant amount of iterations are formed. V guess and $\angle$ are the initial guesses for the solution vector. $\Delta P/Q$ is the difference between power flow of first iteration and current iteration. V result and $\angle$ result are the Vector solution of Eq. 1.1.

Iter.	V guess (p.u.)	$\angle$ guess (degr.)	V results (p.u.)	$\angle$ results (degr.)	ΔP (p.u.)	ΔQ (p.u.)	Converged
126514	1	0	0.9820	-22.7570	1.9422	-0.9262	No
156329	1	10	1.0203	-1.0222	0.8010	-0.4264	No
3392753	1	20	1.0258	19.0616	-0.4120	-0.1329	No
867535	0.99	20	1.0062	23.0715	-0.3982	-0.0555	No
835672	0.97	20	0.9665	23.1346	-0.3715	0.0856	No
2367897	0.97	19	0.9673	21.1310	-0.2517	0.0650	No
2	0.97	16.5	0.9679	16.1265	0.0461	0.0044	Yes

nificantly lower, namely 10^{-4}, making the final solution shown in Eq. 1.1 more accurate by yielding smaller power mismatches. Ideally, this is closest to 0 to satisfy Eq. 1.5. Thus, the hand calculations yield less satisfactory results with power mismatches close to the high threshold of 0.1. Secondly, MatPower considers the angle shift caused by the branch model in Fig. 3.1 when calculating losses. Therefore, the losses are defined as shown in Eq. 5.1 [22]. This was something that could not be taken into account for the hand calculations. Lastly, MatPower ran the power flow the case study, while for the hand calculations only one branch of the 31-branches system was tested. Thus, the influence the power flows of other branches have on the branch analysed in Fig. 3.7 cannot be considered for hand calculations.

$$Losses_{branch} = \frac{|\frac{V_{from}}{\tau e^{j\theta_{shift}}} - V_{to}|^2}{Z_{branch}} \tag{5.1}$$

The hand calculations were performed to determine if the MatPower implementation was done correctly. However, it could be concluded that hand calculations are less accurate approximation for several reasons. Due to the complexity, mistakes are easier to be committed. Furthermore, hand calculations use rougher approximations to converge for the power flows, since the threshold could be considered high for this project and the fact that the influence of other branches was not considered. However, both hand calculations and MatPower make use of iterative minimization. Concluding, MatPower is an open source-tool that gives more satisfactory solutions, as well as faster. Therefore, the system of this scale, 28 bus bars and 31 branches, are recommended to solve with MatPower or other algorithms available with low threshold and fast convergence. The $\Delta P/Q$ in Tab. 5.4 lied within the allowed limits. Hence, hand calculations are not a wrong approximation, were the system power flows solved completely by this methodology.

Table 5.4: Results for voltage profile and losses are compared for MatPower and hand calculations.

	V bus 23 (p.u.)	∠ bus 23 (degr.)	V bus 24 (p.u.)	∠ bus 24 (degr.)	Plosses br. 23-24 (MW)	Qlosses (MVAr) br. 23-24
MatPower	0.9776	18.5814	0.9801	19.2510	0.0607	0.3465
Hand	0.9679	16.1265	1.0157	19.0616	0.1925	1.0978

5.2. Test Models for operating conditions

After completing the implementation of the test models for each farm, the different test models are run and the results are analysed. During this analysis, the results for each farm are inspected to determine the satisfaction of the hypotheses made in Sec. 4.1.

Firstly, the 3-D plot is made by plotting the parameters of interest against each other. For every operating condition:

1. On the Y-axis: the active power losses/ reactive power losses.

2. On the X-axis: the reactive power demand

3. On the Z-axis: the average voltage magnitude of the system.

This plot is generated to prove whether the relationship described in Eq. 4.3 is satisfied. The same procedure is done for the reactive power losses to prove whether the relationship described in Eq. 4.4 is satisfied. Secondly, the losses on the Y-axis are replaced by reactive power injections. This plot is generated to prove whether the relationship described Eq. 4.6 is satisfied. Eventually, the relation between the setpoints Q and the average voltage of each dispatch is inspected.

5.2.1. Wind farm

Active and reactive power losses.   The test models for the wind farm were run for the three o.c., as described in Sec. 4.2. The result of this test is shown in Fig. 5.1. In Fig. 5.1, the quadratic relation is seen between the active power losses and voltages approximately centered around V = 1.0 p.u., as described in Eq. 4.3. This is satisfied for all wind speeds. The peak of the parabolas shown in Fig. 5.1 is defined as the voltage for which the active power losses reach minimal value. This is because the system is considered to be most stable when the average voltage is equal to the voltage of the slack node, i.e. 1 p.u. [35]. Ideally, this peak corresponds to the normal o.c. Hence, the PCC in Figs. 4.2, 4.3 will behave solely as a resistive element. In such a case, the reactive demand is 0 MVAr. Hence, the expected minima coordinates were $minima_{ideal}$ = [**minimum loss value   0   1**]. However, the power flows are not solved analytically, for which there is an unspecified insignificant margin of error for the final solution of Eq. 1.1. Therefore, the parabola is centered around other coordinates than initially expected. For the dispatches ran for v = 7.5 m/s, minima = [**0.02667   - 18.1   1.001**], for v = 14 m/s, minima = [**1.02   15.92   1.006**]. The width of the parabolas is reasonably wide. This compensates for this error, since the loss value for a reactive demand of 0 MVAr, its deviation for P ranges from $| 0.00346 |< \Delta P <| 0.004 | MW$. For Q this deviation ranges from
$| 0.14 |< \Delta Q <| 0.179 | MVAr$. Concluding, this deviation is so small that it can be neglected. The ideal coordinates can be assumed. Therefore, it can be concluded that for each o.c. setpoints of Q = 0 MVar result in the lowest losses.

Fig. 5.1 depicts that the higher the available reactive power generation and subsequently, allowable total reactive power demand, the more the graph is extended for certain wind speed. For the nominal wind speed v = 7.5 m/s, the graph is the most extended, since Fig. 3.4 shows that the strings generate maximum reactive power. Using Fig. 3.4, for v = 14 m/s reactive power generation is less and for v = 14 m/s the least. Concluding, the non-ideal capability curve explained in Subsec. 3.2.2 was implemented correctly, improving the accuracy of the model.

Fig. 5.1 shows that the higher the active power generation (e.g. the higher the wind speeds), the higher the active power losses. This satisfies Ohm's law described in Eq. 4.2, since higher active power generation results in higher currents, which give rise to higher losses in the branches. The exact numbers are shown in Tab. 5.6. Furthermore, for normal and high o.c. Fig. 5.1 shows that voltages lower than 1.0 p.u. result in higher losses than voltages higher than 1.0. p.u. Eq. 4.2 clarifies this observation. For a constant impedance, voltages higher than 1.0 p.u. result in lower currents. Therefore, the active power losses will be lower. As higher wind

speeds will cause a higher power flow, which will lead to a higher current, this influence becomes larger for higher wind speeds as shown in Fig. 5.1. On the other hand, low wind speeds will cause such a low power flow that the influence of the difference in active power losses between V_{max} and V_{min} is negligible as shown in Tab. 5.5. In conclusion, the influence of higher power flow on the losses is only satisfied for the normal and high o.c..

An interesting observation made in the result was that for the nominal wind speed, the parabolic relation seems to be most symmetric. A Q demand of the same value, but an opposite sign will cause approximately the same amount of P/Q losses. This is seen by the highest and lowest X-values of the blue graph in Fig. 5.1. This is not satisfied by the extreme wind speeds. However, for low wind speeds, it can be neglected due to the minimalist magnitude of the losses. As explained in the paragraph above, Eq. 4.2 will cause higher losses for low voltage profiles. Therefore, the relation between voltage and P is symmetric, but does not extend equally. A similar positive or negative power demand causes an equal deviation from the V_{slack} for the voltage, but this voltage will cause higher losses if it is below V_{slack}. The reason for this symmetry solely for nominal wind speed cannot be explained. One possible explanation could be that the nominal wind speed is not generating enough active power to make a significant difference in the current generation between positive and negative Q demands, to depict a difference in power loss for lower or higher voltage profiles.

Finally, the P_{loss} and Q_{loss} of the branches are compared in order to justify the hypothesis made in Sec. 4.1. The values in Tab. 5.7 are obtained from Figs. 5.1 and App. A.20. From these values can be concluded that the hypothesis made in Sec. 4.1 is indeed justified. The Q_{loss} are significantly higher than the P_{loss} as shown in Tab. 5.7.

Table 5.5: Difference in active power losses between V_{max} and V_{min} for each o.c. expressed in MW

Operating condition	$P_{loss_{V_{min}}}$ - $P_{loss_{V_{max}}}$ [MW]
Low generation (4 m/s)	-0.027303
Nominal generation (7.5 m/s)	0.0311
High generation (14 m/s)	0.155

Table 5.6: Active power losses for different operating conditions expressed in MW

Operating condition	Maximum active power losses [MW]
Low generation (4 m/s)	0.03588
Nominal generation (7.5 m/s)	0.5019
High generation (14 m/s)	1.269

Table 5.7: Maximum active and reactive power losses for each o.c.. This overview visualizes the fact that higher wind speeds, e.g. higher generation, give rise to higher active power losses as well as reactive power losses.

O.c.	Max. P losses (MW)	Max. Q losses (MVAr)
Low generation (4 m/s)	0.03588	1.775
Nominal generation (7.5 m/s)	0.5019	22.42
High generation (14 m/s)	1.269	50.47

Reactive power injections. From the result of Fig. 5.2, a negative linear relation is seen for the three wind speeds, between the voltage magnitude and total reactive injected power. The droop relation described by Eq. 4.6, predicts this behavior. Furthermore, it is not possible to make a differentiation between the Q-relation for three different wind speeds. This satisfies the hypotheses made in Sec. 4.1, which was explained by the fact that the droop coefficient R_u does not change for different wind speeds. This coefficient changes if the system configuration changes. Hence, it will change for solar and hybrid farm results. Additionally, the hypotheses based on Eq. 4.6 stated that the higher the allowable range of reactive power demand, the more the relationship is extended between voltage and injection. This is seen in Fig. 5.2 since the blue graph, for nominal wind speed and thus highest Q_{range} extends the most compared to a smaller extension for the red
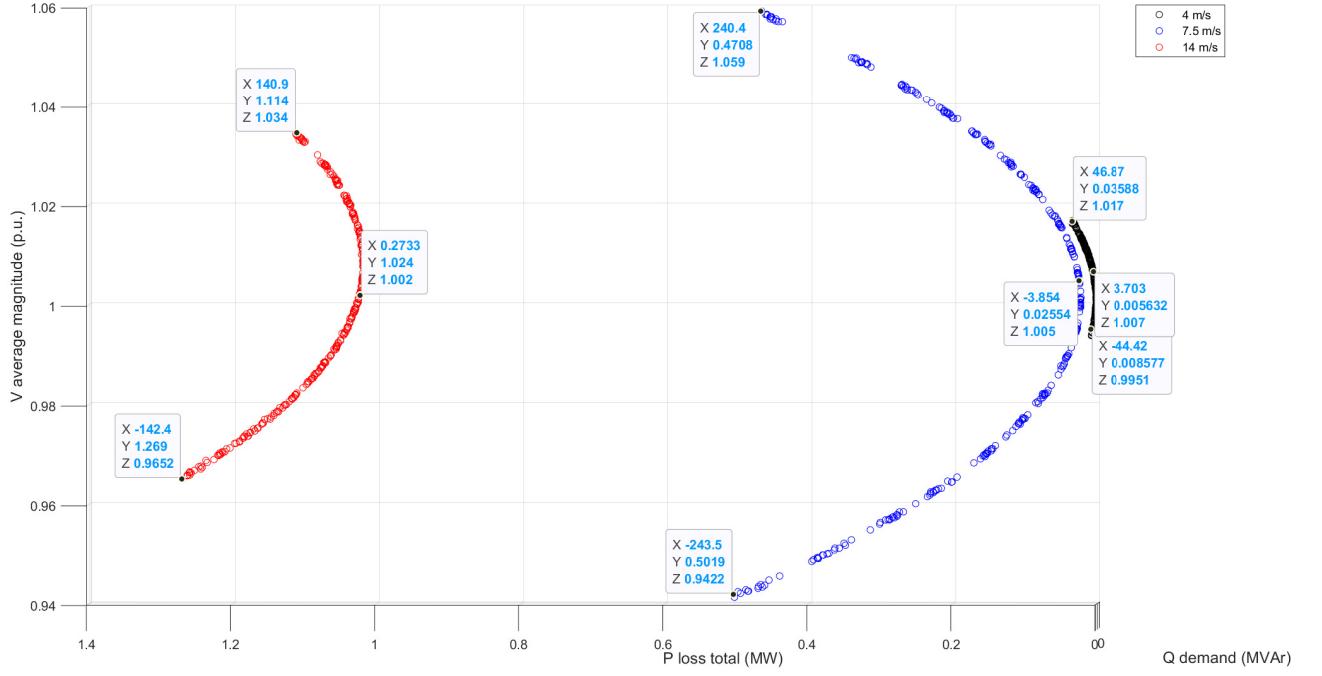
Figure 5.1: 3-D plot of the relation of the average voltage magnitude (p.u.), active power losses and random Q demands for the wind farm. This plot is generated in order to show the relations in a clear and visualizable manner. In this plot the relation of the average voltage magnitudes (p.u.) and the active power losses is emphasized.

graph, i.e. 14 m/s and the smallest extension for the black graph, i.e. 4 m/s. The difference between extension for 4 m/s and 7.5 m/s is reasonably small. The max and min for 4 m/s are 38.32 MVAr and 36.69 MVAr. While for 7.5 m/s this is 39.63 MVAr and 34.72 MVAr. The generation for reactive power is highest for 7.5 m/s. If the reactive power generation had an influence on the injection, the graph would be most extended for this wind speed. However, from Eqs. 3.5, 3.6, the active power generation increases for an increase in wind speed. In conclusion, in a linear relation, the higher the active power flow through the system, the higher the reactive power injections. Lastly, it should be noted that the injections made in the systems are reasonably high if a maximum demand of 240 MVAr is made in the system. Therefore, it will be interesting to inspect the components responsible for such behavior.

Reactive power demand.   In Fig. 5.3 the relation is seen between voltage and reactive power demand from the PCC. The same relation is seen when analysing the 3-D relation plot for reactive power losses. This relation can be described as a positive linear dependence between voltage and power demand. Eq. 4.7 describes an exponential load model [33]. Using Eq. 4.7 with a k_{qu}, it could be derived that the relation shown in Fig. 5.3 describes a constant current load. Since further definition of this term is not part of the scope of this project, the reader is advised to study [33] for a deepened explanation about the exponential load model concept.

Losses in the system.   Since the reactive power losses and injections in the system are relatively high compared to the active power losses, it was decided to inspect which components are responsible for this behavior of the system. It can be seen from Fig. 5.4 that most losses are formed at branches 1, 4 and 5. The equivalent branch bus indication are branches 1-2, 3-4 and 5-6. From App. A.3, this is the branch to the PCC and the branches model for the reactance of the two main transformers. There are several reasons the highest losses are formed at these branches. Firstly, the reactance of the transformers is 0.0625 p.u., which is very high compared to other branches of the system. Secondly, these three branches deal with the highest power flows in the system, using Eq. 4.2, causing more losses. The branch will always pass the total active and reactive power generation of the system to the PCC. In conclusion, if an accurate model is desired, the effects of the transformer losses should be inspected for different test conditions.
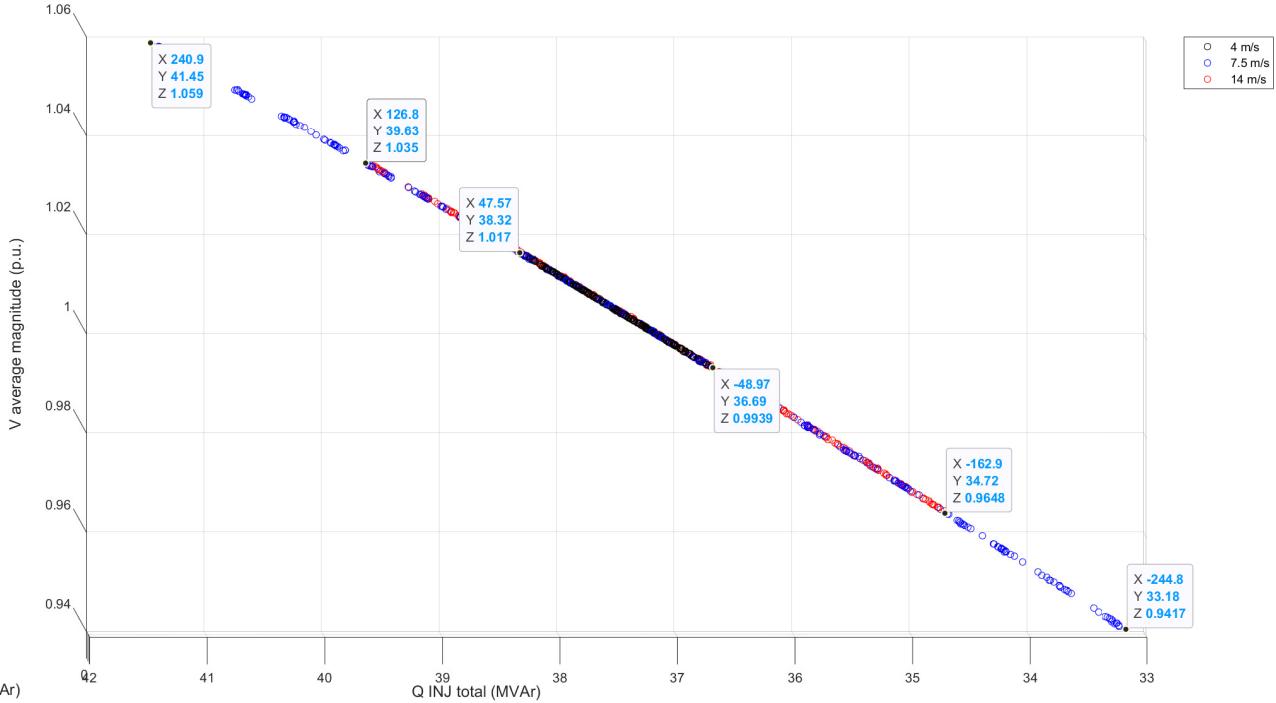
Figure 5.2: 3-D plot of the relation of the average voltage magnitude (p.u.), the sum of the reactive power injections of the branches and random Q demands for the wind farm. This plot is generated in order to show the relations in a clear and visualizable manner. In this plot the relation of the average voltage magnitudes (p.u.) and sum of the reactive power injections is emphasized.

5.2.2. Shunt reactor on wind farm

When the shunt reactor is connected, the WTG strings will receive the same reactive power setpoints. However, an additional -12 MVAr is generated by the shunt reactor and delivered to the PCC, making the reactive power delivered to the PCC more negative. Because of this negative addition of reactive power, the power factor will never be equal to 1, since the Eq. 4.1 if Q is unequal to 0 MVAr at all times. A lower power factor at the PCC, indicates that the behavior of the system will become more capacitive. Following the explanation given in Sec. 4.1, if the PCC behaves as a capacitive element, the average voltage magnitude is lowered. Furthermore, there will be an increase in reactive power losses.

The results are shown in App. A.27, A.28, A.29. The same relations seem to be satisfied as for the wind farm with the shunt disconnected. Therefore, the hypotheses of Sec. 4.1 will not be analysed for the system configuration. Solely, a comparison will be made between the shunt (dis)connection.

With the results plotted in App. A.27, A.28, it can be concluded that the voltage is indeed lowered. Two similar Q demands are used as reference points to analyse the system behavior for shunt disconnected and connected, namely 3-D sample 1 connected = [**-243.5   0.5019   0.9422**] and 3-D sample 1 disconnected = [**-242.5   0.5153   0.9361**]. However, the voltage difference is so small for similar Q demands made to the two system configurations, namely $\Delta V = 0.0056 p.u.$, that it could be considered to be negligible. The same is concluded for the active power losses behavior to be negligible, since $\Delta P = 0.0134 MW$.

In App. A.28, the difference in reactive power losses cannot be neglected anymore. Again, two sample points are used as a reference. 3-D sample 2 connected = [**-242.4   22.08   0.9425**] and 3-D sample 2 disconnected = [**-242.5   24.37   0.9361**]. $\Delta Q = 2.29 MVAr$, making the difference caused by the shunt necessary to take into account. If this is neglected for reactive power losses, there is the possibility that the wrong optimization setpoints are calculated.

The voltage- injection relation with the shunt connected in App. A.29, seems to be reasonably the same as the voltage-injection for the shunt disconnected Fig. 5.2. This was not unexpected, since initially it was thought
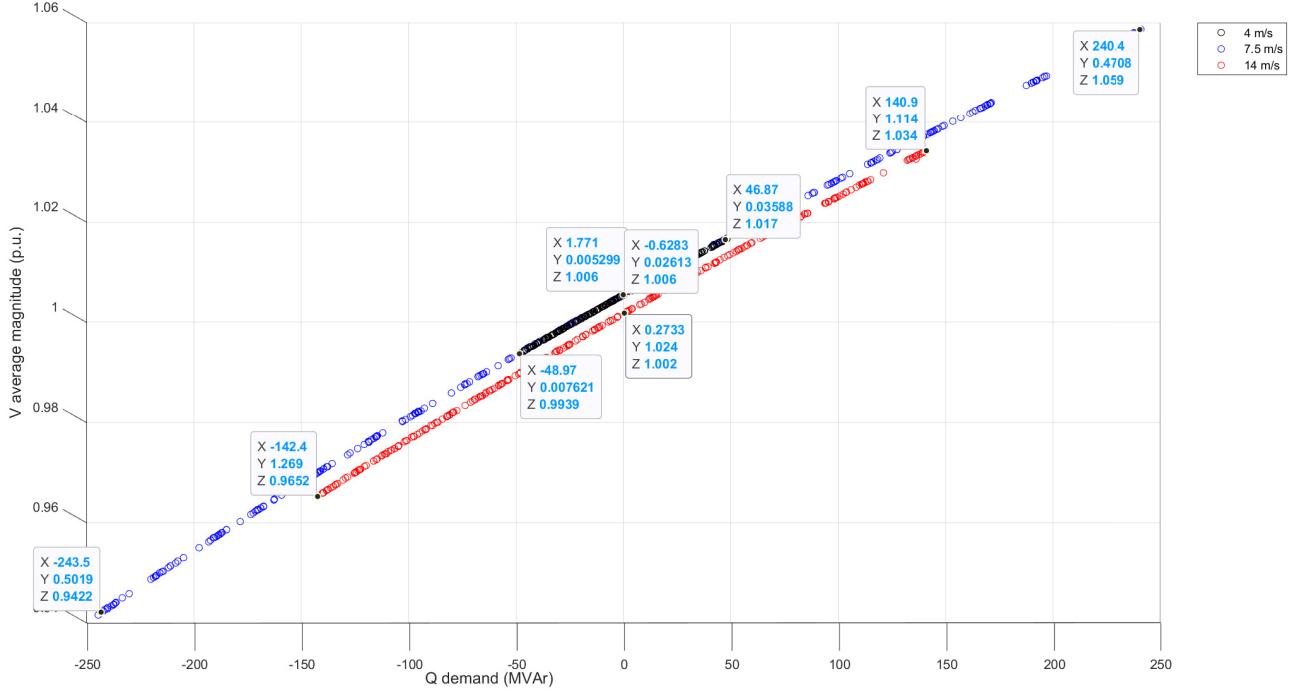
Figure 5.3: 3-D plot of the relation of the average voltage magnitude (p.u.), active power losses and random Q demands for the wind farm. This plot is generated in order to show the relations in a clear and visualizable manner. In this plot the relation of the average voltage magnitudes (p.u.) and the random Q demands is emphasized.

that the droop coefficient changes for every update of the system configuration [32]. If it is analysed, what exactly makes the voltage-injection relation to change, it is the active power flow that influences this. The shunt reactor solely provides negative reactive power to the system. Hence, the active power flow is not of influence, since the linear relation is relatively the same.

5.2.3. Solar farm

In App. A.7.7, the data of the test models designed for the solar irradiances of Tab. 4.3, is processed and its results are plotted. The most important sample points are shown in Tab. 5.8. The data indicate that the effect the solar farm has on the system behavior is minimal. The average voltage magnitude barely deviates from the slack node voltage of 1 p.u., which indicates the power flows are so small, that the system is considered to be stable. In addition, because of this small voltage difference, using Eqs. 4.4, 4.3, the losses are very small. The results prove this estimation to be correct. On the other hand, the results indicate that the losses are higher for voltage magnitudes above 1 p.u. While the hypotheses predicted higher losses for voltage magnitudes below 1 p.u. The explanation for this, is that although this is contrary to the expected, the losses are of such magnitude, that the difference is negligible. Because of this small difference, the results are not sufficient to disprove the hypotheses. Furthermore, the hypotheses are satisfied for the wind farm and hybrid farm, which cause more fluctuations in the system behaviour for different generations.

The relations for losses and injections explained in Sec. 4.1 are satisfied. In conclusion, the system behavior is very stable with the implementation of the solar farm. Therefore, the solar farm can be combined with the wind farm, without a negative effect on the system behavior. The expectation is that the hybrid farm will not lead to violation of system constraints if the wind farm did not cause this behavior already. This discussion is elaborated in Subsec. 5.2.4.

5.2.4. Hybrid farm

Active and reactive power losses. The test models were run for the hybrid farm in the same way as they were run for the wind farm as described in Sec. 4.2. It was expected that for the hybrid farm the same 3-D will be visible as shown and elaborated for the wind farm, described in Subsec. 5.2.1. However, the active
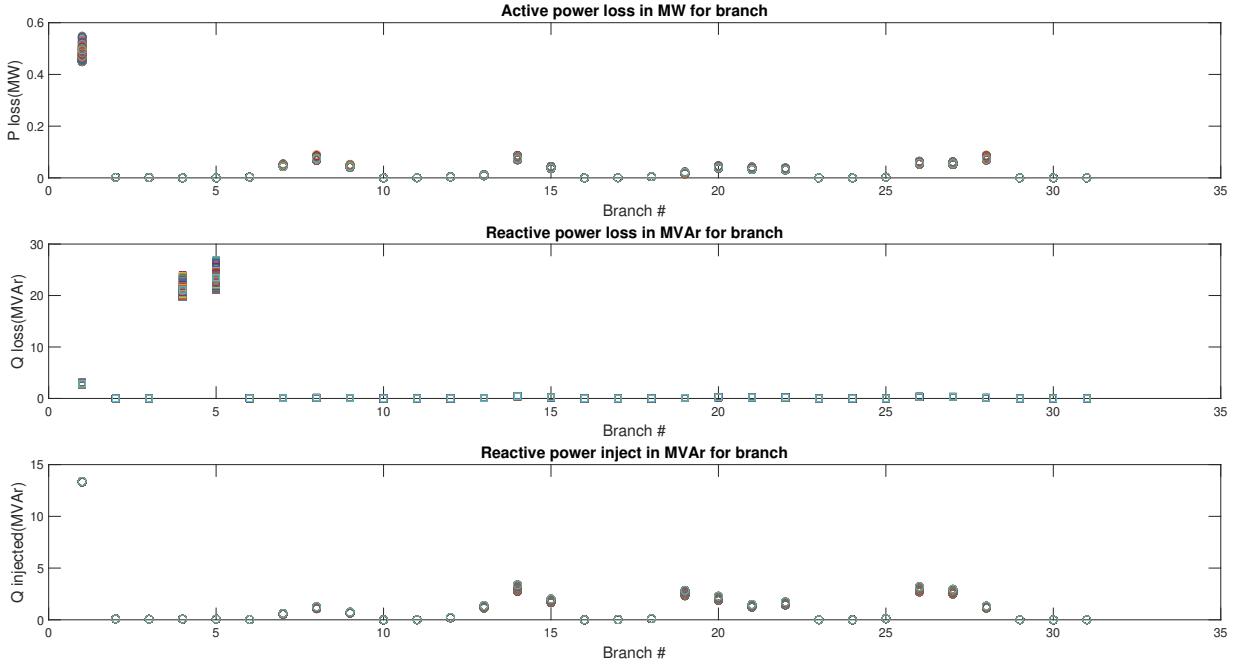
Figure 5.4: Active, reactive, injective losses in the each branch of the wind farm system with a wind speed of 14 m/s. The 2 busses connected to the specified branch are shown in App. A.16.

Table 5.8: The maximum and minimum of every average voltage magnitude for every o.c. with the active power losses, reactive power losses and reactive power injections belonging to these voltages. These results correspond to the solar farm visualized in App.A.7.7.

	V max.(p.u.)	Ploss (MW)	Qloss (MVAr)	Qinj (MVAr)	V min (p.u.)	Ploss (MW)	Qloss (MVAr)	Qinj (MVAr)
Irr.100 W/m2	1.001	0.002102	0.05042	19.46	1	0.0009225	0.01844	19.43
Irr.500 W/m2	1.002	0.01903	0.4438	19.49	0.9995	0.01575	0.3508	19.4
Irr.800 W/m2	1.003	0.045	1.044	19.52	0.9987	0.4098	0.9209	19.37

power generation in each o.c. will be higher for the hybrid farm, since additional power is generated by the photovoltaic strings. App. A.40 visualizes indeed the same relation as shown in Fig. 5.1 for the wind farm. However, as illustrated by Tab. 5.9, there is a significant difference in the number of losses. Since the power generation for the hybrid farm is higher than that of the wind farm, both the active and reactive power losses will be higher. The exact values are shown in Tab. 5.9. Furthermore, Fig. 5.1 and Tab. 5.9 show that the higher the generation, the difference between the losses of each farm. These results are in line with the hypotheses made in Sec. 4.1.

From Tab. 5.10, it can be seen that the boundary voltage magnitudes increase for maximum and minimum voltage magnitudes. Firstly, the available reactive power is higher for the hybrid farm, since both wind and solar farm deliver their reactive capacity. Because of this availability, the PCC can make higher reactive power requests, having a more capacitive or inductive behavior shown in Figs. 4.3, 4.2. Therefore, the voltage minimum and maximum increase according to Sec. 4.1.

Table 5.9: Overview of the active and reactive power losses comparison of the wind and hybrid farm for each o.c..

O.c.	$Ploss_{max}$ W.F. (MW)	$Ploss_{max}$ H.F. (MW)	$Qloss_{max}$ W.F. (MVAr)	$Qloss_{max}$ H.F. (MVAr)
Low gen. (4 m/s)	0.03588	0.04188	1.775	2.207
Nominal gen. (7.5 m/s)	0.5019	0.5266	22.69	25.72
High gen. (14 m/s)	1.269	1.481	56.84	72.5

Table 5.10: Comparison of Aggregated model wind and hybrid farm boundary voltage magnitudes. Column 1 indicates the wind operating conditions. W.F. are the losses and injections for the wind farm. H.F. is the same hybrid farm.

O.c.	V_{max} W.F. (p.u.)	V_{max} H.F. (p.u.)	V_{min} W.F. (p.u.)	V_{min} H.F. (p.u.)
Low gen. (4 m/s)	1.017	1.022	0.9939	0.9941
Nominal gen. (7.5 m/s)	1.097	1.074	0.9422	0.9292
High gen. (14 m/s)	1.072	1.046	0.9652	0.9506

Reactive power injections   For the reactive power injections, it was expected that the same linear relation will hold as shown in Fig. 5.2 for the wind farm and as explained in Eq. 4.6. As shown in App. A.41, this linear relation also holds for the hybrid farm. However, the maximum injected reactive power for the hybrid farm is significantly higher than that of the wind farm as shown in Tab. 5.11. This is in line with Eq. 4.6, since a higher average voltage magnitude in the hybrid farm results in a larger maximum injected reactive power. The linear line shown in Fig. 5.2 is extended in App. A.41.

Table 5.11: Maximum reactive power injections for the wind and hybrid farm.

Farm	Maximum reactive power injection (MVAr)
Wind farm	41.45
Hybrid farm	47.97

5.2.5. String level
The test models of the wind farm on string level are expected to visualize the same relations as described in Subsec. 5.2.1. However, for string level modeling losses in the string are taken into account as described in Subsec. 3.2.1, while being neglected in the aggregated model. Expected is this will result in higher active and reactive power losses. The results of the string level modeling and testing are shown in App. A.48. App. A.48 visualizes the same relations derived from the simplified model shown in Fig. 5.1. Hence, the hypotheses of Sec. A.19 are satisfied for a more complex model of the transmission system. What can already be noticed, is that the power losses and injections are higher compared to the wind farm aggregated model, as expected. In Tab. 5.12, the results are put next to each other and analysed. For low wind speed, the difference is not significant, but rather noticeable by a $\Delta P_{loss} = 0.9422 MW$ and $\Delta Q_{loss} = 1.6449 MVAr$. With increasing wind speeds this difference becomes significant, especially for the active power losses. For a high generation, the total active power losses become approximately 11 times higher compared to the aggregated model. When the aggregated model was used, the smallest diameter for a cable type was 1000 mm2. On string level, different cables are used, ranging from a diameter of 240-630 mm2. Tab. 3.2 indicates that this decrease in cross-sectional area results in a higher resistance. The same could be concluded from the basic Eq. 5.2, indicating a higher resistance for a smaller area. Using Eq. 4.5, one can conclude that this will result in higher system losses. Additionally, by inspection App. A.55 it can be seen that the branches in the strings cause more losses compared to the branches of Fig. 5.4, which are close to 0 MW, except for the PCC. The same conclusion is drawn for the reactive power losses. Furthermore, it is justified by the linear relation explained in Sec. 4.1.

$$R = \rho \frac{l}{A} \tag{5.2}$$

Table 5.12: Comparison of Aggregated model wind farm and String level model wind farm losses. Column 1 indicates the wind operating conditions. W.F. are the losses and injections for the aggregated model. String W.F. is the same for the string level model.

O.c.	$Ploss_{max}$ W.F. (MW)	$Ploss_{max}$ String W.F. (MW)	$Qloss_{max}$ W.F. (MVAr)	$Qloss_{max}$ String W.F. (MVAr)
Low gen. (4 m/s)	0.03588	0.1301	1.775	1.785
Nominal gen. (7.5 m/s)	0.5019	6.383	22.69	28.02
High gen. (14 m/s)	1.269	14.13	56.84	71.87

From Tab. 5.13, the boundary voltage magnitudes have increased for both symmetric sides from 1 p.u. The reactive power demands are the same for both models. However, due to an increase in losses caused by the increase in branches, the system will be less stable when trying to satisfy the load demand. Therefore, the voltages will have a higher ΔV difference compared to the slack node voltage of 1 p.u.

Table 5.13: Comparison of Aggregated model wind farm and String level model wind farm boundary voltage magnitudes. Column 1 indicates the wind operating conditions. W.F. are the losses and injections for the aggregated model. String W.F. is the same for the string level model.

O.c.	V_{max} W.F. (p.u.)	V_{max} String W.F. (p.u.)	V_{min} W.F. (p.u.)	V_{min} String W.F. (p.u.)
Low gen. (4 m/s)	1.017	1.025	0.9939	0.9995
Nominal gen. (7.5 m/s)	1.059	1.097	0.9422	0.9106
High gen. (14 m/s)	1.034	1.072	0.9652	0.9483

Tab. 5.14 indicate an increase in reactive power injection. This is expected if it is considered, that the amount of bus bars increase in the system configuration. With an increase in bus bars, the aggregation of reactive injection in the system will increase as well by 15.28 MVAr. In App. A.50, the droop coefficient of Eq. 4.6 is the same as to the aggregated model of Fig. 5.2. This could be derived from the direction coefficients in the graph. For both models this is approximately -0.015 p.u./MVAr. Further analysis shall be put to determine if this was expected, but for the sake of this project, it is not relevant to achieve the project objective.

Table 5.14: Maximum reactive power injections for the aggregated model and string level model.

Farm	Maximum reactive power injection (MVAr)
Wind farm	41.45
String level wind farm	56.73

5.3. Prototype

The test profiles are tested, for which the power flows are shown in App. A.8. The prototype shows that the system model works as expected, since the 17500 were run in order to find the optimal setpoints and the final setpoints yield a converging power flow within the physical boundaries of the system [6]. Although not noted in the Figs., no voltage violations were provoked by the optimal setpoints for the strings. From the Figs. in App. A.8 it can be seen that the highest reactive power losses occur at the transformers, as was already shown in Fig. A.55.

Furthermore, to find the optimal setpoints for the test profiles of Tab. 4.5, the shunt reactor had to be connected to the system configuration. Delivering exactly -12 MVAr to the system, this indicates that the system is constantly generating reactive power that shall be absorbed by the shunt reactor. Moreover, this explains why the safety branches between main bus bars are connected, i.e. to compensate active or reactive power generated in the system. This could be to compensate losses or prevent bus voltage violations or branch apparent power limits.

Note, the reactive power values delivered to the PCC are different to the requested power by the PCC indicated in Tab. 4.5. This is because the optimization algorithm has a higher weighting factor, i.e. more importance, to reduce the active power losses in the system. Therefore, in all occasions delivering the maximum active power possible [6].

6

Conclusion

The project aimed to design a trustworthy model, i.e. as accurate as possible, that can show the effects on the system behavior for different operating conditions. The different operating conditions vary from normal generation and load demand to an extremely low or high generation with extremely negative or positive load demands. The inspection of these conditions is desired, to determine if the requirements formulated at the PCC are satisfied. When this is not the case, the transmission system is not allowed to deliver power. This is unwanted and therefore avoided. Hence, if this model proves to satisfy this goal, it could be used by optimisation algorithms to determine actual optimal setpoints of the system configuration. In this manner, requirements are satisfied as frequently as possible. Additionally, with an accurate model, inspections could be made based on the model, concerning future expansion of the transmission system with an increase of RES.

It was required to design a PV system for the case study used. This PV would be designed based on two main criterias. Firstly, deliver slightly more apparent power allowed by the system configuration, i.e. considering the apparent power limits of components, in order to give the control scheme [4] the opportunity to come up with control solutions. Secondly, the implementation of this PV system has to be done in a realistic and rule-based manner. Eventually, the design has to result in stable power flows and not violate any voltage physical constraints.

For the project objectives to be achieved, general requirements were formulated in Chap. 2. If these are satisfied, the model will prove to be trustworthy. Subsequently, the system model had to update the system parameters after every setpoints/ dispatch generation iteration. After each update, power flows are run according to the procedure explained in Fig. 4.1, to determine for which combination of parameters, e.g. WTG apparent power generation, reactive power demands by PCC, shunt connection status, the physical constraints of the system are violated. In addition, the power losses and injections are calculated, since these are of importance for the optimal setpoint calculation. The original power losses serve as reference values for this calculation.

To show that the system is able to update itself and provide the information shown in Fig. 1.2 for every node system configuration, the prototype will consist of snapshots of the results after the power flow is ran for a combination of power generation and load demand. Then, this is done again after the system parameters are processed by the optimisation scheme [6]. The result of this optimal power flow is set next to the normal power flow, depicting the model's accuracy and optimisation algorithm's contribution to this calculation.

6.1. Conclusions
In the introduction, Chap. 1, the main problem was divided into smaller research questions. Firstly, to determine when system components were modeled correctly, the non-ideal characteristics were inspected. It was found that the transformer losses could be modeled by an equivalent leakage reactance. In addition, the active and reactive capability curves of the WTGs were considered. After implementing this behavior, the system was able to converge for power flows in nominal operating conditions of the wind farm. This is

as expected since the system configuration of the case study [24] was designed such it converges for nominal load demands and average (nominal) power generation. Furthermore, after comparing with the hand results, proving that the used tool for system modeling is accurate with maximum allowed power mismatch of 1e-4 p.u., or 0.01 MW/MVAr. For nominal load demands with a reactive power Q ≈ 0 MVAr, the average voltage magnitude was close to 1 p.u., i.e. the voltage of the slack node (PCC). If the demand is zero, the PCC does not behave as a reactive element. Therefore, the voltage magnitude of the left terminal (system configuration) and the right terminal (PCC) of the reactance model of Fig. 4.3 are equal. In conclusion, the basic characteristics were modeled correctly.

The non-ideal components' behavior was modeled to inspect a difference in power generation and losses. This is indeed the case, based on the reactive power generation range for wind speeds. According to the capability curve of Fig. 3.4, for high wind speeds, i.e. above 14 m/s, the reactive power of the system would become lower than for nominal wind speeds in the range of 7-14 m/s. The wind farm results show that for a wind speed of 14 m/s, the wind farm produces Q ≈ 140 MVAr, compared to Q ≈ 240 MVAr for nominal wind speed. Furthermore, the results of individual branches loss, show there is an increase of Q loss of ≈ 20 MVAr at the transformer branch and PCC branch, as expected considering the modeled leakage reactance and the length and cable type of the PCC branch. In conclusion, components are modeled correctly.

The relation held between voltage magnitudes and power losses seemed to satisfy Eqs. 4.3, 4.4. The Figs. of the 3-D relation plots, clearly showed a parabolic relation symmetric around the voltage of the slack node. With the results of the wind farm at nominal wind speed as an example, with a voltage higher than 1 p.u., active power losses would increase from 0.02554 MW (v = 1.005 p.u.) to 0.4708 MW (v = 1.059 p.u.). For reactive power losses this increased from 0.2571 MVAr to 22.42 MVAr . With a voltage lower than 1 p.u. the active and reactive power increases to 0.5019 MW and 22.69 MVAr(v = 0.9422 p.u.). This increase is caused by higher load demands up to the maximum generation of the strings. In conclusion, the difference in power loss between voltages higher or lower than the slack node voltage are insignificant compared to a power generation of ≈ 360 MW. For higher wind speeds, the difference in losses between voltages higher and lower than 1 p.u. becomes more notable since following from Ohm's Law lower voltages increase the losses in the system. For a wind speed of 14 m/s, the $\Delta P = 0.155 MW$ and $\Delta Q = 6.37 MVAr$. For the hybrid farm this difference is increased.

For the reactive injection losses, Eq. 4.6 indicates that the losses would decrease linearly for lower voltages. Fig. 5.2, for 7.5 m/s, this injection would decrease with a slope of -0.015 p.u./MVAr, i.e. -2e-3 MVAr/V, from 41.45 MVAr (v = 1.059 p.u.) to 33.18 MVAr (v = 0.9417 p.u.). This difference is significant in magnitude, making the availability of this relation for purposes of the control scheme important [4].

The relation between load demands and voltage magnitudes has a linearly increasing relation as shown for an exponential load model of Eq. 4.7. The slope coefficient is 0.125 MVAr/V. For a substation where the voltage can vary from $\approx 32 - 36 kV$, this relation is needed for control and optimisation schemes.

The relations between the parameters described above are influenced directly by the dispatch profiles. The effects of active power losses are analysed for three different wind speeds. A low wind speed of 4 m/s, generates 5 MW. Subsequently, it was expected to see the least amount of losses for low wind speed. The losses will increase with increasing wind speed since the power generation increase according to Eqs. 3.5, 3.6, up to $\approx 360 MW$. Using the wind farm as an example, if this reasoning is followed, the maximal active power losses for the wind speed increases from 0.03588 MW (4 m/s), to 0.5019 MW (7.5 m/s), to 1.269 MW (14 m/s) and for reactive loss from 1.775 MVAr (4 m/s), to 22.69 MVAr (7.5 m/s), to 56.84 MVAr (14 m/s). The same increase was seen for losses in the solar farm and hybrid with increasing wind speed and/or solar irradiance. In conclusion, the hypotheses made in Sec. 4.1 was correct.

The relation between voltage magnitudes and injection losses or load demands, seem to be independent from the dispatch profiles, since there is no change in the linear coefficient for different wind speeds. However, the graph of the injection or load demand is extended for nominal wind speed compared to other conditions, since reactive power generation is maximal in this case. Using Eq. 3.8, for the solar farm, the graph is extended according to increasing solar irradiance.

For an analysis between a change in system configuration the wind-, solar- and hybrid farm are compared. The same conclusion was derived as for the comparison of dispatch profiles. The solar farm produces 36 MW, $P_{loss} = 0.045 MW$ and $Q_{loss} = 1.044 MVAr$. The wind farm produces 363 MW $P_{loss} = 1.269 MW$ and $Q_{loss} = 56.84 MVAr$. The hybrid farm produces 399 MW $P_{loss} = 1.481 MW$ and $Q_{loss} = 72.5 MVAr$. In conclu-

sion, if the available power generation is higher, the apparent power losses increase. For a better overview of this behavior, see Tabs. 5.10.

Furthermore, the shunt reactor makes the total reactive power flow 12 MVAr more negative for all dispatches. The wind farm with a nominal wind speed dispatch is used as example. The voltage profile is lowered by $\approx \Delta V = 0.0056 p.u.$. Subsequently, the maximum losses increase with $\Delta P = 0.0134 MW$ and $\Delta Q = 2.29 MVAr$. This difference caused by the shunt shall be taken into account. If this is neglected for reactive power losses, there is the possibility that the wrong optimisation setpoints are calculated.

Eventually, the analysis of the aforementioned parameters for the modeling of the WTG farm on string level resulted indeed in an improved model. For the aggregated wind farm under normal o.c., $P_{loss_{max}} = 0.5019 MW$ and $Q_{loss_{max}} = 22.69 MVAr$, while for the string level farm $P_{loss_{max}} = 6.383$ MW and $Q_{loss_{max}} = 28.02 MVAr$. Moreover, the relations of the aforementioned parameters still hold. These results show that active power losses differ significantly, which can give different results concerning the satisfaction of the requirements at the PCC. In conclusion, modeling on string levels resulted in a more accurate and useful model.

From the results in Chap. 5, it can be concluded that the system is relatively stable. For each of the farms, none of the busses violate voltage constraints, i.e. lower than 0.8576 p.u. or higher than 1.1424 p.u. Moreover, no violations are made at the cables, since the apparent power flows are lower than the cable ratings. This makes the future expansion of the system configuration with additional PV or WTG strings feasible. There is no violations of the system constraints, i.e. cable ratings or voltage limits to the input of the transformer. In conclusion, the model on string level can be considered trustworthy for the use of power control at the PCC and serves as a reference model for future expansion. Mandatory requirements are satisfied such that the system meets the functional requirements formulated. The project objective has been satisfied. However, several problems were encountered. Mainly, there were concerns about which system parameters require more testing models to determine its effects on the system behavior. This is discussed further in Sec. 6.2.

6.2. Recommendations

6.2.1. Discussion
During the research interesting remarks were made about procedures and results. The following points should be taken into account when carrying out when modeling the power flows:

- When extreme conditions are being tested, probabilistic distributions do not have to be necessarily implemented, but can rather be used to check whether the extreme conditions can be satisfied.

- The cables have to be modeled accurately in order to have meaningful power flows. Branches, which are not modeled accurately will result in high losses and extreme voltage violations.

6.2.2. Points for future research
For future research, it is recommended to inspect the losses caused by the transformers in the system. The transformers significantly generate more losses than the other components in the system, seen in Fig. 5.4 as branches 4 and 5. If a more accurate model is desired, its effect should be analysed carefully. It could be the case, that a small change in the tap ratio in order to calculate optimal setpoints, yields high losses. Hence, making the system behavior sensitive and unreliable if not analysed. Furthermore, it is recommended to use a 3-winding transformer model rather than a 2-winding transformer to improve the accuracy for realistic system behavior. The reason the accuracy is improved by this, is because the transformer are responsible for the limitations in the system for voltage and power flow, making it the weakest component to take into consideration when modeling a similar transmission system.

Another component that is recommended to analyse more carefully, are the WTGs. Although, both aggregated model and individual WTG model are used for analysis, the capability curve used was static. However, this is not the case, since as explained in Subsec. 3.2.2, the capability curve is a function that changes of reactive power output with the voltage magnitude as the input parameter. For the individual WTG model this is a negligible effect, due to its small difference in reactive power output. When the aggregated model is used, this difference increases, making the difference significant. To future research it is recommended to analyse the effects this function for capability curve has on the complete system behavior.

Furthermore, research shall be put into the behavior of the remaining system components for normal and extreme operating conditions. This is not analysed during this project, but is particularly of interest, since it yields which components make the system more unstable or cause highest losses. By determining this beforehand, less power flows shall be run by the optimisation algorithm. Previously, this algorithm will run sufficient power flows to determine from which nodes the power flows should be reduced or increased to determine this optimal setpoint.

Bibliography

[1] L. Webb, "How has the renewable energy market changed in the last decade?." `https://www.nesgt.com/blog/2020/01/how-has-the-renewable-energy-market-changed-in-the-last-decade`, January 2020. Accessed on 2020-05-01.

[2] E. E. Agency, "Making clean renewable energy happen." `https://www.eea.europa.eu/signals/signals-2017/articles/making-clean-renewable-energy-happen`, November 2017. Accessed on 2020-05-10.

[3] I.Munteanu, *Optimal control of wind energy systems: towards a global approach.*

[4] D. Groenenberg and L. Beijnen, "Active- and reactive power control in a wind- and solar park," bsc graduation thesis, Delft University of Technology, July 2020.

[5] A. Etxegarai, P. Eguia, E. Torres, G. Buigues, and A. Iturregi, "Current procedures and practices on grid code compliance verification ofrenewable power generation," *Renewable and sustainable energy reviews*, February 2015.

[6] A. Neagu and J. Bai, "Design of an optimisation unit considering physical system boundaries and technical constraints," bsc graduation thesis, Delft University of Technology, July 2020.

[7] A. C. Tobar, E. Bullich-Massague, M. Arruages-Penalba, and O. Gomis-Bellmunt, "Reactive power capability analysis of a photovoltaic generator for large scale power plants," *5th IET International Conference on Renewable Power Generation (RPG)*, 2016. DOI: 10.1049/cp.2016.0574.

[8] A. Glimm and G. Stagg, "Automatic calculation of load flows," *AIEEE Transaction on Power Apparatus and Systems*, vol. 76, pp. 817–828, October 1957.

[9] W. Tinney and C. Hart, "Power flow solution by newton's method," *IEEE Transaction on Power Apparatus and Systems*, vol. PAS-86, no. 11, pp. 1449–1460, November 1967.

[10] S. Conti and S. Raiti, "Probabilistic load flow for distribution networks with photovoltaic generators part 1: Theoretical concepts and models," *International Conference on Clean Electrical Power*, May 2007. DOI: 10.1109/ICCEP.2007.384199.

[11] K. Divya and P. N. Rao, "Models for wind turbine generating systems and their application in load flow studies," *Electric Power Systems Research*, vol. 76, pp. 844–856, June 2006. DOI: 10.1016/j.epsr.2005.10.012.

[12] A. Abdelaziz, M. M. Othman, M. Ezzat, and A. Mahmoud, "A novel monte carlo based modeling strategy for wind based renewable energy sources," *Eighteenth International Middle East Power Systems Conference (MEPCON)*, December 2016. DOI: 10.1109/MEPCON.2016.7836897.

[13] Z.-S. Zhang, Y.-Z. Sun, J. Lin, L. Cheng, and G.-J. Li, "Versatile distribution of wind power output for a given forecast value," *IEEE Power and Energy Society General Meeting*, July 2012.

[14] K. Hagan and O. Oyebanjo, "A probabilistic forecasting model for accurate estimation of pv solar and wind power generation," *IEEE Power and Energy Conference at Illinois (PECI)*, February 2016.

[15] S. Walker, "Building mounted wind turbines and their suitability for the urban scale—a review of methods of estimating urban wind resource," *Energy and buildings*, August 2011.

[16] F. Mahmood, A. Resen, and A. Khamees, "Wind characteristic analysis based on weibull distribution of al-salman site, iraq," *Energy reports*, February 2020.

[17] N. Zulkilfi, N. Razali, M. Marsadek, and A. Ramasamy, "Probabilistic analysis of solar photovoltaic output based on historical data," *IEEE 8th International Power Engineering and Optimization Conference (PEOCO2014)*, March 2014.

[18] A. Etxegarai, P. Eguia, E. Torres, G. Buigues, and A. Iturregi, "Incorporation of probabilistic solar irradiance and normally distributed load for the assesment of atc," *8th International Conference on Computing, Communication and Networking Technologies (ICCCNT)*, July 2017.

[19] R. Ramakrishna, A. Scaglione, V. Vittal, E. Dall'Anese, and A. Bernstein, "A model for joint probabilistic forecast of solar photovoltaic power and outdoor temperature," *IEEE Transactions on Signal Processing*, vol. 67, no. 24, November 2019.

[20] P. Priyadharshini and M. M. T. Ansari, "Modeling and analysis of wind farms in load flow studies," *International Conference on Computation of Power, Energy, Information and Communication (ICCPEIC)*, April 2015. DOI: 10.1109/ICCPEIC.2015.7259482.

[21] A. E. Feijoo and J. Cidras, "Modeling and analysis of wind farms in the load flow analysis," *IEEE Transactions on Power Systems*, vol. 15, no. 1, February 2000. DOI:10.1109/ICCPEIC.2015.7259482.

[22] R. D. Zimmerman and C. Murillo-Sánchez, "Matpower user's manual," 2019.

[23] ██

[24] ██

[25] J. Conroy and R. Watson, "Aggregate modelling of wind farms containing full-converter wind turbine generators with permanent magnet synchronous machines: transient stability studies," *IET Renewable Power Generation*, vol. 3, no. 1, December 2008.

[26] T. kabel, "Power and signal cable 0,6/1 kv, pvc insulated and sheathed." `http://www.tim-kabel.hr/content/view/272/343/lang,english/`, 2020. Accessed on 2020-06-10.

[27] Sunpower, "Sunpower x-series." `https://us.sunpower.com/sunpower-x-series-x22-360-residential-solar-panel` September 2017. Accessed on 2020-05-05.

[28] ██

[29] ESIG, "Reactive power capability and interconnection requirements for pv and wind plants." `https://www.esig.energy/wiki-main-page/reactive-power-capability-and-interconnection-requirements-for-pv-and-wind-plants/`, 2020. Accessed on 2020-05-05.

[30] T. Delft, "Dutch pv portal." `https://www.tudelft.nl/en/eemcs/the-faculty/departments/electrical-sustainable-energy/photovoltaic-materials-and-devices/dutch-pv-portal/`, 2020. Accessed on 2020-05-05.

[31] S. International, "Solar power analysis and design specifications," 2017. Accessed on 2020-05-10.

[32] Y. Li, Z. Xu, J. Zhang, and K. Meng, "Variable droop voltage control for wind farm," *IEEE Transactions on Sustainable Energy*, vol. 9, no. 1, January 2018.

[33] W. group C4.605, *Modelling and aggregation of loads in flexible power networks.* 2014.

[34] K. Schoenmaker, "Functional design specification central wind farm controller," December 2019.

[35] B. L.Kunjumuhammed, S.Kuenzel, *Simulation of power system with renewables.* 2020.

A

Appendix

A.1. Group interaction
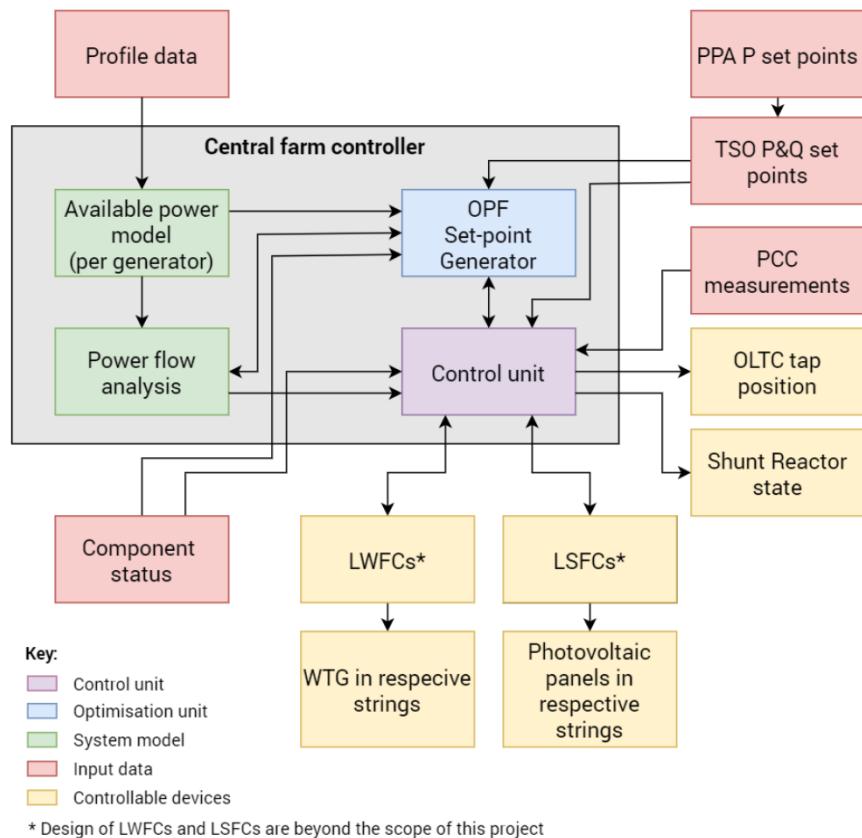
Figure A.1: Overview of interaction between the three components that together form the optimisation unit.

A.2. Transmission system configuration overview
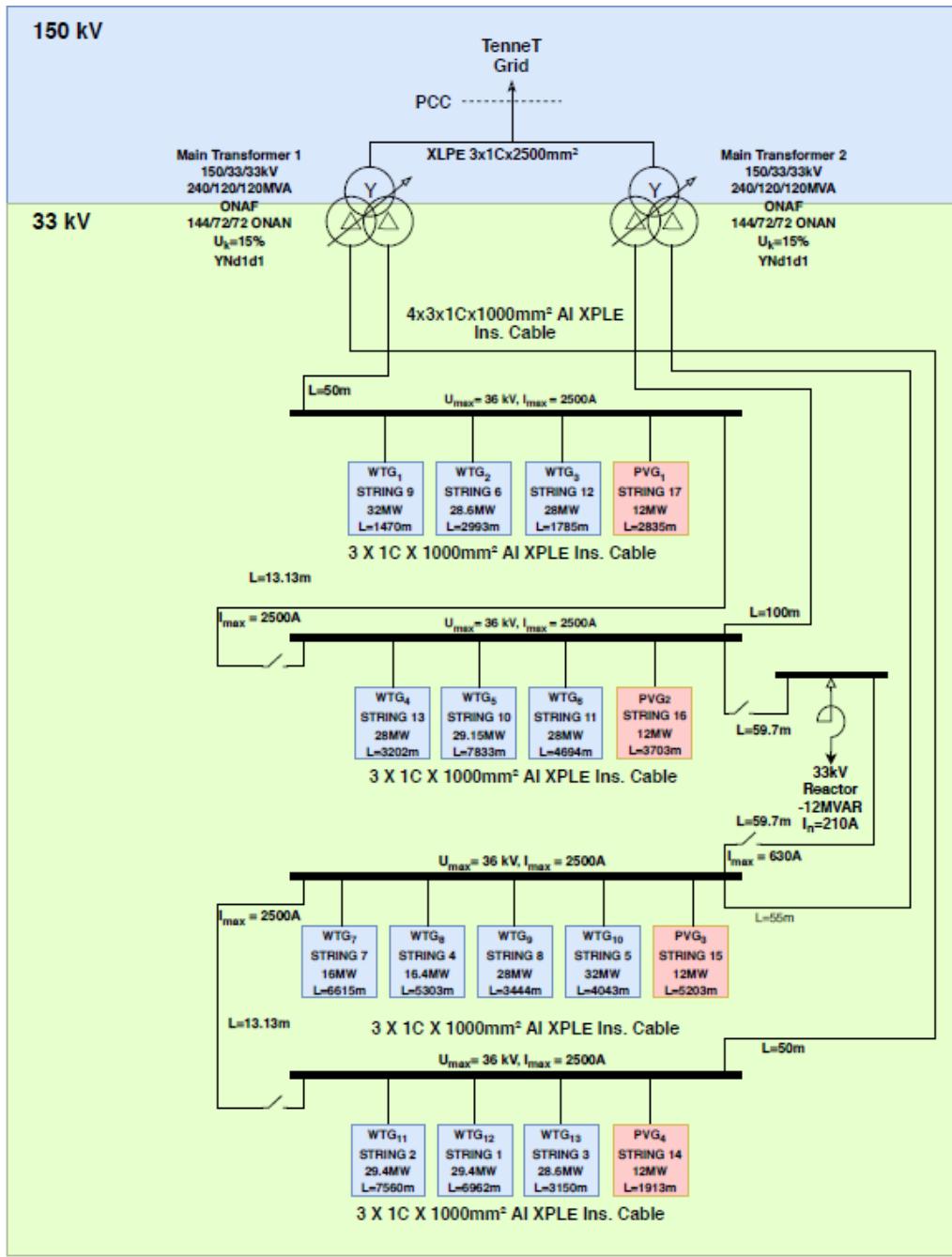
Figure A.2: Schematic of case system.
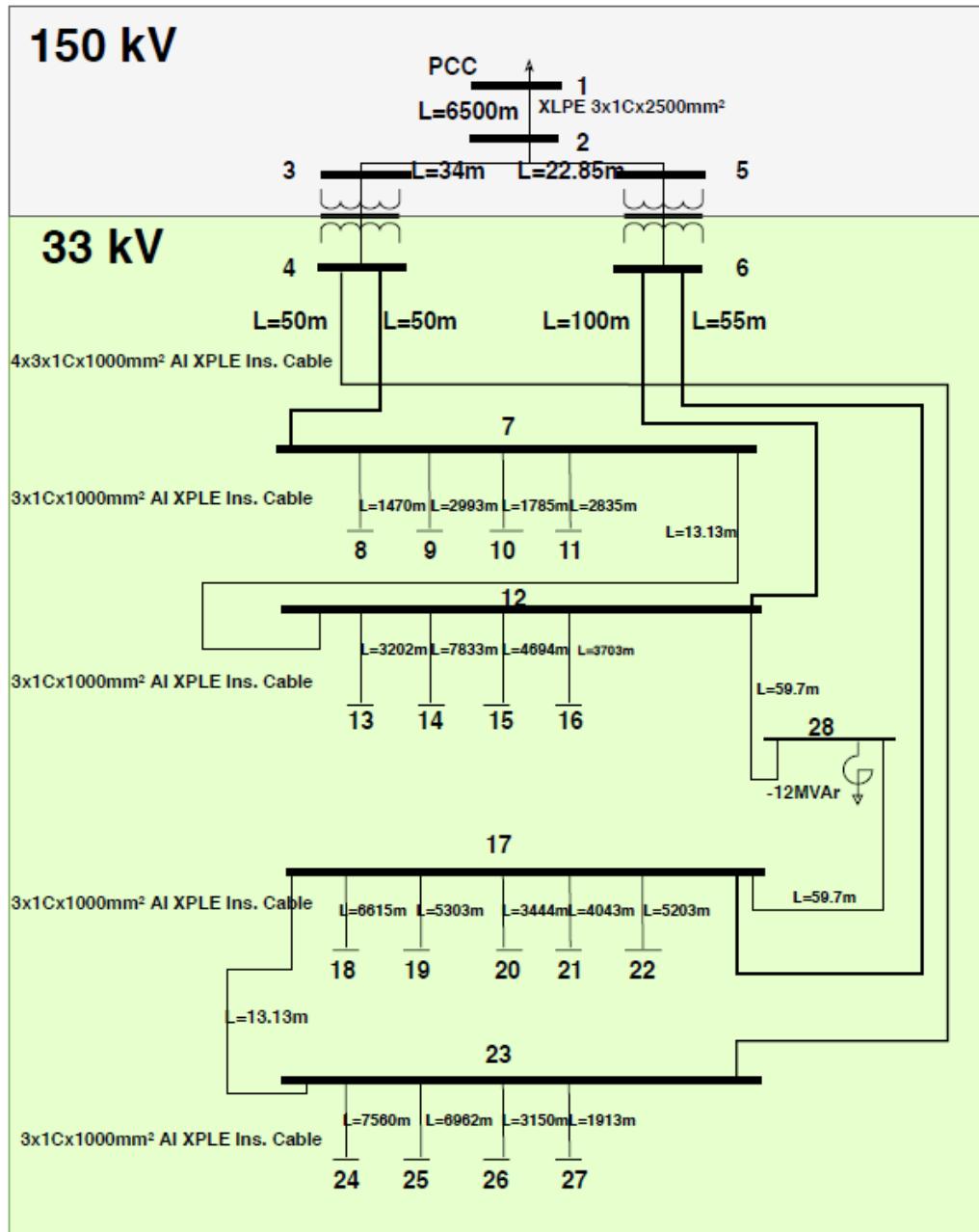
Figure A.3: Overview of case system used in MatPower. Bus numbers are specified and the length between the busses. Furthermore, the cable type for each section of branches.

A.3. Other overviews

String	Index	Address		WPZ Type	P_nom [kW]	P_string [MW]
Bus 25	1	A27-01	E-138	A	4200	
	2	A27-02	E-138	A	4200	
	3	A27-03	E-138	A	4200	
	4	A27-04	E-138	A	4200	29.4
	5	A27-05	E-138	A	4200	
	6	A27-06	E-138	A	4200	
	7	A27-07	E-138	A	4200	
Bus 24	8	A27-11	E-138	A	4200	
	9	A27-12	E-138	A	4200	
	10	A27-13	E-138	A	4200	
	11	A27-14	E-138	A	4200	29.4
	12	A27-15	E-138	A	4200	
	13	A27-16	E-138	A	4200	
	14	A27-17	E-138	A	4200	
Bus 26	15	A27-08	E-138	A	4200	
	16	A27-09	E-138	A	4200	
	17	A27-10	E-138	A	4200	
	18	ADW-05	E-115	C	4200	29.4
	19	ADW-06	E-115	C	4200	
	20	ADW-07	E-115	C	4200	
	21	ADW-08	E-115	C	4200	
Bus 19	22	ADW-01	E-138	A	4200	
	23	ADW-02	E-138	A	4200	16.8
	24	ADW-03	E-115	C	4200	
	25	ADW-04	E-115	C	4200	
Bus 21	26	ADW-11	E-126	B	4000	
	27	ADW-12	E-126	B	4000	
	28	ADW-13	E-126	B	4000	
	29	ADW-14	E-126	B	4000	32
	30	ADW-15	E-126	B	4000	
	31	ADW-16	E-126	B	4000	
	32	ADW-17	E-126	B	4000	
	33	ADW-18	E-126	B	4000	
Bus 9	34	ADO-01	E-138	A	4200	
	35	ADO-02	E-138	A	4200	
	36	ADO-03	E-138	A	4200	
	37	ADO-04	E-115	C	4200	29.4
	38	ADO-05	E-115	C	4200	
	39	ADO-06	E-115	C	4200	
	40	ADO-07	E-115	C	4200	
Bus 18	41	ADW-19	E-126	B	4000	
	42	ADW-20	E-126	B	4000	16
	43	ADO-20	E-126	B	4000	
	44	ADO-22	E-126	B	4000	

Figure A.4: Overview of different ███████ TG types connected to each string of the transmission system [23] [24].

Bus						
Bus 20	45	ADO-14	E-126	B	4000	
	46	ADO-15	E-126	B	4000	
	47	ADO-16	E-126	B	4000	
	48	ADO-17	E-126	B	4000	28
	49	ADO-18	E-126	B	4000	
	50	ADO-19	E-126	B	4000	
	51	ADO-21	E-126	B	4000	
Bus 8	52	ADO-08	E-115	C	4200	
	53	ADO-09	E-115	C	4200	
	54	ADO-10	E-115	C	4200	
	55	ADO-11	E-126	B	4000	33
	56	ADO-12	E-126	B	4000	
	57	ADO-13	E-126	B	4000	
	58	ADW-09	E-115	C	4200	
	59	ADW-10	E-115	C	4200	
Bus 14	60	SCH-01	E-103	D	2350	
	61	SCH-02	E-103	D	2350	
	62	SCH-03	E-103	D	2350	
	63	SCH-04	E-103	D	2350	
	64	SCH-05	E-103	D	2350	
	65	SCH-06	E-103	D	2350	29.15
	66	SCH-07	E-103	D	2350	
	67	SCH-08	E-103	D	2350	
	68	SCH-09	E-103	D	2350	
	69	LPT-11	E-126	B	4000	
	70	LPT-12	E-126	B	4000	
Bus 15	71	LPT-04	E-126	B	4000	
	72	LPT-05	E-126	B	4000	
	73	LPT-06	E-126	B	4000	
	74	LPT-07	E-126	B	4000	28
	75	LPT-08	E-126	B	4000	
	76	LPT-09	E-126	B	4000	
	77	LPT-10	E-126	B	4000	
Bus 10	78	LPT-03	E-126	B	4000	
	79	RDT-08	E-115	C	4200	
	80	RDT-09	E-115	C	4200	
	81	RDT-10	E-115	C	4200	28.8
	82	RDT-11	E-126	B	4000	
	83	RDT-12	E-126	B	4000	
	84	RDT-13	E-115	C	4200	
Bus 13	85	RDT-01	E-126	B	4000	
	86	RDT-02	E-126	B	4000	
	87	RDT-03	E-126	B	4000	
	88	RDT-04	E-115	C	4200	28.8
	89	RDT-05	E-115	C	4200	
	90	RDT-06	E-115	C	4200	
	91	RDT-07	E-115	C	4200	
					Total	**Total**
					358.15	358.15

Figure A.5: Overview of different ▮▮▮▮ TG types connected to each string of the transmission system [23] [24].

A.4. Cable modeling

A.4.1. Cable configurations
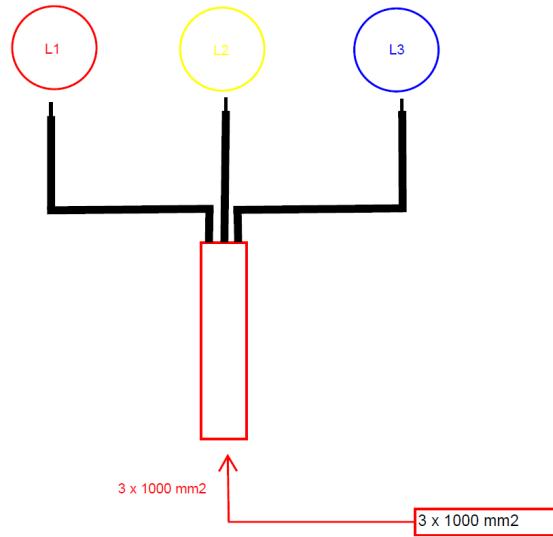
Figure A.6: Cable configuration for a 3x1000mm2 XLPE Al cable. Data from [23].
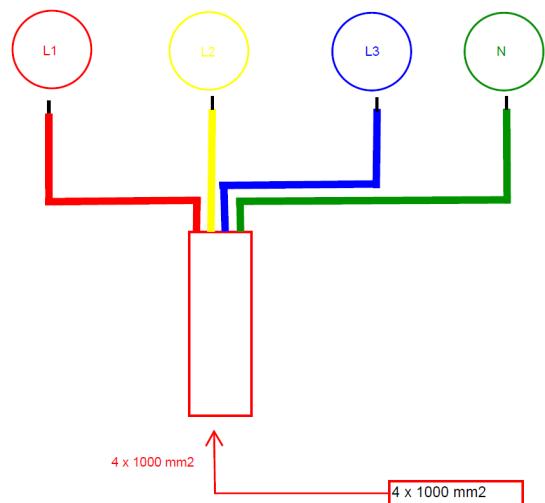
Figure A.7: Cable configuration for a 4x1000mm2 XLPE Al cable. Data from [23].
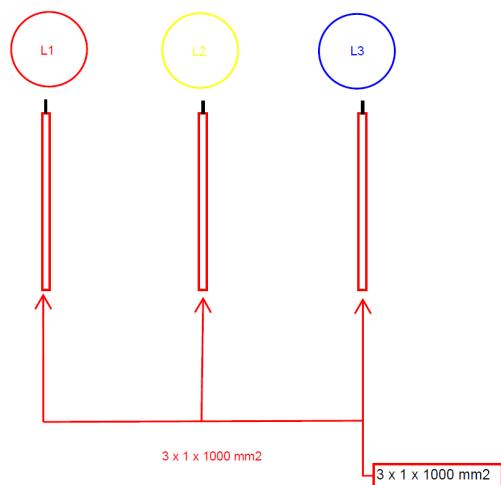
Figure A.8: Cable configuration for a 3x1x1000mm2 XLPE Al cable. Data from [23].

A.4.2. Branch calculations

Power Base(MVA)	100
Frequency (rad/s)	314.1592654 2 * pi * 50
Schematics	
- Visual	https://app.diagrams.net/#G19lkrn58XQq1Cf3l2TUfGfg6DbHJpP-a03
- Configuration	https://app.diagrams.net/#G1soRX8OS1u6B6LxdbMUrvngw27k8BDYeG

Branch	Vbase(kV)	Zbase(Ohm)	Zreal (Ohm/km)	Zim(Ohm/km)	C(e-6* F/km)	Length (km)	Zreal(Ohm)	Zim(Ohm)	Bs(e-6* Siemens)	Zreal (p.u.)	Zim (p.u.)	Bs (p.u.)	Rate (MVA)
1-2	150	225	0.0119	0.06788	0.29	6.5	0.07735	0.44122	592.1902153	0.0003437777	0.0019609777	0.1332427984	400
2-3	150	225	0.0356	0.101	0.366	0.034	0.0012104	0.003434	3.909397899	0.0000053795	0.0001526222	0.0008796145	400
2-5	150	225	0.0356	0.101	0.366	0.02285	0.00081346	0.00230785	2.627345352	0.0000036153	0.0001025711	0.0005911527	400
3-4	33	10.89			0.2025	0	0	0	63.61725124	0	0.0625	0.0006927918	240
5-6	33	10.89			0.2025	0	0	0	63.61725124	0	0.0625	0.0006927918	240
4-7	33	10.89	0.007275	0.0415	1.52	0.05	0.00036375	0.002075	23.87610417	0.0000334022	0.0001905417	0.0002600107	185.19
7-8	33	10.89	0.0291	0.166	0.38	1.47	0.042777	0.08134	526.468097	0.0039280991	0.0074692378	0.0057332375	46.2977
7-9	33	10.89	0.0291	0.166	0.38	2.993	0.0870963	0.1656126667	1071.917697	0.0079978236	0.0152077747	0.0116731837	46.2977
7-10	33	10.89	0.0291	0.166	0.38	1.785	0.0519435	0.09877	639.2826892	0.0047698347	0.0090697887	0.0069617884	46.2977
7-11	33	10.89	0.0291	0.166	0.38	2.835	0.0824985	0.15687	1015.33133	0.0075756198	0.0144049586	0.0110569581	46.2977
7-12	33	10.89	0.0291	0.166	0.38	0.0133	0.00038703	0.0007359333	4.763282782	0.0000355394	0.0000675788	0.0000518721	46.2977
6-12	33	10.89	0.007275	0.0415	1.52	0.1	0.0007275	0.0010375	191.0088334	0.0000668044	0.0000952708	0.0020800861	185.19
12-13	33	10.89	0.0291	0.166	0.38	3.202	0.0310594	0.1771773333	1146.769283	0.0028521028	0.0162692725	0.0124883175	46.2977
12-14	33	10.89	0.0291	0.166	0.38	7.833	0.0759801	0.433426	2805.32286	0.0069770523	0.0398003673	0.0305499659	46.2977
12-15	33	10.89	0.0291	0.166	0.38	4.694	0.0455318	0.2597346667	1681.116495	0.0041810651	0.0238507499	0.0183073586	46.2977
12-16	33	10.89	0.0291	0.166	0.38	3.703	0.0359191	0.2048993333	1326.198206	0.0032983562	0.0188153657	0.0144422984	46.2977
12-17	33	10.89	0.0291	0.166	0.38	0.0597	0.00057909	0.0033034	21.38105128	0.0000531763	0.0003033425	0.0002328398	46.2977
6-17	33	10.89	0.007275	0.0415	1.52	0.055	0.000400125	0.000570625	105.0548583	0.0000367424	0.0000523989	0.0011440474	185.19
17-18	33	10.89	0.0291	0.166	0.38	6.615	0.0641655	0.36603	2369.106436	0.0058921487	0.0336115702	0.0257995690	46.2977
17-19	33	10.89	0.0291	0.166	0.38	5.303	0.0514391	0.2934326667	1899.224706	0.0047235169	0.0269454148	0.0206825705	46.2977
17-20	33	10.89	0.0291	0.166	0.38	3.444	0.0334068	0.190568	1233.439541	0.0030676584	0.0174993572	0.0134321566	46.2977
17-21	33	10.89	0.0291	0.166	0.38	4.043	0.0392171	0.2237126667	1447.966337	0.0036012029	0.0205429446	0.0157683534	46.2977
17-22	33	10.89	0.0291	0.166	0.38	5.203	0.0504691	0.2878993333	1863.41055	0.0046344444	0.0264370370	0.0202925408	46.2977
17-23	33	10.89	0.0291	0.166	0.38	0.0133	0.00012901	0.0007359333	4.763282782	0.0001184664	0.0000675788	0.0000518721	46.2977
4-23	33	10.89	0.007275	0.0415	1.52	0.05	0.00036375	0.00051875	95.50441668	0.0000334022	0.0000476354	0.0010400430	185.19
23-24	33	10.89	0.0291	0.166	0.38	7.56	0.073332	0.41832	2707.550213	0.0067333884	0.0384132231	0.0294852218	46.2977
23-25	33	10.89	0.0291	0.166	0.38	6.962	0.0675314	0.3852306667	2493.381559	0.0062012304	0.0353747168	0.0271529251	46.2977
23-26	33	10.89	0.0291	0.166	0.38	3.15	0.091665	0.1743	1128.145922	0.0084173553	0.0160055096	0.0122855090	46.2977
23-27	33	10.89	0.0291	0.166	0.38	1.913	0.0556683	0.1058526667	685.1248092	0.0051118732	0.0097201714	0.0074610091	46.2977
12-28	33	10.89	0.0291	0.166	0.38	0.05917	0.001721847	0.0032740733	21.19123626	0.0001581126	0.0003006849	0.0002307725	46.2977
17-28	33	10.89	0.0291	0.166	0.38	0.05917	0.001721847	0.0032740733	21.19123626	0.0001581126	0.0003006849	0.0002307725	46.2977
7-36		33	0.0291	0.166	0.38	1.47	0.014259	0.08134	526.468097	0.0013093663	0.0074692378	0.0057332375	46.2977
36-31		33	0.0283	0.163	0.35	0.037	0.0003490333333	0.0020101033333	12.20508746	0.00003205081	0.00018460361	0.00013291340	46.2977

Figure A.9: Excel sheet of the branch calculations performed in order to determine the branch resistances, reactances, susceptances and rates for the aggregated model.

Branch													
31-30	33	10.89	0.0469	0.177	0.32	0.651	0.0101773	0.038409	196.3369745	0.0009345546	0.003526997724	0.0021381096	36.86
30-29	33	10.89	0.125	0.196	0.22	0.588	0.0245	0.038416	121.9189277	0.0022497704	0.003527640003	0.0013276971	20.86
29-129	33	10.89	0.125	0.196	0.22	0.583	0.024291666667	0.03808933333	120.8822021	0.0022306397	0.003497643090	0.0013164071	20.86
31-35	33	10.89	0.125	0.196	0.22	0.53	0.02208333333	0.03462666667	109.892911	0.0020278543	0.003179675540	0.0011967338	20.86
35-34	33	10.89	0.0469	0.177	0.32	0.62	0.009692666667	0.03658	186.9875948	0.0008900520	0.003359044990	0.0020362949	36.86
30-33	33	10.89	0.125	0.196	0.22	2.069	0.08620833333	0.1351746667	428.9970433	0.0079162840	0.01241273339	0.0046717778	20.86
33-32	33	10.89	0.125	0.196	0.22	0.641	0.02670833333	0.04187866667	132.9082188	0.0024525558	0.003845607590	0.0014473705	20.86
7-44	33	10.89	0.0291	0.166	0.38	2.993	0.0290321	0.1656126667	1071.917697	0.0026659412	0.01520777472	0.0116731837	46.2977
44-43	33	10.89	0.0283	0.163	0.35	0.037	0.0003490333333	0.002010333333	12.20508746	0.0000320508	0.0001846036	0.0001329134	46.2977
43-42	33	10.89	0.0469	0.177	0.32	0.599	0.009364366667	0.035341	180.654144	0.0008599051	0.003245270890	0.0019673236	36.86
42-41	33	10.89	0.0469	0.177	0.32	0.604	0.009442533333	0.035636	182.1621084	0.0008670829	0.003272359960	0.0019837453	36.86
41-40	33	10.89	0.078	0.19	0.26	0.599	0.015574	0.03793666667	146.781492	0.0014301193	0.003483624120	0.0015984504	28.29
40-39	33	10.89	0.125	0.196	0.22	0.599	0.02495833333	0.03913466667	124.199724	0.0022918579	0.003593633300	0.0013525349	20.86
39-38	33	10.89	0.125	0.196	0.22	0.541	0.02254166667	0.03534533333	112.1737073	0.0020699418	0.003245668800	0.0012215716	20.86
38-37	33	10.89	0.206	0.208	0.19	0.52	0.03570666667	0.03605333333	93.11680626	0.0032788490	0.003310682580	0.0010140420	16.28
7-52	33	10.89	0.0291	0.166	0.38	1.785	0.0173145	0.09877	639.2826892	0.0015899449	0.003906978879	0.0069617884	46.2977
52-48	33	10.89	0.0283	0.163	0.35	0.037	0.0003490333333	0.002010333333	12.20508746	0.0000320508	0.0001846036	0.0001329134	46.2977
48-47	33	10.89	0.078	0.19	0.26	0.525	0.01365	0.03325	128.6482192	0.0012534435	0.003053259870	0.0014009791	28.29
47-46	33	10.89	0.125	0.196	0.22	0.536	0.02233333333	0.03501866667	111.1369817	0.0020508111	0.003215671870	0.0012102817	20.86
47-49	33	10.89	0.125	0.196	0.22	2.961	0.123375	0.193452	613.948886	0.0113292011	0.017764187330	0.0066859033	20.86
46-45	33	10.89	0.125	0.196	0.22	0.536	0.02233333333	0.03501866667	111.1369817	0.0020508111	0.003215671870	0.0012102817	20.86
48-51	33	10.89	0.125	0.196	0.22	0.53	0.02208333333	0.03462666667	109.892911	0.0020278543	0.003179675540	0.0011967338	20.86
51-50	33	10.89	0.125	0.196	0.22	0.525	0.021875	0.0343	108.8561855	0.0020087236	0.003149678600	0.0011854438	20.86
12-60	33	10.89	0.0291	0.166	0.38	3.202	0.0310594	0.1771773333	1146.769283	0.0028521028	0.01626972758	0.0124883175	46.2977
60-59	33	10.89	0.0283	0.163	0.35	0.037	0.0003490333333	0.002010333333	12.20508746	0.0000320508	0.0001846036	0.0001329134	46.2977
59-58	33	10.89	0.0778	0.19	0.26	0.536	0.01390026667	0.03394666667	131.3437057	0.0012764248	0.003117232930	0.0014303330	28.29
58-57	33	10.89	0.0469	0.177	0.32	0.541	0.008457633333	0.031919	163.1617561	0.0007766421	0.002931037640	0.0017768315	36.86
57-56	33	10.89	0.0469	0.177	0.32	0.536	0.008379466667	0.031624	161.6537916	0.0007694643	0.002903948570	0.0017604098	36.86
56-55	33	10.89	0.125	0.196	0.22	0.536	0.02233333333	0.03501866667	111.1369817	0.0020508111	0.003215671870	0.0012102817	20.86
55-54	33	10.89	0.206	0.208	0.19	0.536	0.03680533333	0.03716266667	95.98193877	0.0033797367	0.003341254974	0.0010452433	16.28
54-53	33	10.89	0.206	0.208	0.19	0.588	0.040376	0.040768	105.2936194	0.0037070716	0.003743617990	0.0011464751	16.28
12-72	33	10.89	0.0291	0.166	0.38	7.833	0.0759801	0.433426	2805.32286	0.0069770523	0.039800036731	0.0305499659	46.2977
72-71	33	10.89	0.0283	0.163	0.35	0.037	0.0003490333333	0.002010333333	12.20508746	0.0000320508	0.0001846036	0.0001329134	46.2977
71-70	33	10.89	0.0469	0.177	0.32	0.504	0.0078792	0.029736	152.002819	0.0007235261	0.002730578510	0.0016553106	36.86
70-69	33	10.89	0.0469	0.177	0.32	0.887	0.01386676667	0.052333	267.5128977	0.0012733486	0.004805601466	0.0029132154	36.86
69-68	33	10.89	0.0469	0.177	0.32	0.546	0.0085358	0.032214	164.6697206	0.0007838200	0.002958126720	0.0017932532	36.86

Figure A.10: Excel sheet of the branch calculations performed in order to determine the branch resistances, reactances, susceptances and rates for the aggregated model.

68-67	33	10.89	0.0778	0.19	0.26	0.541	0.01402993333	0.03426333333	132.5689268	0.0012883318	0.0031463116	0.0014436756	28.29
67-66	33	10.89	0.0778	0.19	0.26	0.494	0.01281106667	0.03128666667	121.0518481	0.0011764064	0.0028729721	0.0013182564	28.29
66-65	33	10.89	0.0778	0.19	0.26	0.536	0.01390026667	0.03394666667	131.3437057	0.0012764248	0.0031172329	0.0014303329	28.29
65-64	33	10.89	0.125	0.196	0.22	0.567	0.023625	0.037044	117.5646803	0.0021694214	0.0034016528	0.0012802793	20.86
64-63	33	10.89	0.125	0.196	0.22	0.551	0.02295833333	0.03599866667	114.2471585	0.0021082032	0.0033056626	0.0012441515	16.28
63-62	33	10.89	0.206	0.208	0.19	0.551	0.03783533333	0.03820266667	98.66800048	0.0034743189	0.0035080050	0.0010744945	16.28
62-61	33	10.89	0.206	0.208	0.19	0.515	0.03536333333	0.03570066667	92.22145236	0.0032473217	0.0032788490	0.0010042916	16.28
12-79	33	10.89	0.0291	0.166	0.38	4.694	0.0455318	0.2597346667	1681.116495	0.0041810655	0.0238507499	0.0183073586	46.2977
79-78	33	10.89	0.0283	0.163	0.35	0.037	0.0003490333333	0.0002010333333	12.20508746	0.0000320508	0.0001846036	0.0001329134	46.2977
78-77	33	10.89	0.0469	0.177	0.32	0.52	0.008129333333	0.03068	156.8283053	0.0007464952	0.0028172635	0.0017078602	36.86
77-76	33	10.89	0.0469	0.177	0.32	0.488	0.007629066667	0.028792	147.1773327	0.0007005570	0.0026438934	0.0016027611	36.86
76-75	33	10.89	0.0778	0.19	0.26	0.499	0.01294073333	0.03160333333	122.2770693	0.0011883134	0.0029020508	0.0013315972	28.29
75-74	33	10.89	0.125	0.196	0.22	0.499	0.02079166667	0.03260133333	103.4652125	0.0019092439	0.0029936945	0.0011267361	20.86
74-73	33	10.89	0.206	0.208	0.19	0.499	0.03426466667	0.03459733333	89.35631986	0.0031464340	0.0031769819	0.0009730903	16.28
73-72	33	10.89	0.206	0.208	0.19	0.499	0.03426466667	0.03459733333	89.35631986	0.0031464340	0.0031769819	0.0009730903	16.28
17-83	33	10.89	0.0778	0.19	0.26	6.615	0.171549	0.41895	1620.967562	0.0157528925	0.0384710743	0.0176523367	28.29
83-82	33	10.89	0.125	0.196	0.22	1.082	0.04508333333	0.07069066667	224.3474146	0.0041398836	0.0064913376	0.0024431433	20.86
82-81	33	10.89	0.206	0.208	0.19	1.754	0.1204413333	0.1216106667	314.0901504	0.0110598102	0.0111671870	0.0034204417	16.28
81-80	33	10.89	0.206	0.208	0.19	0.546	0.037492	0.037856	97.77264658	0.0034427915	0.0034762167	0.0010647441	16.28
17-87	33	10.89	0.0291	0.166	0.38	5.303	0.0514391	0.2934326667	1899.224706	0.0047235168	0.0269451484	0.0206825570	46.2977
87-86	33	10.89	0.125	0.196	0.22	0.536	0.02233333333	0.03501866667	111.1369817	0.0020508111	0.0032156718	0.0012102817	20.86
86-85	33	10.89	0.125	0.196	0.22	0.578	0.02408333333	0.03776266667	119.8454766	0.0022115090	0.0034676461	0.0013051172	20.86
85-84	33	10.89	0.206	0.208	0.19	0.572	0.03927733333	0.03965866667	102.4284869	0.0036067340	0.0036417508	0.0011154462	16.28
17-95	33	10.89	0.0291	0.166	0.38	3.444	0.0334068	0.190568	1233.439541	0.0030676584	0.0174993572	0.0134321566	46.2977
95-94	33	10.89	0.0283	0.163	0.35	0.037	0.0003490333333	0.0002010333333	12.20508746	0.0000320508	0.0001846036	0.0001329134	46.2977
94-93	33	10.89	0.0469	0.177	0.32	0.588	0.0091924	0.034692	177.3366221	0.0008441138	0.0031856749	0.0019311958	36.86
93-92	33	10.89	0.0469	0.177	0.32	0.562	0.008785933333	0.033158	169.4952069	0.0008067891	0.0030448117	0.0018458028	36.86
92-91	33	10.89	0.0778	0.19	0.26	0.646	0.01675293333	0.04091333333	158.2985706	0.0015383777	0.0037569635	0.0017238714	28.29
91-90	33	10.89	0.125	0.196	0.22	0.541	0.02254166667	0.03534533333	112.1737073	0.0020699418	0.0032456688	0.0012215716	20.86
90-89	33	10.89	0.206	0.208	0.19	0.583	0.04003266667	0.04042133333	104.3982655	0.0036760942	0.0037117845	0.0011368971	16.28
89-88	33	10.89	0.206	0.208	0.19	1.113	0.076426	0.077168	199.3057796	0.0070179981	0.0070861340	0.0021704399	16.28
17-104	33	10.89	0.0291	0.166	0.38	4.043	0.0392171	0.2237126667	1447.966337	0.0036012029	0.0205429446	0.0157683534	46.2977
104-101	33	10.89	0.0283	0.163	0.35	0.037	0.0003490333333	0.0002010333333	12.20508746	0.0000320508	0.0001846036	0.0001329134	46.2977
101-100	33	10.89	0.0469	0.177	0.32	1.628	0.02545106667	0.096052	490.9932327	0.0023371043	0.0088202022	0.0053469163	36.86
101-103	33	10.89	0.125	0.196	0.22	0.567	0.023625	0.037044	117.5646803	0.0021694214	0.0034016528	0.0012802793	20.86

Figure A.11: Excel sheet of the branch calculations performed in order to determine the branch resistances, reactances, susceptances and rates for the model on string level.

Branch													Rate
103-102	33	10.89	0.206	0.208	0.19	0.567	0.038934	0.039312	101.533133	0.0035752066	0.00360991735	0.0011056958	16.28
100-99	33	10.89	0.0778	0.19	0.26	0.567	0.0147042	0.03591	138.9400767	0.0013502479	-0.0032975206	0.0015130574	28.29
99-98	33	10.89	0.125	0.196	0.22	0.572	0.02383333333	0.03737066667	118.6014059	0.00218855218	0.00343164983	0.0012915693	20.86
98-97	33	10.89	0.206	0.208	0.19	0.567	0.038934	0.039312	101.533133	0.0035752066	0.00360991735	0.0011056958	16.28
97-96	33	10.89	0.206	0.208	0.19	0.725	0.04978333333	0.05026666667	129.8263164	0.00457147229	0.0046158552	0.0014138085	16.28
23-112	33	10.89	0.0291	0.166	0.38	7.56	0.073332	0.41832	2707.550213	0.00673384291	0.03841322314	0.02948522182	46.2977
112-111	33	10.89	0.0283	0.163	0.35	0.037	0.0003490333333	0.002010333333	12.20508746	0.0000320508	0.0001846036	0.0001329134	46.2977
111-110	33	10.89	0.0469	0.177	0.32	0.651	0.0101773	0.038409	196.3369745	0.0009345546	0.0035269972	0.0021381096	36.86
110-109	33	10.89	0.0469	0.177	0.32	0.641	0.01002096667	0.037819	193.3210456	0.0009201989	0.0034728191	0.0021052661	36.86
109-108	33	10.89	0.0778	0.19	0.26	0.667	0.01729753333	0.04224333333	163.4444994	0.0015883868	0.0038790939	0.0017799105	28.29
108-107	33	10.89	0.125	0.196	0.22	0.651	0.027125	0.042532	134.98167	0.0024908172	0.0039056014	0.0014699503	20.86
107-106	33	10.89	0.125	0.196	0.22	0.672	0.028	0.043904	139.3359174	0.0025711662	0.0040315886	0.0015173681	20.86
106-105	33	10.89	0.206	0.208	0.19	0.656	0.04504533333	0.04548266667	117.4704325	0.0041363942	0.0041765534	0.0012792530	16.28
23-120	33	10.89	0.0291	0.166	0.38	6.962	0.0675314	0.3852306667	2493.381559	0.0062012304	0.0353747168	0.0271529251	46.2977
120-119	33	10.89	0.0283	0.163	0.35	0.037	0.0003490333333	0.002010333333	12.20508746	0.0000320508	0.0001846036	0.0001329134	46.2977
119-118	33	10.89	0.0469	0.177	0.32	0.583	0.009114233333	0.034397	175.8286577	0.0008369360	0.0031585585	0.0019147740	36.86
118-117	33	10.89	0.0469	0.177	0.32	0.578	0.009036066667	0.034102	174.3206932	0.0008297558	0.0031314967	0.0018983523	36.86
117-116	33	10.89	0.0778	0.19	0.26	0.583	0.01511913333	0.03692333333	142.8607843	0.0013883501	0.0033905723	0.0015557539	28.29
116-115	33	10.89	0.125	0.196	0.22	0.609	0.025375	0.039788	126.2731751	0.0023301193	0.0036536271	0.0013751148	20.86
115-114	33	10.89	0.125	0.196	0.22	0.683	0.02845833333	0.04462266667	141.6167137	0.0026132537	0.0040975818	0.0015442206	20.86
114-113	33	10.89	0.206	0.208	0.19	0.614	0.04216133333	0.04257066667	109.9494597	0.0038715641	0.0039091521	0.0011973496	16.28
23-128	33	10.89	0.0291	0.166	0.38	3.15	0.030555	0.1743	1128.145922	0.0028057851	0.0160055096	0.0122885090	46.2977
128-124	33	10.89	0.0469	0.177	0.32	0.037	0.0005784333333	0.002183	11.15893711	0.0000531160	0.0002004591	0.0001215208	36.86
124-123	33	10.89	0.125	0.196	0.22	0.578	0.02408333333	0.03776266667	119.8454766	0.0022115090	0.0034676461	0.0013051172	20.86
123-122	33	10.89	0.125	0.196	0.22	0.578	0.02408333333	0.03776266667	119.8454766	0.0022115090	0.0034676461	0.0013051172	20.86
122-121	33	10.89	0.206	0.208	0.19	0.578	0.03968933333	0.04007466667	103.5029116	0.0036445668	0.0036799510	0.0011271467	16.28
124-127	33	10.89	0.0778	0.19	0.26	4.043	0.1048484667	0.2560566667	990.7138098	0.0096279583	0.0235130088	0.0107888733	28.29
127-126	33	10.89	0.125	0.196	0.22	0.677	0.02820833333	0.04423066667	140.372643	0.0025902969	0.0040615855	0.0015286580	20.86
126-125	33	10.89	0.206	0.208	0.19	0.614	0.04216133333	0.04257066667	109.9494597	0.0038715641	0.0039091521	0.0011973496	16.28

Figure A.12: Excel sheet of the branch calculations performed in order to determine the branch resistances, reactances, susceptances and rates for the model on string level.

From Trafo to WTG													Type Turbine	
STRING 7														
string: L:1470 m														
31-137	0.63	0.003969	0.028222	0.028496	0.19	0.15	0.0014111	0.0014248	26.86061719	0.3555303603	1.663329937	0.00000010660(	4.6	C
35-136	0.4	0.0016	0.028222	0.028496	0.19	0.16	0.001505173333	0.001519786667	28.651325	0.9407333333	2.2832	0.0000004584;	4.5	B
34-135	0.63	0.003969	0.028222	0.028496	0.19	0.15	0.0014111	0.0014248	26.86061719	0.3555303603	1.663329937	0.00000010660(	4.6	C
30-132	0.63	0.003969	0.028222	0.028496	0.19	0.15	0.0014111	0.0014248	26.86061719	0.3555303603	1.663329937	0.00000010660(	4.6	C
33-134	0.63	0.003969	0.028222	0.028496	0.19	0.15	0.0014111	0.0014248	26.86061719	0.3555303603	1.663329937	0.00000010660(	4.6	C
32-133	0.63	0.003969	0.028222	0.028496	0.19	0.15	0.0014111	0.0014248	26.86061719	0.3555303603	1.663329937	0.00000010660(	4.6	C
29-131	0.4	0.0016	0.028222	0.028496	0.19	0.16	0.001505173333	0.001519786667	28.651325	0.9407333333	2.2832	0.0000004584;	4.5	B
129-130	0.4	0.0016	0.028222	0.028496	0.19	0.16	0.001505173333	0.001519786667	28.651325	0.9407333333	2.2832	0.0000004584;	4.5	B
string: L:2993 m														
43-144	0.63	0.003969	0.028222	0.028496	0.19	0.15	0.0014111	0.0014248	26.86061719	0.3555303603	1.663329937	0.00000010660(	4.6	C
42-143	0.63	0.003969	0.028222	0.028496	0.19	0.15	0.0014111	0.0014248	26.86061719	0.3555303603	1.663329937	0.00000010660(	4.6	C
41-142	0.63	0.003969	0.028222	0.028496	0.19	0.15	0.0014111	0.0014248	26.86061719	0.3555303603	1.663329937	0.00000010660(	4.6	C
40-141	0.63	0.003969	0.028222	0.028496	0.19	0.15	0.0014111	0.0014248	26.86061719	0.3555303603	1.663329937	0.00000010660(	4.6	C
39-140	0.63	0.003969	0.028222	0.028496	0.19	0.22	0.002069613333	0.002089706667	39.39557188	0.5214445284	0.5265070967	0.00000015636	5	A
38-139	0.63	0.003969	0.028222	0.028496	0.19	0.22	0.002069613333	0.002089706667	39.39557188	0.5214445284	1.726507097	0.00000015636	5	A
37-138	0.63	0.003969	0.028222	0.028496	0.19	0.22	0.002069613333	0.002089706667	39.39557188	0.5214445284	1.726507097	0.00000015636	5	A
string: L:1785 m														
48-149	0.63	0.003969	0.028222	0.028496	0.19	0.15	0.0014111	0.0014248	26.86061719	0.3555303603	1.663329937	0.00000010660(	4.6	C
51-151	0.63	0.003969	0.028222	0.028496	0.19	0.15	0.0014111	0.0014248	26.86061719	0.3555303603	1.663329937	0.00000010660(	4.6	C
50-150	0.63	0.003969	0.028222	0.028496	0.19	0.15	0.0014111	0.0014248	26.86061719	0.3555303603	1.663329937	0.00000010660(	4.6	C
47-148	0.4	0.0016	0.028222	0.028496	0.19	0.16	0.001505173333	0.001519786667	28.651325	0.9407333333	2.2832	0.0000004584;	4.5	B
49-147	0.4	0.0016	0.028222	0.028496	0.19	0.16	0.001505173333	0.001519786667	28.651325	0.9407333333	2.2832	0.0000004584;	4.5	B
46-146	0.4	0.0016	0.028222	0.028496	0.19	0.16	0.001505173333	0.001519786667	28.651325	0.9407333333	2.2832	0.0000004584;	4.5	B
45-145	0.63	0.003969	0.028222	0.028496	0.19	0.15	0.0014111	0.0014248	26.86061719	0.3555303603	1.663329937	0.00000010660(	4.6	C
STRING 12														
string: L:3202 m														
59-158	0.63	0.003969	0.028222	0.028496	0.19	0.15	0.0014111	0.0014248	26.86061719	0.3555303603	1.663329937	0.00000010660(	4.6	C
58-157	0.63	0.003969	0.028222	0.028496	0.19	0.15	0.0014111	0.0014248	26.86061719	0.3555303603	1.663329937	0.00000010660(	4.6	C
57-156	0.63	0.003969	0.028222	0.028496	0.19	0.15	0.0014111	0.0014248	26.86061719	0.3555303603	1.663329937	0.00000010660(	4.6	C
56-155	0.63	0.003969	0.028222	0.028496	0.19	0.15	0.0014111	0.0014248	26.86061719	0.3555303603	1.663329937	0.00000010660(	4.6	C
55-154	0.4	0.0016	0.028222	0.028496	0.19	0.16	0.001505173333	0.001519786667	28.651325	0.9407333333	2.2832	0.0000004584;	4.5	B
54-153	0.4	0.0016	0.028222	0.028496	0.19	0.16	0.001505173333	0.001519786667	28.651325	0.9407333333	2.2832	0.0000004584;	4.5	B
53-152	0.4	0.0016	0.028222	0.028496	0.19	0.16	0.001505173333	0.001519786667	28.651325	0.9407333333	2.2832	0.0000004584;	4.5	B
string: L:7833 m														
71-169	0.4	0.0016	0.028222	0.028496	0.19	0.16	0.001505173333	0.001519786667	28.651325	0.9407333333	2.2832	0.0000004584;	4.5	B
70-168	0.4	0.0016	0.028222	0.028496	0.19	0.16	0.001505173333	0.001519786667	28.651325	0.9407333333	2.2832	0.0000004584;	4.5	B
69-167	0.4	0.0016	0.028222	0.028496	0.19	0.16	0.001505173333	0.001519786667	28.651325	0.9407333333	3.349866667	0.0000004584;	2.5	D
68-166	0.4	0.0016	0.028222	0.028496	0.19	0.16	0.001505173333	0.001519786667	28.651325	0.9407333333	3.349866667	0.0000004584;	2.5	D

Figure A.13: Excel sheet of the branch calculations performed in order to determine the branch resistances, reactances, susceptances and rates for the model on string level.

67-162	0.4	0.0016	0.028222	0.028496	0.19	0.16	0.001505173333	0.001519786667	28.651325	0.9407333333	3.349866667	0.00000004584;	2.5 D
66-165	0.4	0.0016	0.028222	0.028496	0.19	0.16	0.001505173333	0.001519786667	28.651325	0.9407333333	3.349866667	0.00000004584;	2.5 D
65-161	0.4	0.0016	0.028222	0.028496	0.19	0.16	0.001505173333	0.001519786667	28.651325	0.9407333333	3.349866667	0.00000004584;	2.5 D
64-164	0.4	0.0016	0.028222	0.028496	0.19	0.16	0.001505173333	0.001519786667	28.651325	0.9407333333	3.349866667	0.00000004584;	2.5 D
63-160	0.4	0.0016	0.028222	0.028496	0.19	0.16	0.001505173333	0.001519786667	28.651325	0.9407333333	3.349866667	0.00000004584;	2.5 D
62-163	0.4	0.0016	0.028222	0.028496	0.19	0.16	0.001505173333	0.001519786667	28.651325	0.9407333333	3.349866667	0.00000004584;	2.5 D
61-159	0.4	0.0016	0.028222	0.028496	0.19	0.16	0.001505173333	0.001519786667	28.651325	0.9407333333	3.349866667	0.00000004584;	2.5 D
string: L:4694 m													
78-176	0.4	0.0016	0.028222	0.028496	0.19	0.16	0.001505173333	0.001519786667	28.651325	0.9407333333	2.2832	0.00000004584;	4.5 B
77-175	0.4	0.0016	0.028222	0.028496	0.19	0.16	0.001505173333	0.001519786667	28.651325	0.9407333333	2.2832	0.00000004584;	4.5 B
76-174	0.4	0.0016	0.028222	0.028496	0.19	0.16	0.001505173333	0.001519786667	28.651325	0.9407333333	2.2832	0.00000004584;	4.5 B
75-173	0.4	0.0016	0.028222	0.028496	0.19	0.16	0.001505173333	0.001519786667	28.651325	0.9407333333	2.2832	0.00000004584;	4.5 B
74-172	0.4	0.0016	0.028222	0.028496	0.19	0.16	0.001505173333	0.001519786667	28.651325	0.9407333333	2.2832	0.00000004584;	4.5 B
73-171	0.4	0.0016	0.028222	0.028496	0.19	0.16	0.001505173333	0.001519786667	28.651325	0.9407333333	2.2832	0.00000004584;	4.5 B
72-170	0.4	0.0016	0.028222	0.028496	0.19	0.16	0.001505173333	0.001519786667	28.651325	0.9407333333	2.2832	0.00000004584;	4.5 B
STRING 17													
string: L:6615 m													
83-180	0.4	0.0016	0.028222	0.028496	0.19	0.16	0.001505173333	0.001519786667	28.651325	0.9407333333	2.2832	0.00000004584;	4.5 B
82-179	0.4	0.0016	0.028222	0.028496	0.19	0.16	0.001505173333	0.001519786667	28.651325	0.9407333333	2.2832	0.00000004584;	4.5 B
81-178	0.4	0.0016	0.028222	0.028496	0.19	0.16	0.001505173333	0.001519786667	28.651325	0.9407333333	2.2832	0.00000004584;	4.5 B
80-177	0.4	0.0016	0.028222	0.028496	0.19	0.16	0.001505173333	0.001519786667	28.651325	0.9407333333	2.2832	0.00000004584;	4.5 B
string: L:5303 m													
87-184	0.4	0.0016	0.028222	0.028496	0.19	0.15	0.0014111	0.0014248	26.86061719	0.8819375	2.194847826	0.0000004297(	4.6 C
86-183	0.4	0.0016	0.028222	0.028496	0.19	0.15	0.0014111	0.0014248	26.86061719	0.8819375	2.194847826	0.0000004297(	4.6 C
85-182	0.63	0.003969	0.028222	0.028496	0.19	0.22	0.002069613333	0.00208970666	39.39557188	0.5214445284	1.726507097	0.00000015636:	5 A
84-181	0.63	0.003969	0.028222	0.028496	0.19	0.22	0.002069613333	0.00208970666	39.39557188	0.5214445284	1.726507097	0.00000015636:	5 A
string: L:3444 m													
94-191	0.4	0.0016	0.028222	0.028496	0.19	0.16	0.001505173333	0.001519786667	28.651325	0.9407333333	2.2832	0.00000004584;	4.5 B
93-190	0.4	0.0016	0.028222	0.028496	0.19	0.16	0.001505173333	0.001519786667	28.651325	0.9407333333	2.2832	0.00000004584;	4.5 B
92-189	0.4	0.0016	0.028222	0.028496	0.19	0.16	0.001505173333	0.001519786667	28.651325	0.9407333333	2.2832	0.00000004584;	4.5 B
91-188	0.4	0.0016	0.028222	0.028496	0.19	0.16	0.001505173333	0.001519786667	28.651325	0.9407333333	2.2832	0.00000004584;	4.5 B
90-187	0.4	0.0016	0.028222	0.028496	0.19	0.16	0.001505173333	0.001519786667	28.651325	0.9407333333	2.2832	0.00000004584;	4.5 B
89-186	0.4	0.0016	0.028222	0.028496	0.19	0.16	0.001505173333	0.001519786667	28.651325	0.9407333333	2.2832	0.00000004584;	4.5 B
88-185	0.4	0.0016	0.028222	0.028496	0.19	0.16	0.001505173333	0.001519786667	28.651325	0.9407333333	2.2832	0.00000004584;	4.5 B
string: L:4043 m													
101-197	0.4	0.0016	0.028222	0.028496	0.19	0.16	0.001505173333	0.001519786667	28.651325	0.9407333333	2.2832	0.00000004584;	4.5 B
103-199	0.4	0.0016	0.028222	0.028496	0.19	0.16	0.001505173333	0.001519786667	28.651325	0.9407333333	2.2832	0.00000004584;	4.5 B
102-198	0.4	0.0016	0.028222	0.028496	0.19	0.16	0.001505173333	0.001519786667	28.651325	0.9407333333	2.2832	0.00000004584;	4.5 B
100-196	0.4	0.0016	0.028222	0.028496	0.19	0.16	0.001505173333	0.001519786667	28.651325	0.9407333333	2.2832	0.00000004584;	4.5 B
99-195	0.4	0.0016	0.028222	0.028496	0.19	0.16	0.001505173333	0.001519786667	28.651325	0.9407333333	2.2832	0.00000004584;	4.5 B
98-194	0.4	0.0016	0.028222	0.028496	0.19	0.16	0.001505173333	0.001519786667	28.651325	0.9407333333	2.2832	0.00000004584;	4.5 B
97-193	0.4	0.0016	0.028222	0.028496	0.19	0.16	0.001505173333	0.001519786667	28.651325	0.9407333333	2.2832	0.00000004584;	4.5 B
96-192	0.4	0.0016	0.028222	0.028496	0.19	0.16	0.001505173333	0.001519786667	28.651325	0.9407333333	2.2832	0.00000004584;	4.5 B

Figure A.14: Excel sheet of the branch calculations performed in order to determine the branch resistances, reactances, susceptances and rates for the model on string level.

STRING 23

string: L:7560 m

111-206	0.63	0.003969	0.028222	0.028496	0.19	0.22	0.0020696961333	0.002089706667	39.39557188	0.5214445284	1.726507097	0.00000015636	5 A
110-205	0.63	0.003969	0.028222	0.028496	0.19	0.22	0.0020696961333	0.002089706667	39.39557188	0.5214445284	1.726507097	0.00000015636	5 A
109-204	0.63	0.003969	0.028222	0.028496	0.19	0.22	0.0020696961333	0.002089706667	39.39557188	0.5214445284	1.726507097	0.00000015636	5 A
108-203	0.63	0.003969	0.028222	0.028496	0.19	0.22	0.0020696961333	0.002089706667	39.39557188	0.5214445284	1.726507097	0.00000015636	5 A
107-202	0.63	0.003969	0.028222	0.028496	0.19	0.22	0.0020696961333	0.002089706667	39.39557188	0.5214445284	1.726507097	0.00000015636	5 A
106-201	0.63	0.003969	0.028222	0.028496	0.19	0.22	0.0020696961333	0.002089706667	39.39557188	0.5214445284	1.726507097	0.00000015636	5 A
105-200	0.63	0.003969	0.028222	0.028496	0.19	0.22	0.0020696961333	0.002089706667	39.39557188	0.5214445284	1.726507097	0.00000015636	5 A

string: L:6962 m

119-213	0.63	0.003969	0.028222	0.028496	0.19	0.22	0.0020696961333	0.002089706667	39.39557188	0.5214445284	1.726507097	0.00000015636	5 A
118-212	0.63	0.003969	0.028222	0.028496	0.19	0.22	0.0020696961333	0.002089706667	39.39557188	0.5214445284	1.726507097	0.00000015636	5 A
117-211	0.63	0.003969	0.028222	0.028496	0.19	0.22	0.0020696961333	0.002089706667	39.39557188	0.5214445284	1.726507097	0.00000015636	5 A
116-210	0.63	0.003969	0.028222	0.028496	0.19	0.22	0.0020696961333	0.002089706667	39.39557188	0.5214445284	1.726507097	0.00000015636	5 A
115-209	0.63	0.003969	0.028222	0.028496	0.19	0.22	0.0020696961333	0.002089706667	39.39557188	0.5214445284	1.726507097	0.00000015636	5 A
114-208	0.63	0.003969	0.028222	0.028496	0.19	0.22	0.0020696961333	0.002089706667	39.39557188	0.5214445284	1.726507097	0.00000015636	5 A
113-207	0.63	0.003969	0.028222	0.028496	0.19	0.22	0.0020696961333	0.002089706667	39.39557188	0.5214445284	1.726507097	0.00000015636	5 A

string: L:3150 m

124-217	0.63	0.003969	0.028222	0.028496	0.19	0.15	0.0014111	0.0014248	26.86061719	0.3555303603	1.663329937	0.000000106606	4.6 C
127-220	0.63	0.003969	0.028222	0.028496	0.19	0.22	0.0020696961333	0.002089706667	39.39557188	0.5214445284	1.726507097	0.00000015636	5 A
126-219	0.63	0.003969	0.028222	0.028496	0.19	0.22	0.0020696961333	0.002089706667	39.39557188	0.5214445284	1.726507097	0.00000015636	5 A
125-218	0.63	0.003969	0.028222	0.028496	0.19	0.22	0.0020696961333	0.002089706667	39.39557188	0.5214445284	1.726507097	0.00000015636	5 A
123-216	0.63	0.003969	0.028222	0.028496	0.19	0.15	0.0014111	0.0014248	26.86061719	0.3555303603	0.3589821114	0.000000106606	4.6 C
122-215	0.63	0.003969	0.028222	0.028496	0.19	0.15	0.0014111	0.0014248	26.86061719	0.3555303603	1.663329937	0.000000106606	4.6 C
121-214	0.63	0.003969	0.028222	0.028496	0.19	0.15	0.0014111	0.0014248	26.86061719	0.3555303603	1.663329937	0.000000106606	4.6 C

Transformer impedances

	S [MVA]	V_base [kV]	Leakage [%]	Z_lowside (Im Z_pu)	
Type A	5	0.63	6	0.0047628	1.2
Type B	4.5	0.4	6	0.0021333333	1.333333333
Type C	4.6	0.63	6	0.0051769656	1.304347826
Type D	2.5	0.4	6	0.00384	2.4
Main trafo	240	33	15	0.680625	0.0625

Figure A.15: Excel sheet of the branch calculations performed in order to determine the branch resistances, reactances, susceptances and rates for the model on string level.

A.4.3. Branch connections to bus

MatLab Branch	Branch "from"	Branch "to"
1	1	2
2	2	3
3	2	5
4	3	4
5	5	6
6	4	7
7	7	8
8	7	9
9	7	10
10	7	11
11	7	12
12	6	12
13	12	13
14	12	14
15	12	15
16	12	16
17	12	17
18	6	17
19	17	18
20	17	19
21	17	20
22	17	21
23	17	22
24	17	23
25	4	23
26	23	24
27	23	25
28	23	26
29	23	27
30	12	28
31	17	28

Figure A.16: The numbering of branches in Matpower corresponding with the branches shown in App.A.3.

A.5. Capability curves
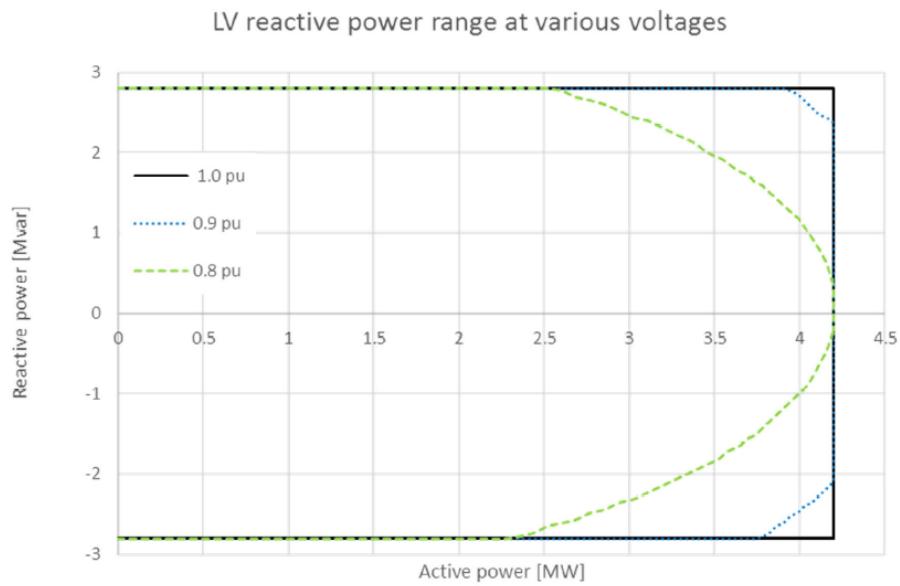
Figure A.17: Common case for relation between P and Q of WTG
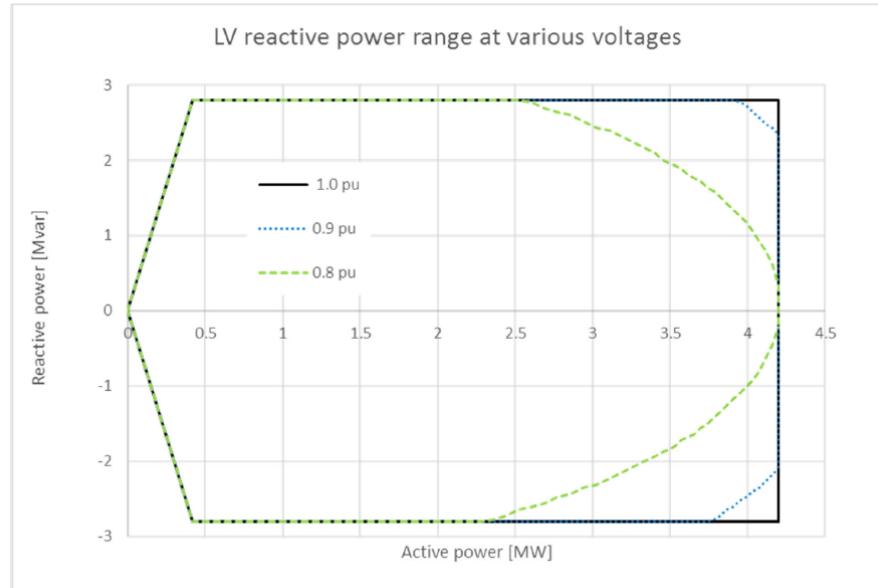
Figure A.18: Non-ideal case for relation between P and Q of WTG

A.6. String level overview
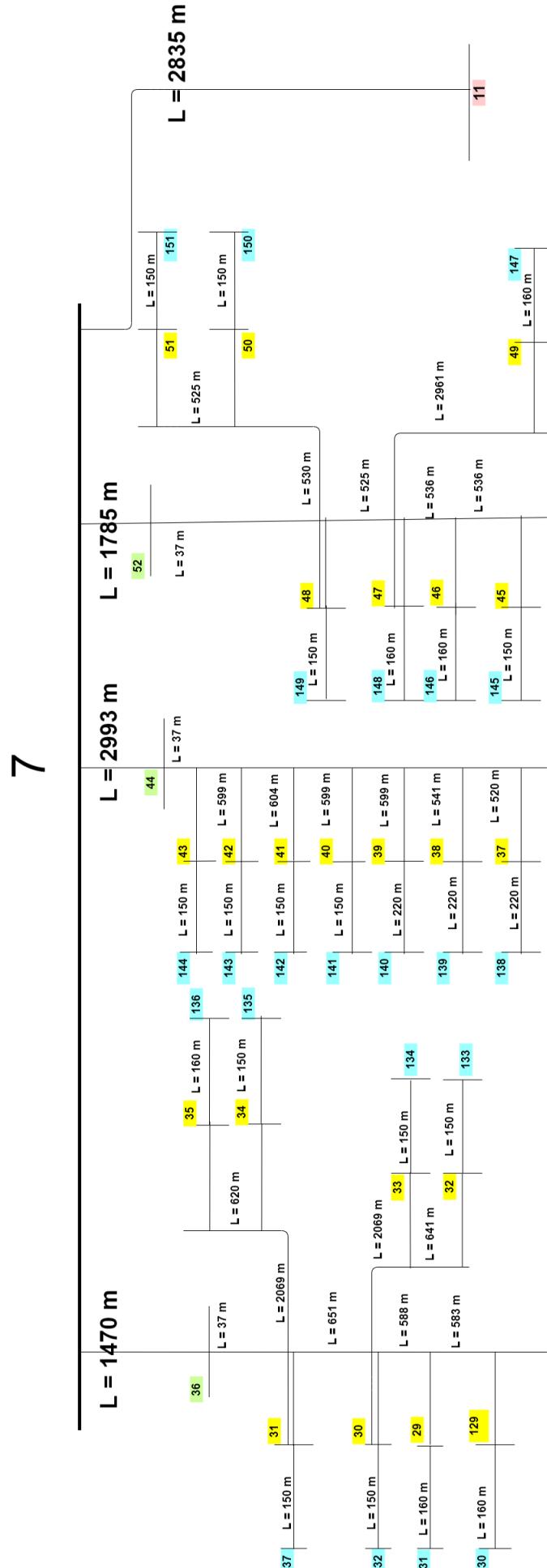
Figure A.19: Visualization of one string connected to bus 7, which is modeled on string level. The same procedure is applied for the remaining WTG strings. The lengths in bold are the same lengths as was previously for the aggregated model. Yellow busses are WTGs, blue busses are transformers, green busses are joint terminals.

A.7. Results
A.7.1. Wind farm Plots
A.7.2. Reactive power losses
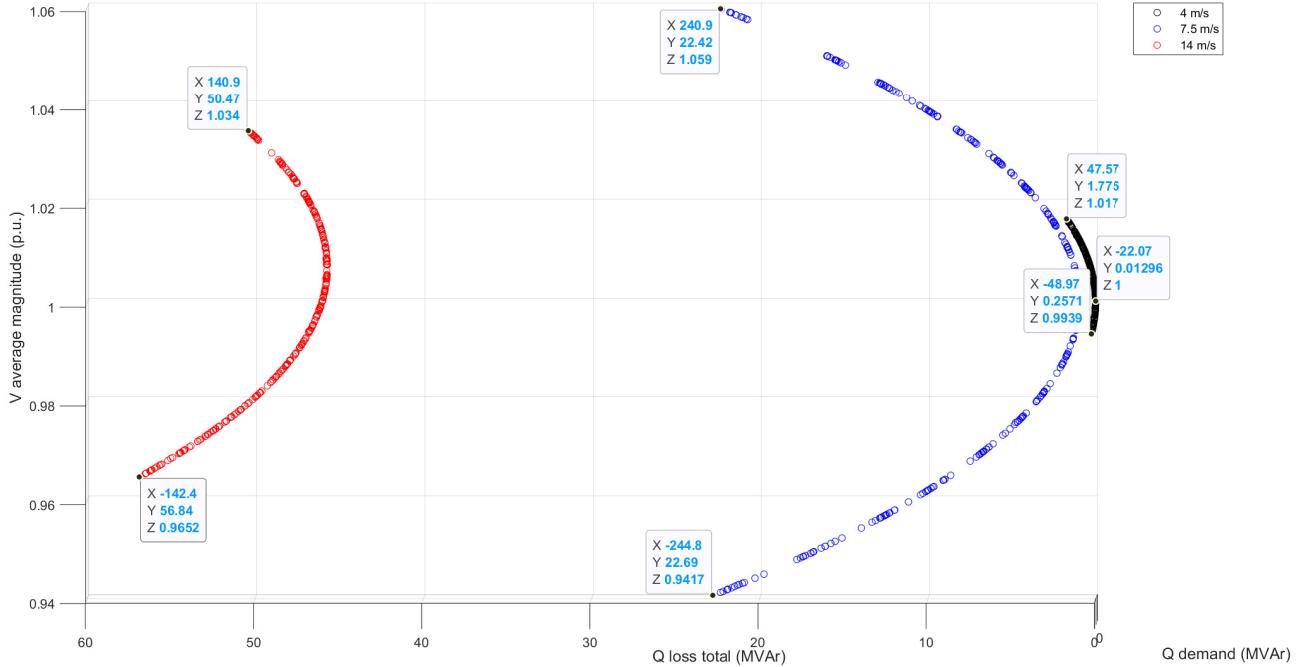
Figure A.20: 3-D plot of the relation of the average voltage magnitude (p.u.), reactive power losses and random Q demands for the wind farm. This plot is generated in order to show the relations in a clear and visualizable manner. In this plot the relation of the average voltage magnitudes (p.u.) and the reactive power losses is emphasized.

A.7.3. Voltage profiles
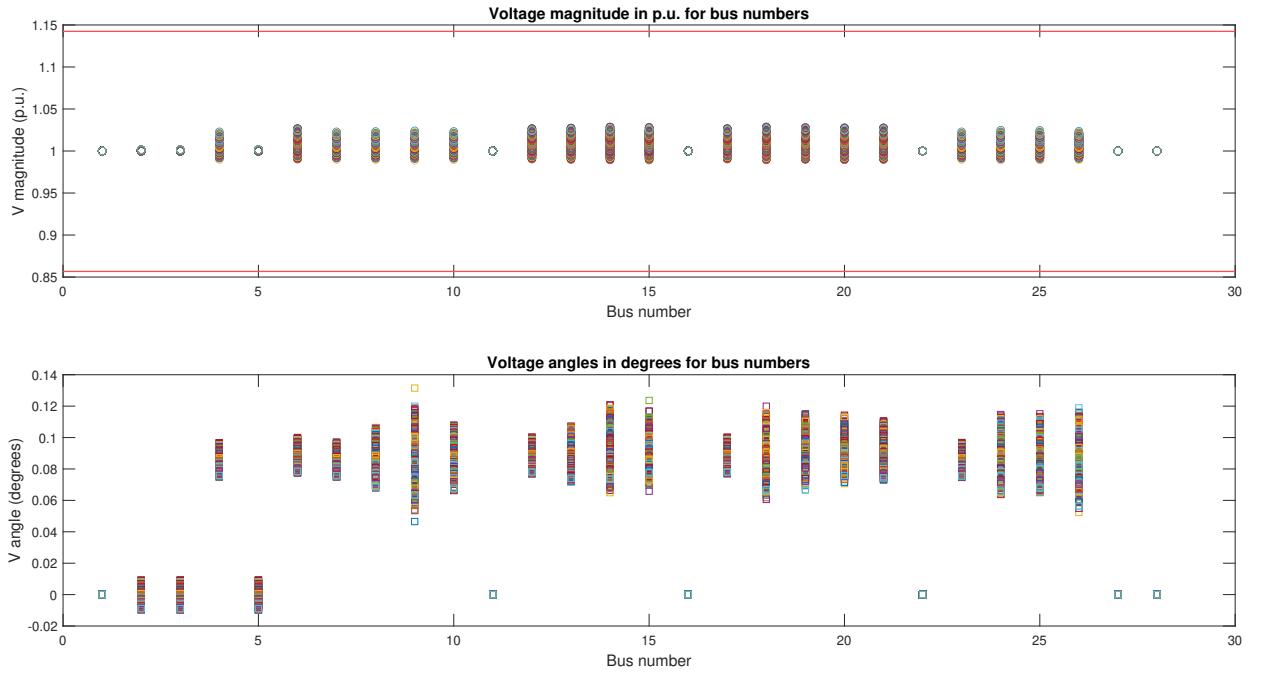
Figure A.21: Voltage magnitude and angle for each bus number of App. A.3 after running power flows for the wind farm at a wind speed of 4 m/s. Most busses deviate from 1 p.u., except for the slack bus, i.e. bus 1.
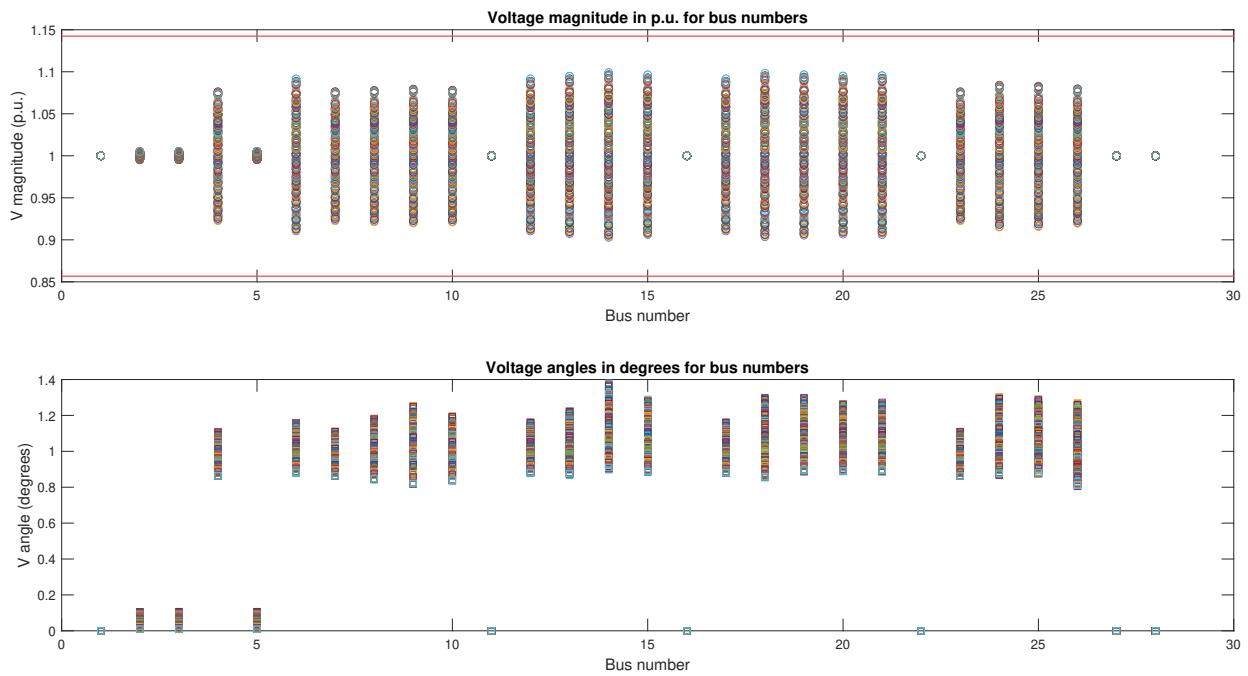
Figure A.22: Voltage magnitude and angle for each bus number of App. A.3 after running power flows for the wind farm at a wind speed of 7.5 m/s. Most busses deviate from 1 p.u., except for the slack bus, i.e. bus 1.
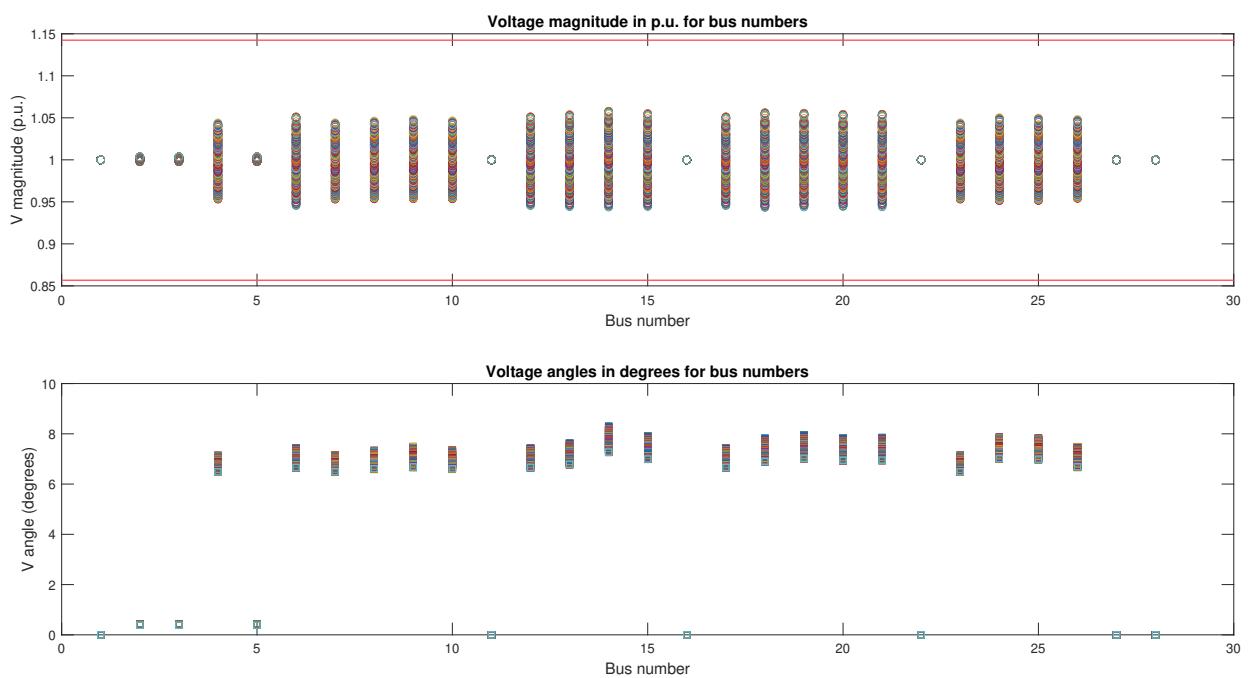

Figure A.23: Voltage magnitude and angle for each bus number of App. A.3 after running power flows for the wind farm at a wind speed of 14 m/s. Most busses deviate from 1 p.u., except for the slack bus, i.e. bus 1.

A.7.4. Power flows through transformer and PCC branch
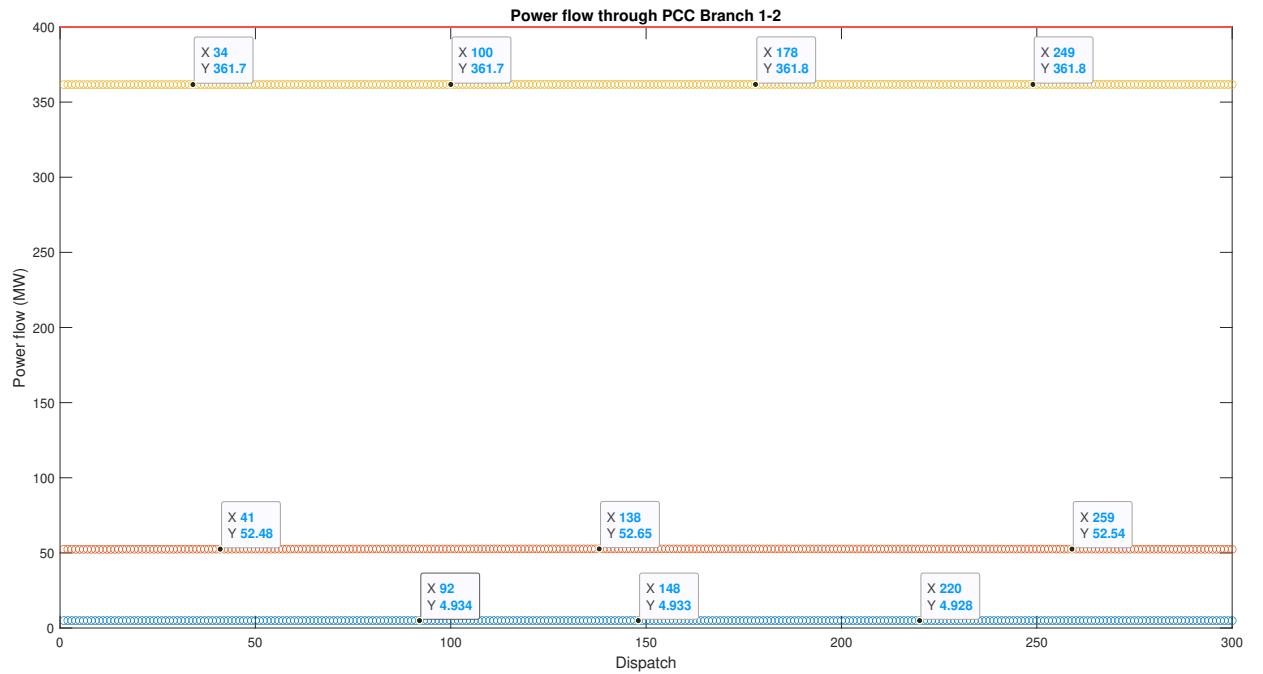
Figure A.24: Power flow through branch 1-2 for the wind farm. From down to up, wind speeds = 4;7.5;14 m/s. The red line visualizes the apparent power limit for this branch.
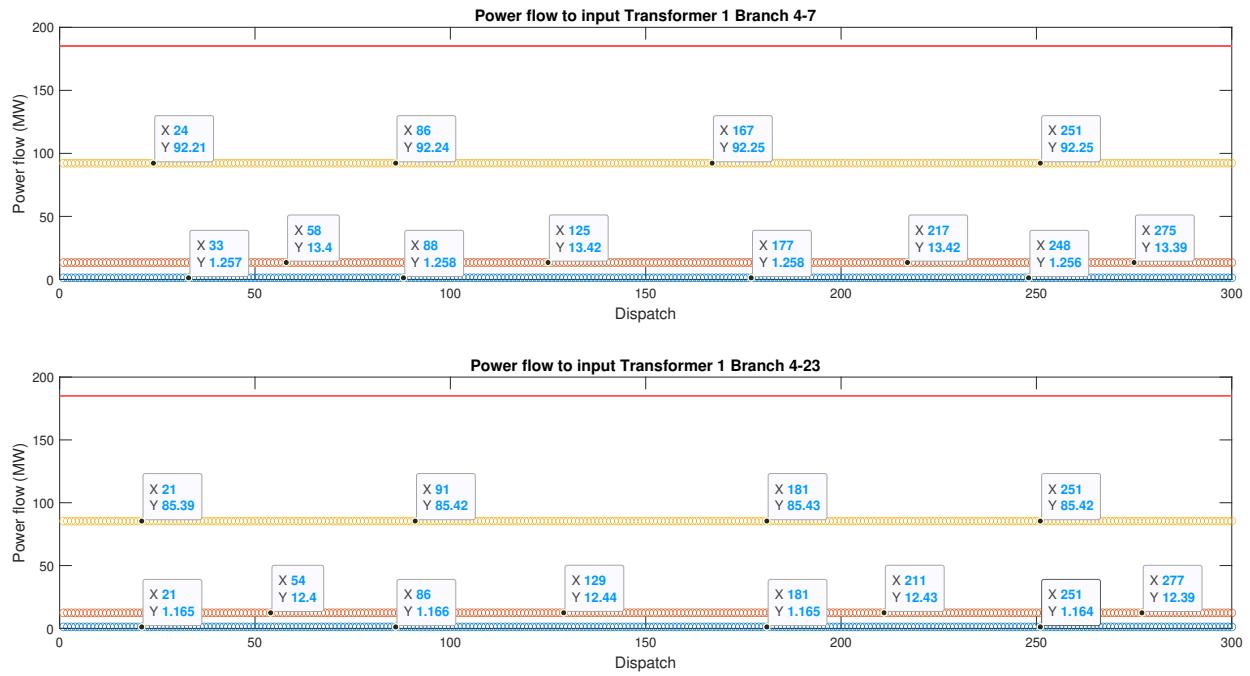
Figure A.25: Power flow through branches 4-7 and 4-23 for the wind farm. From down to up, wind speeds = 4;7.5;14 m/s. The red line visualizes the apparent power limit for this branch.
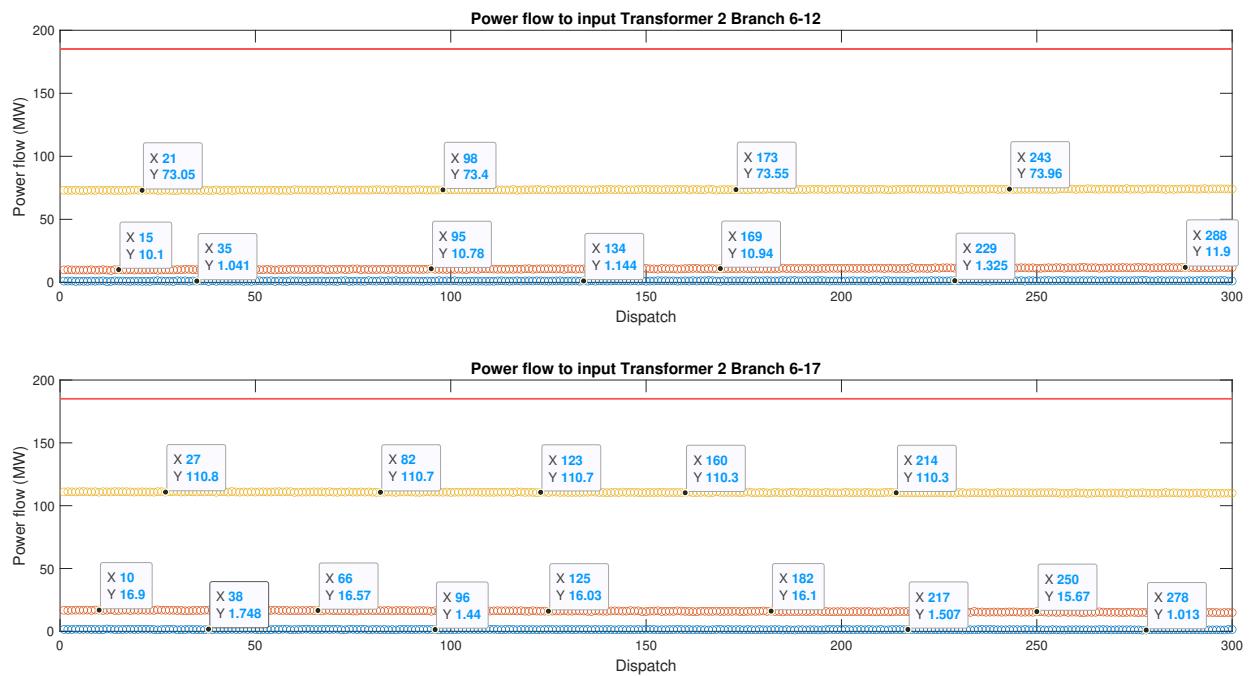
Figure A.26: Power flow through branches 6-12 and 6-17 for the wind farm. From down to up, wind speeds = 4;7.5;14 m/s. The red line visualizes the apparent power limit for this branch.

A.7.5. Wind farm with shunt reactor connection
A.7.6. Power losses
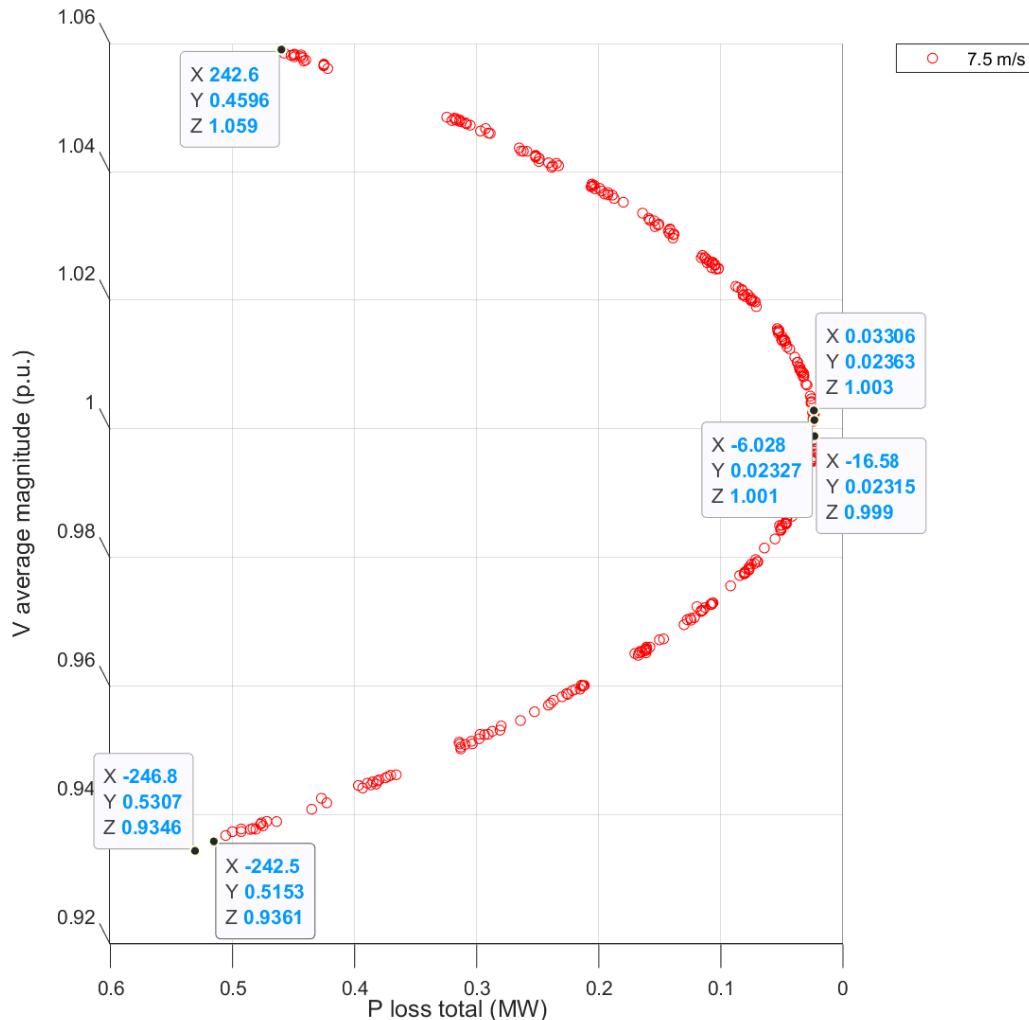
Figure A.27: 3-D relation of the of the average voltage magnitude(p.u.), active power losses and random Q demands for the wind farm, in which the shunt reactor is connected. This plot is generated in order to show the relations in a clear and visualizable manner.
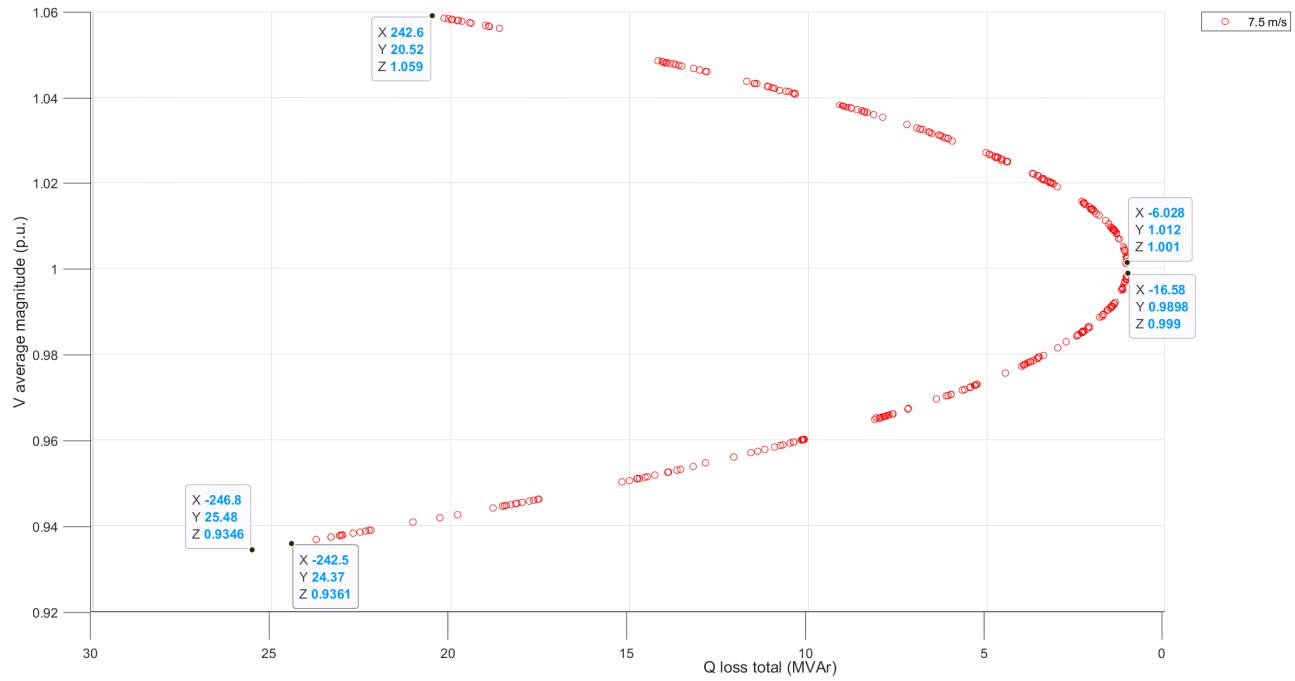
Figure A.28: 3-D relation of the of the average voltage magnitude(p.u.), active power losses and random Q demands for the wind farm, in which the shunt reactor is connected. This plot is generated in order to show the relations in a clear and visualizable manner.
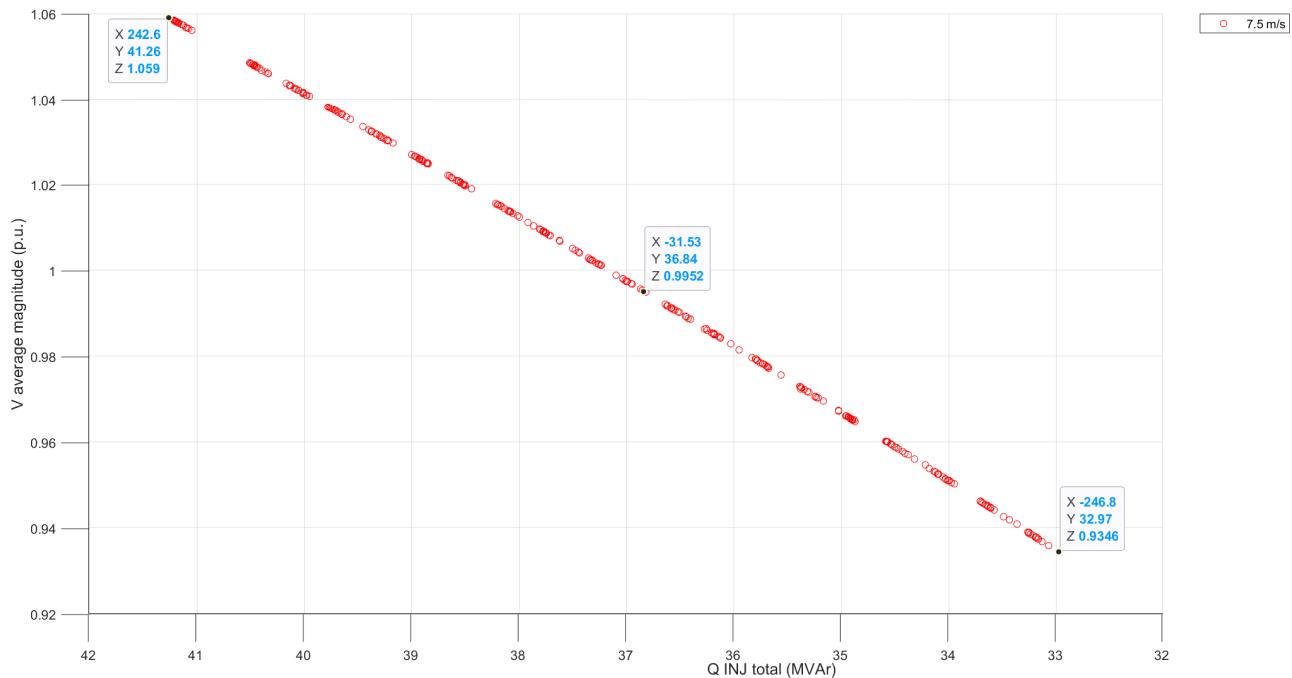
Figure A.29: 3-D relation of the of the average voltage magnitude(p.u.), active power losses and random Q demands for the wind farm, in which the shunt reactor is connected. This plot is generated in order to show the relations in a clear and visualizable manner.

A.7.7. Solar farm Plots
A.7.8. Power losses
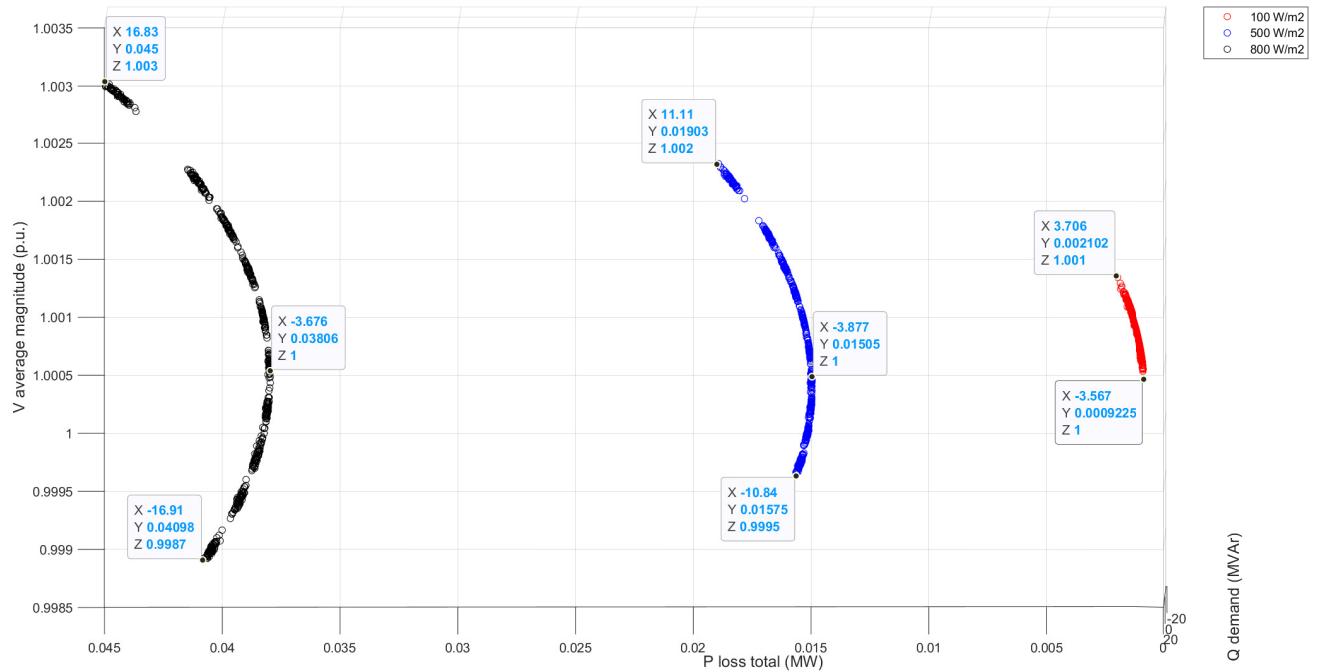
Figure A.30: 3-D plot of the relation of the average voltage magnitude (p.u.), active power losses and random Q demands for the solar farm. This plot is generated in order to show the relations in a clear and visualizable manner.
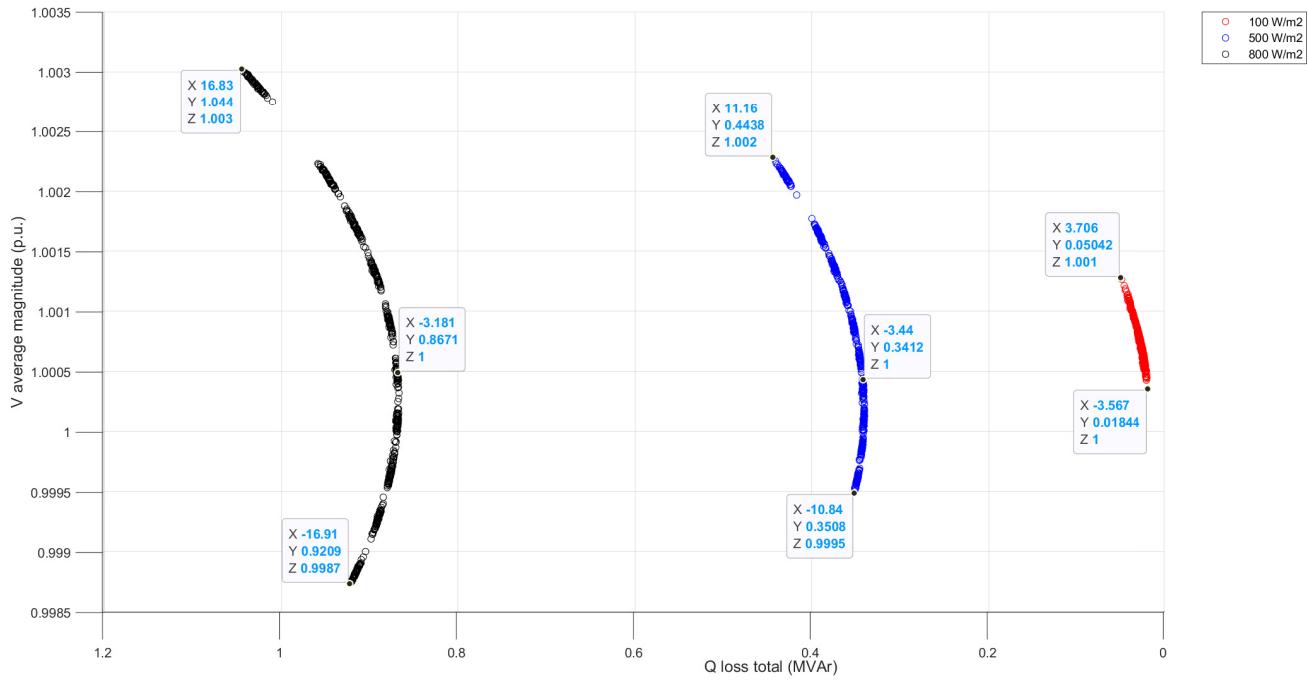
Figure A.31: 3-D plot of the relation of the average voltage magnitude (p.u.), reactive power losses and random Q demands for the solar farm. This plot is generated in order to show the relations in a clear and visualizable manner.
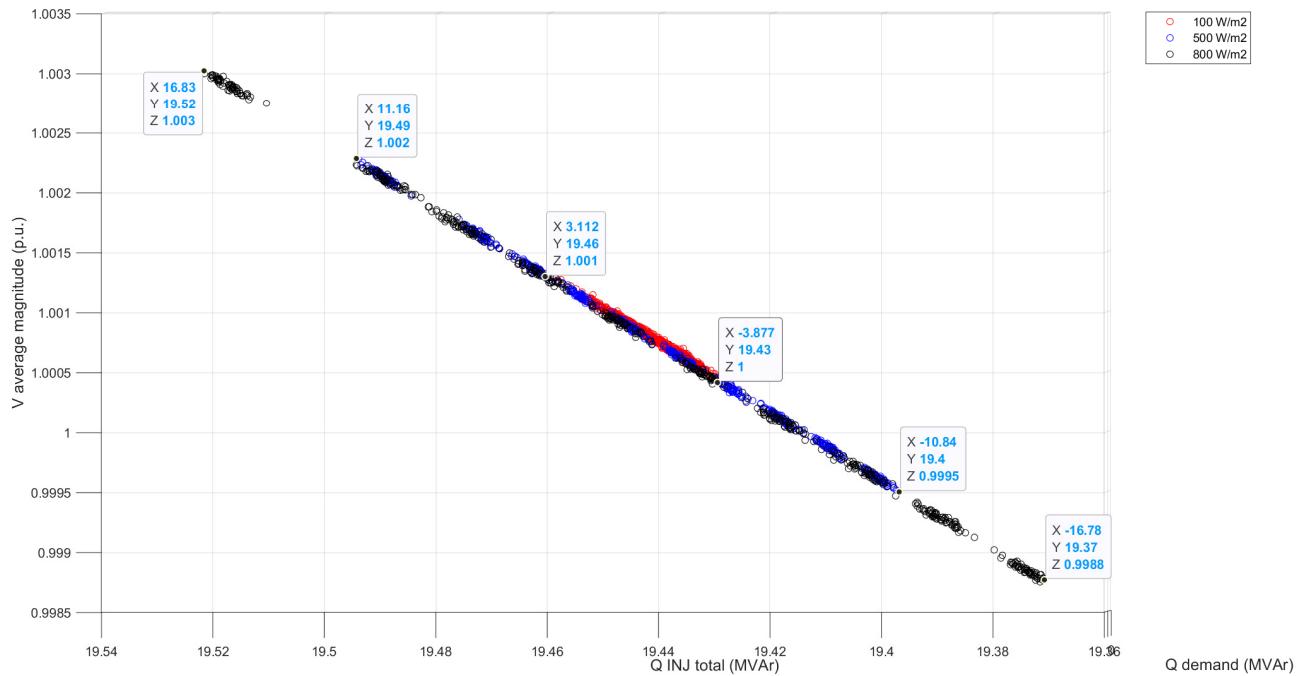
Figure A.32: 3-D plot of the relation of the average voltage magnitude (p.u.), sum of power injections and random Q demands for the hybrid farm. This plot is generated in order to show the relations in a clear and visualizable manner.

## A.7.9. Power flows through transformer and PCC branch
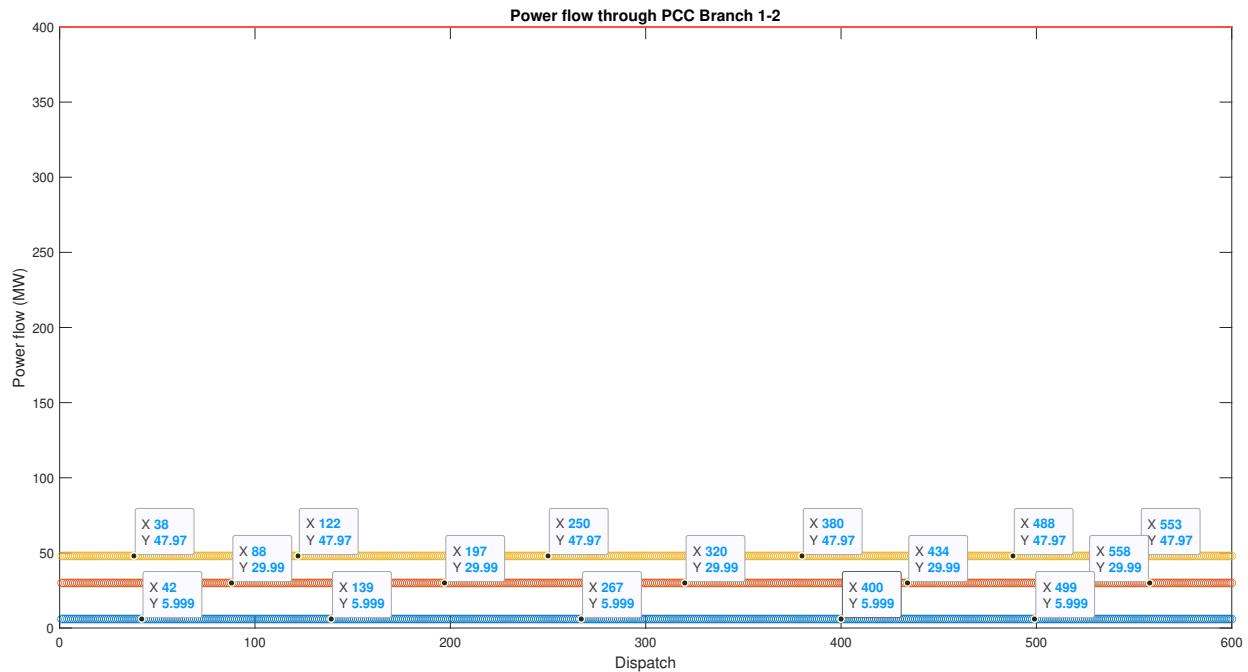
Figure A.33: Power flow through branch 1-2 for the solar farm. From down to up, solar irradiance = 100;500;800 W/m2. The red line visualizes the apparent power limit for this branch.
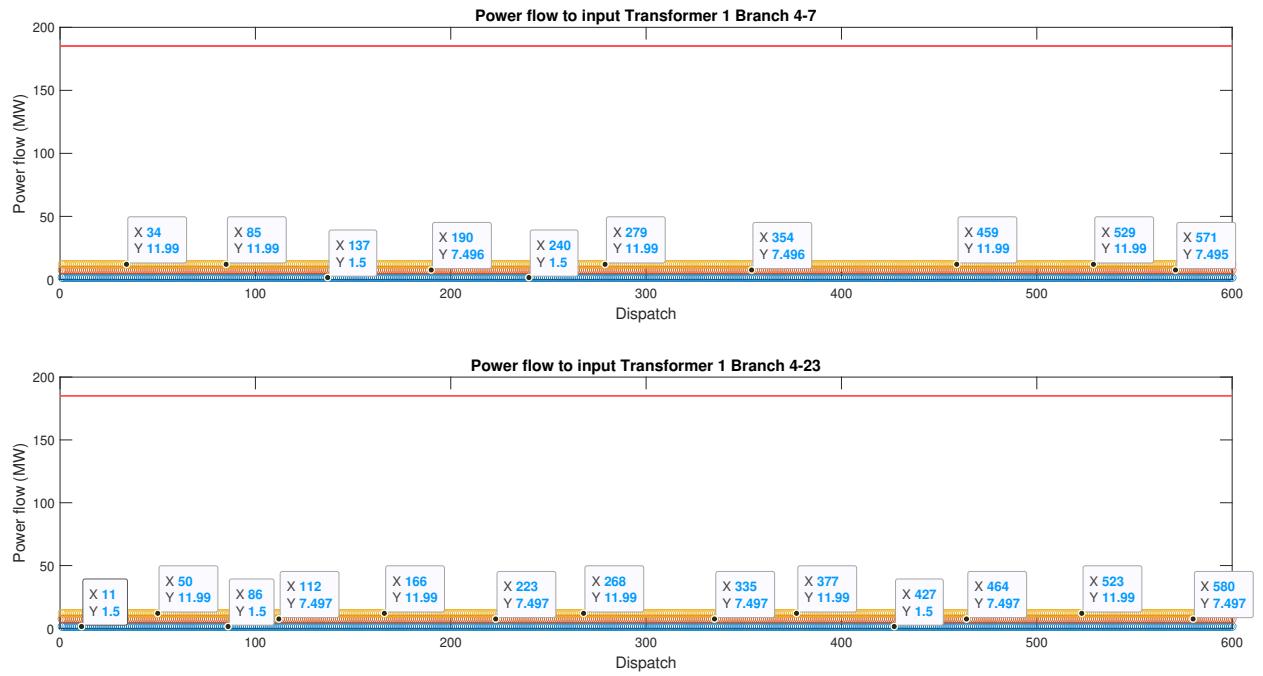
Figure A.34: Power flow through branch 4-7 and 4-23 for the solar farm. From down to up, solar irradiance = 100;500;800 W/m2. The red line visualizes the apparent power limit for this branch.
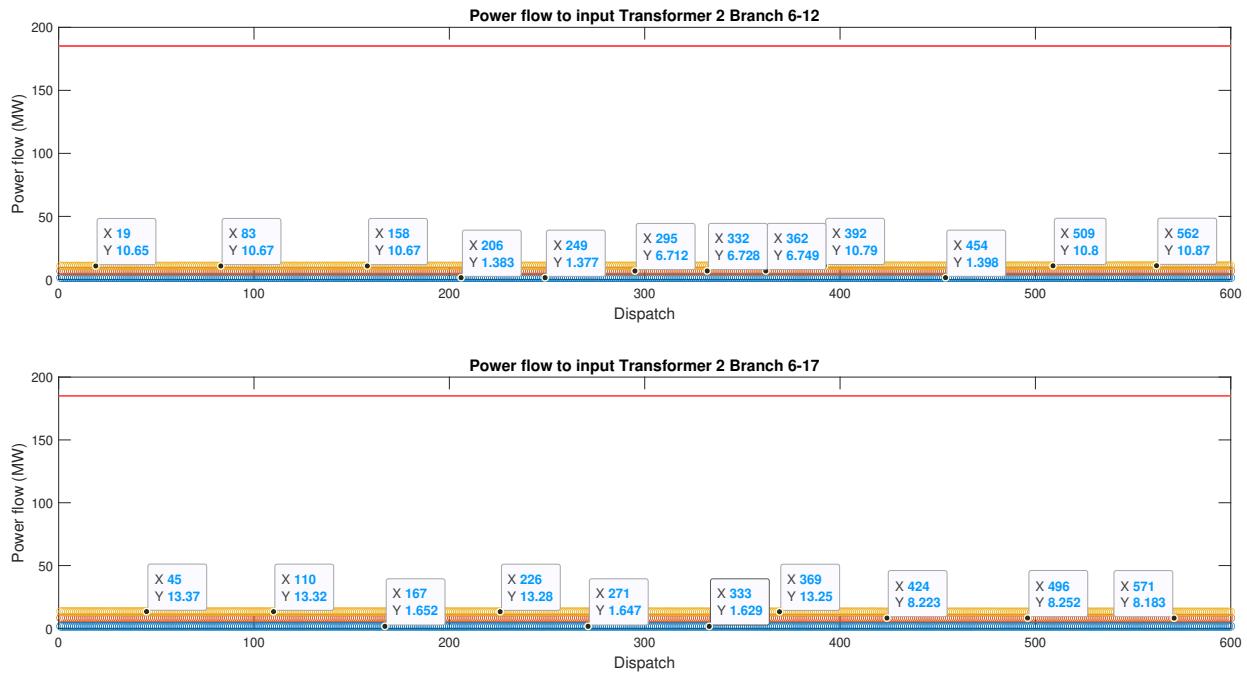
Figure A.35: Power flow through branch 6-12 and 6-17 for the solar farm. From down to up, solar irradiance = 100;500;800 W/m2. The red line visualizes the apparent power limit for this branch.
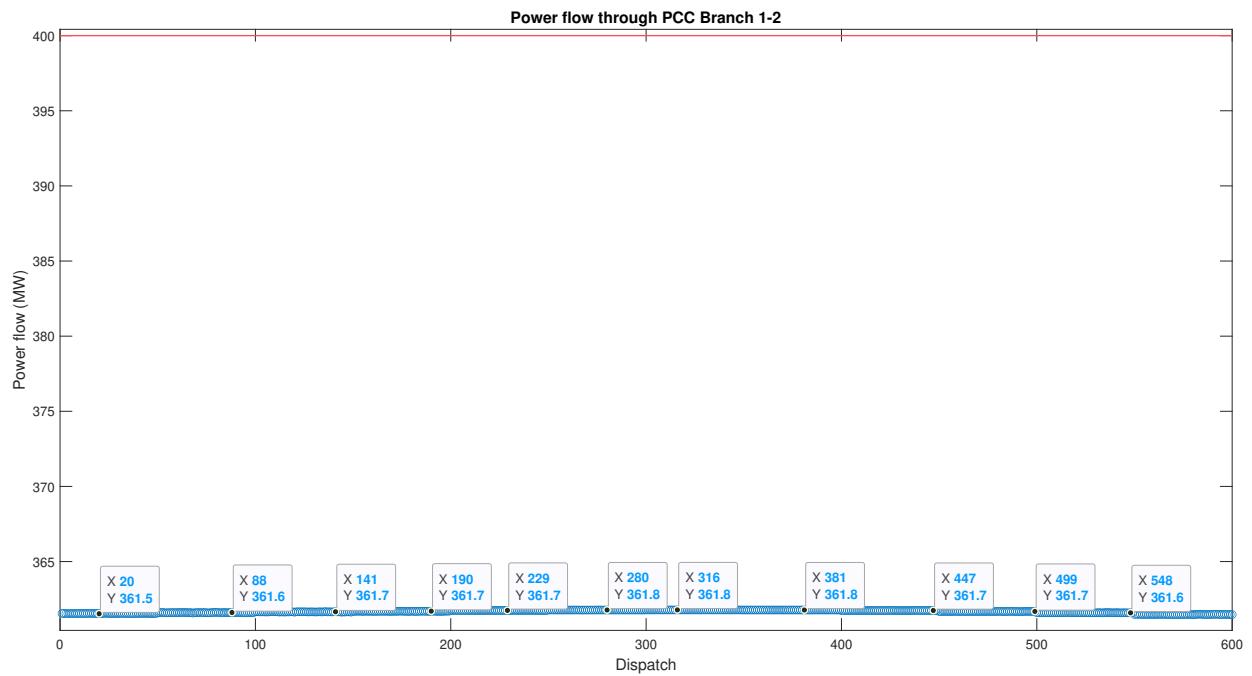
Figure A.36: Power flow through branch 1-2 for the wind farm for 14 m/s. The red line visualizes the apparent power limit for this branch.
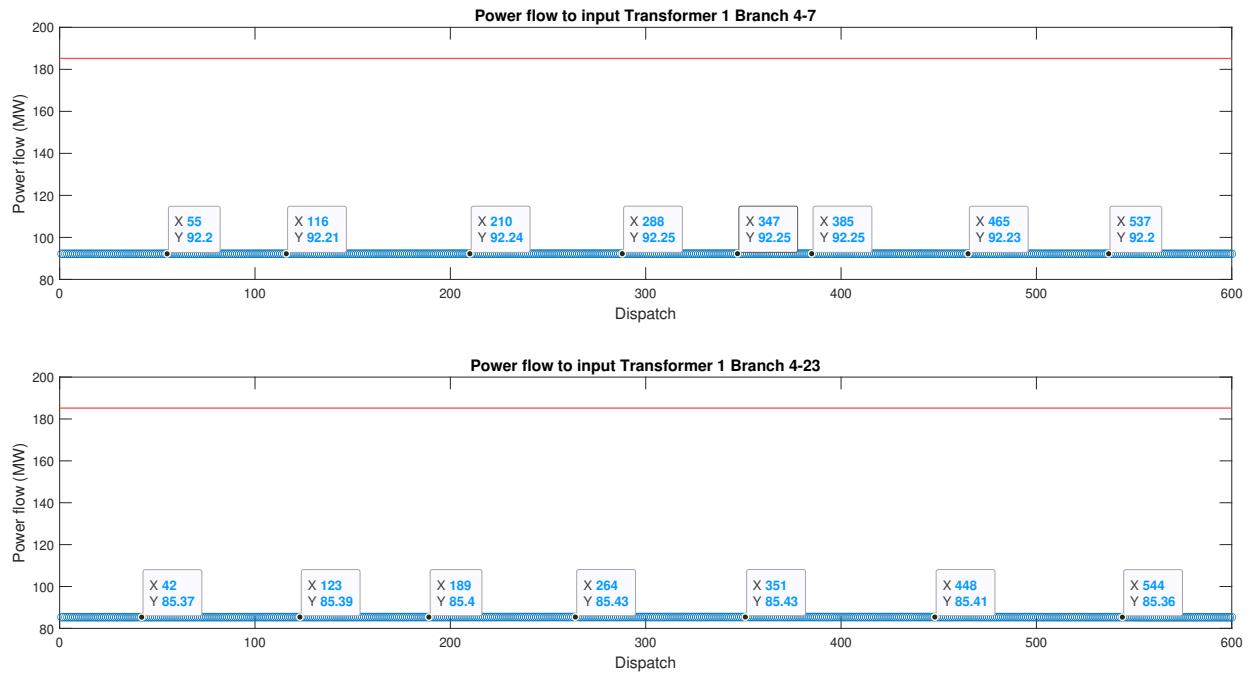
Figure A.37: Power flow through branches 4-7 and 4-23 for the wind farm for 14 m/s. The red line visualizes the apparent power limit for this branch.
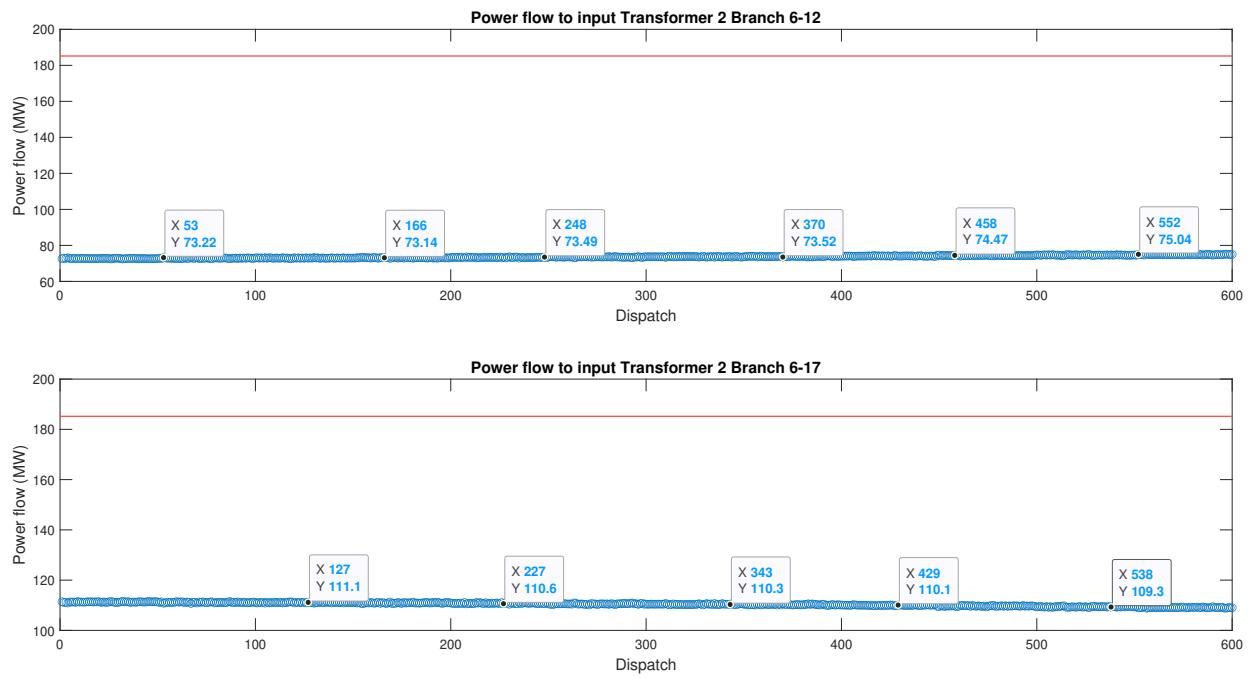
Figure A.38: Power flow through branches 6-12 and 6-17 for the wind farm for 14 m/s. The red line visualizes the apparent power limit for this branch.

A.7.10. Hybrid farm Plots
A.7.11. Power losses
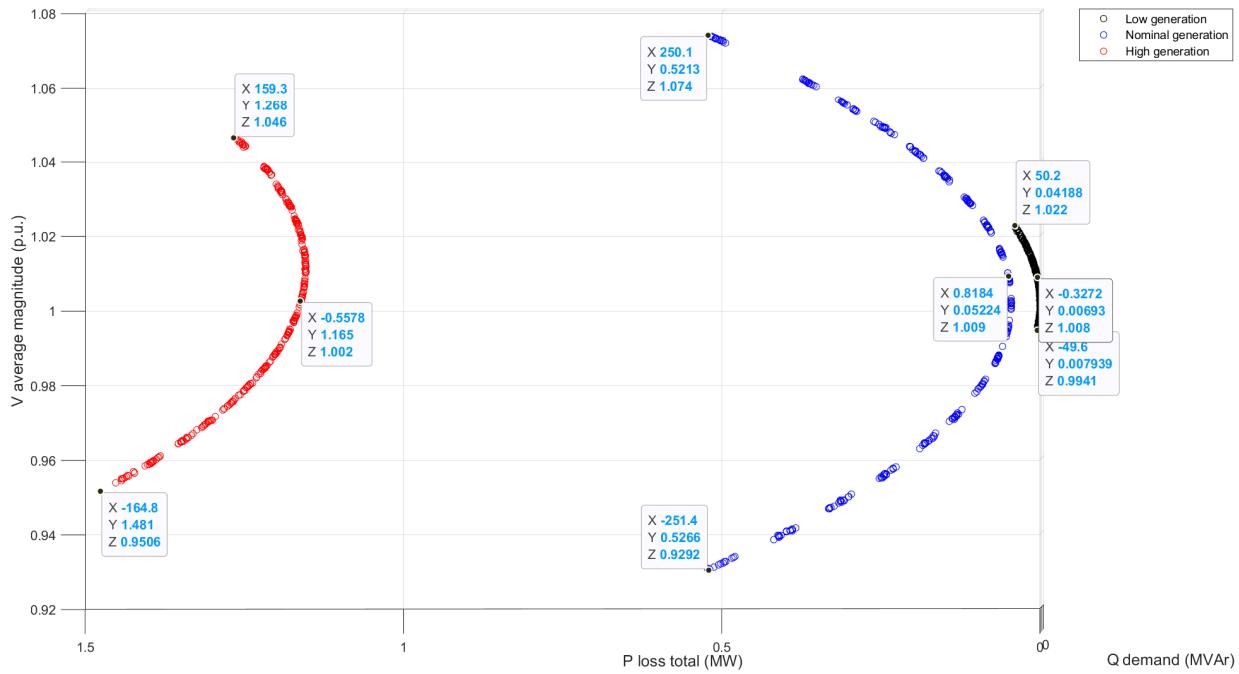
Figure A.39: 3-D plot of the relation of the average voltage magnitude (p.u.), active power losses and random Q demands for the hybrid farm. This plot is generated in order to show the relations in a clear and visualizable manner.
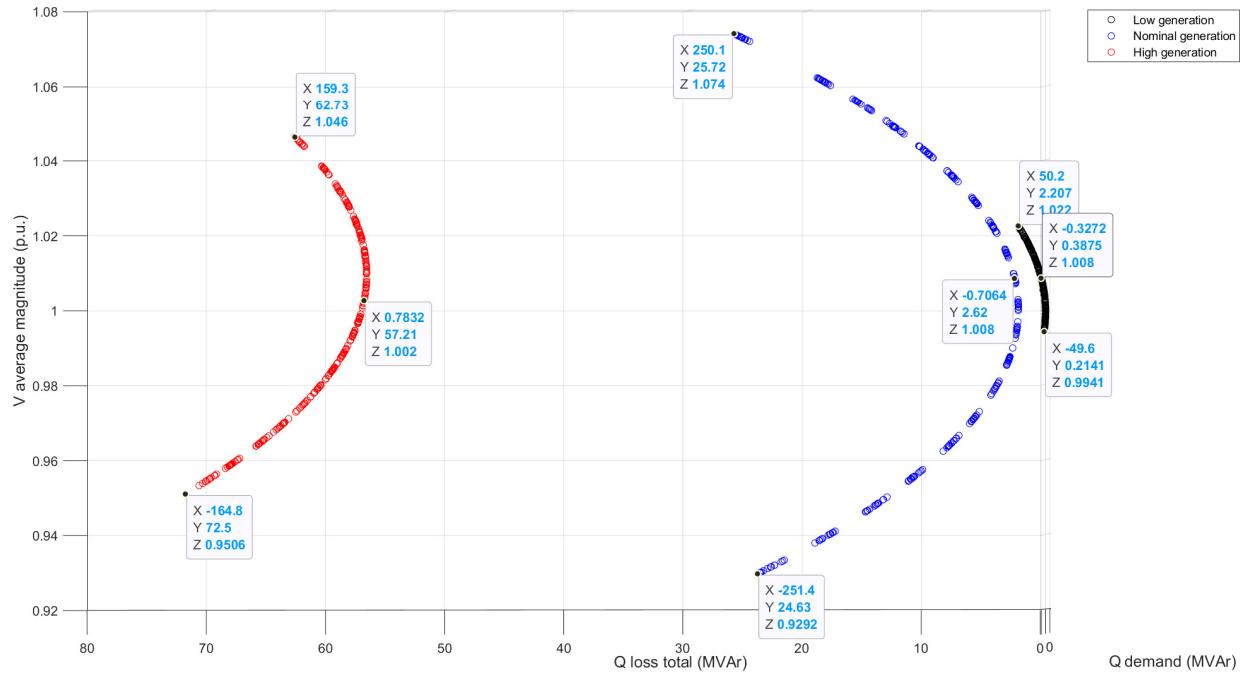
Figure A.40: 3-D plot of the relation of the average voltage magnitude (p.u.), reactive power losses and random Q demands for the hybrid farm. This plot is generated in order to show the relations in a clear and visualizable manner.
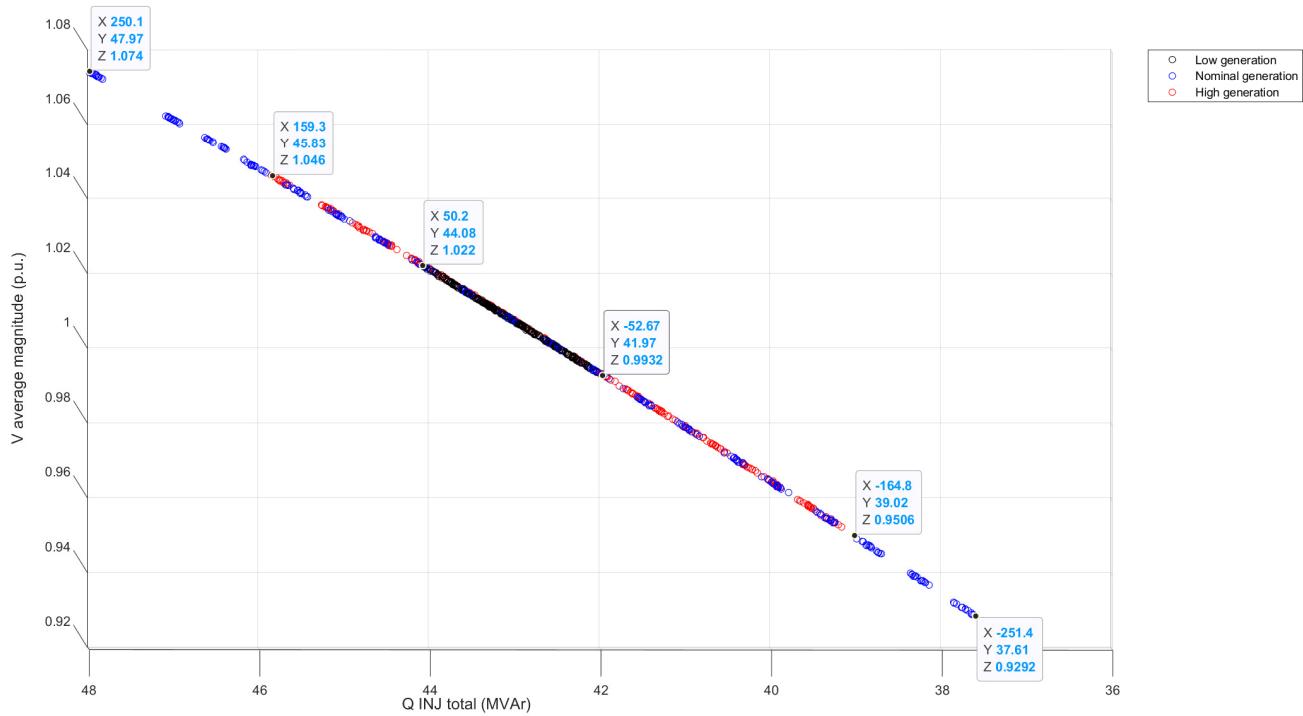
Figure A.41: 3-D plot of the relation of the average voltage magnitude (p.u.), sum of power injections and random Q demands for the hybrid farm. This plot is generated in order to show the relations in a clear and visualizable manner.

A.7.12. Voltage profiles
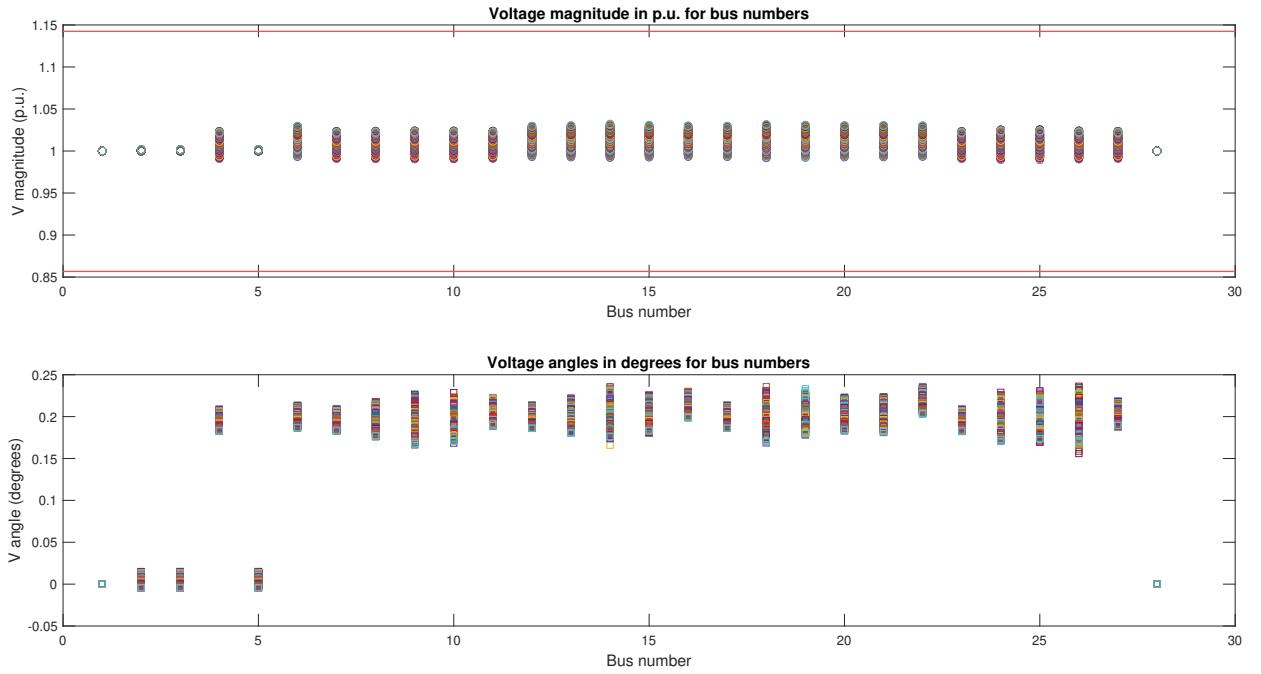
Figure A.42: Voltage magnitude and angle for each bus number of App. A.3 after running power flows for the hybrid farm at low generation (4 m/s and 100 W/m2). Most busses deviate from 1 p.u., except for the slack bus, i.e. bus 1.
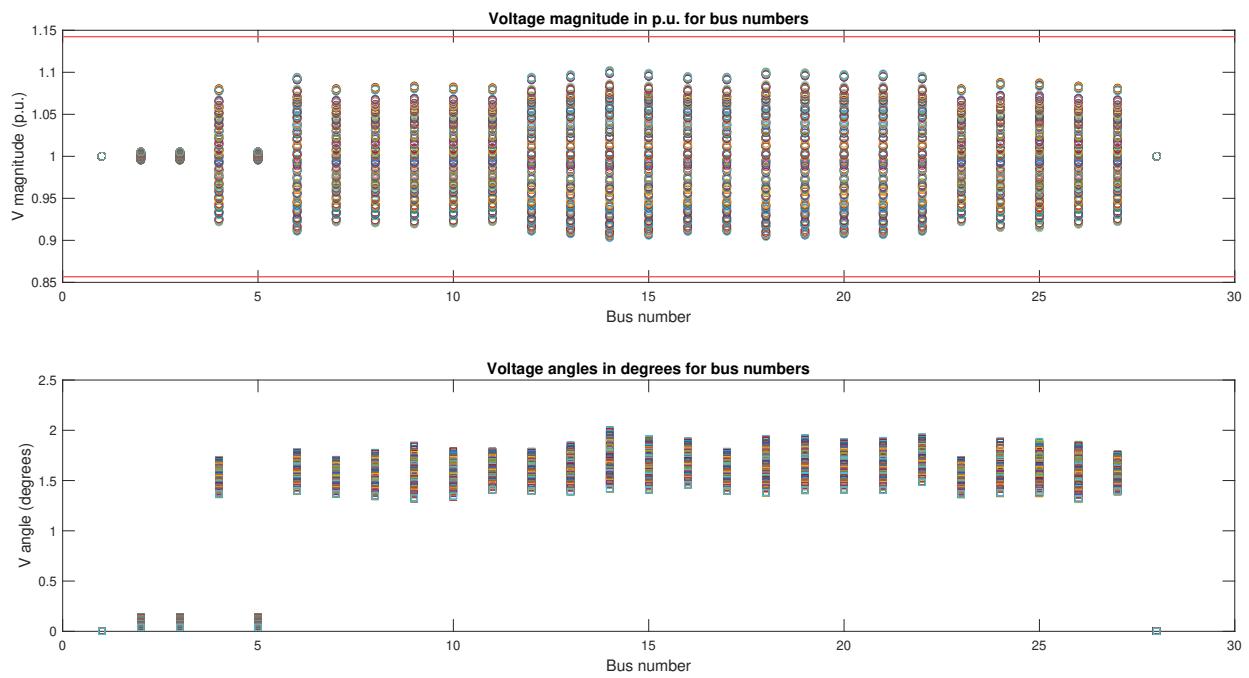
Figure A.43: Voltage magnitude and angle for each bus number of App. A.3 after running power flows for the hybrid farm at low generation (7.5 m/s and 500 W/m2). Most busses deviate from 1 p.u., except for the slack bus, i.e. bus 1.
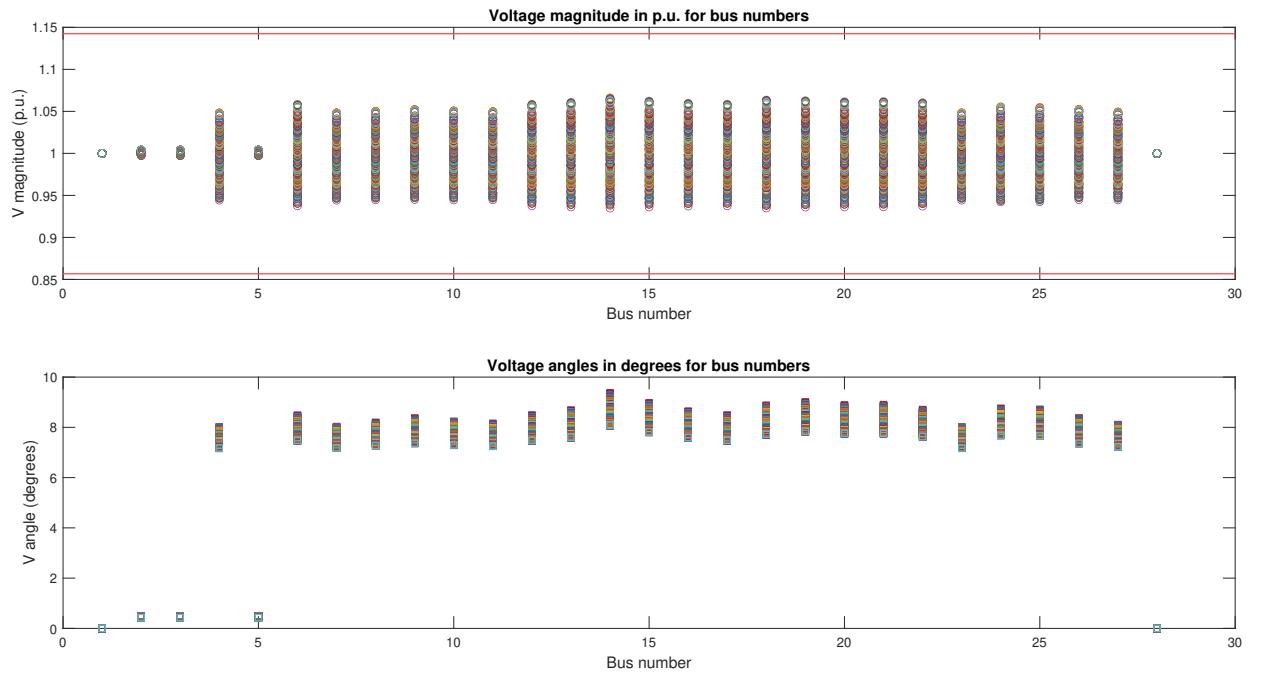
Figure A.44: Voltage magnitude and angle for each bus number of App. A.3 after running power flows for the hybrid farm at low generation (14 m/s and 800 W/m2). Most busses deviate from 1 p.u., except for the slack bus, i.e. bus 1.

A.7.13. Power flows through transformer and PCC branch
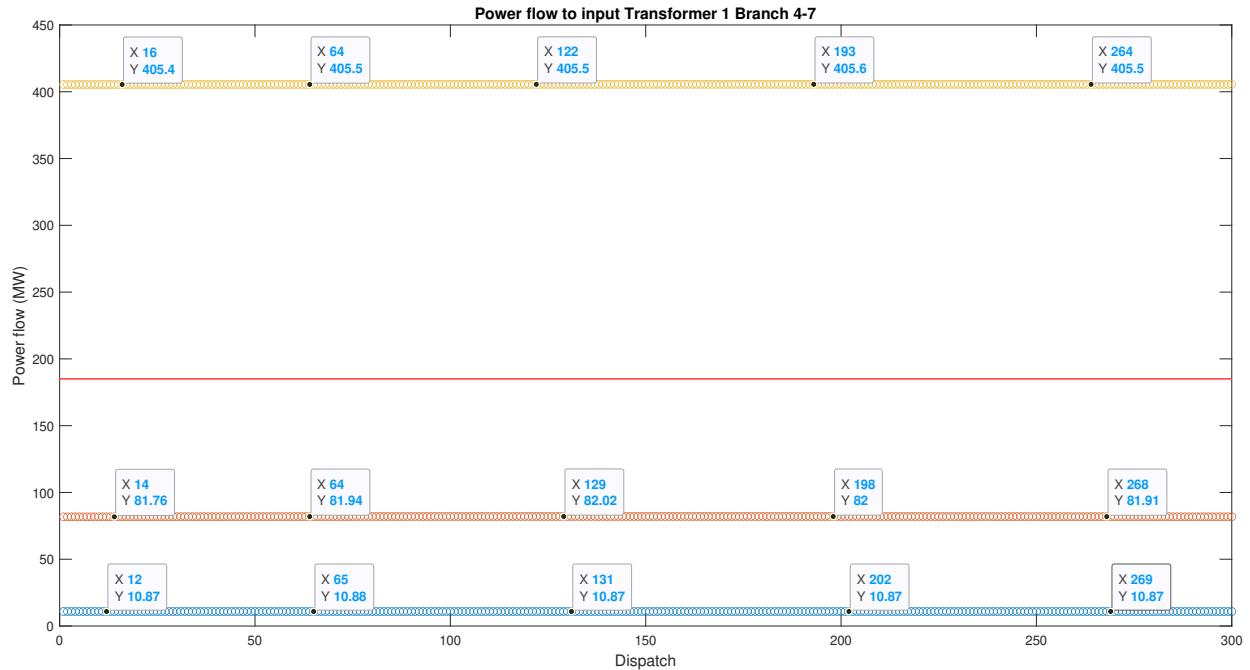
Figure A.45: Power flow through branch 1-2 for the hybrid farm. From down to up, active power generation: low; normal; high. The red line visualizes the apparent power limit for this branch
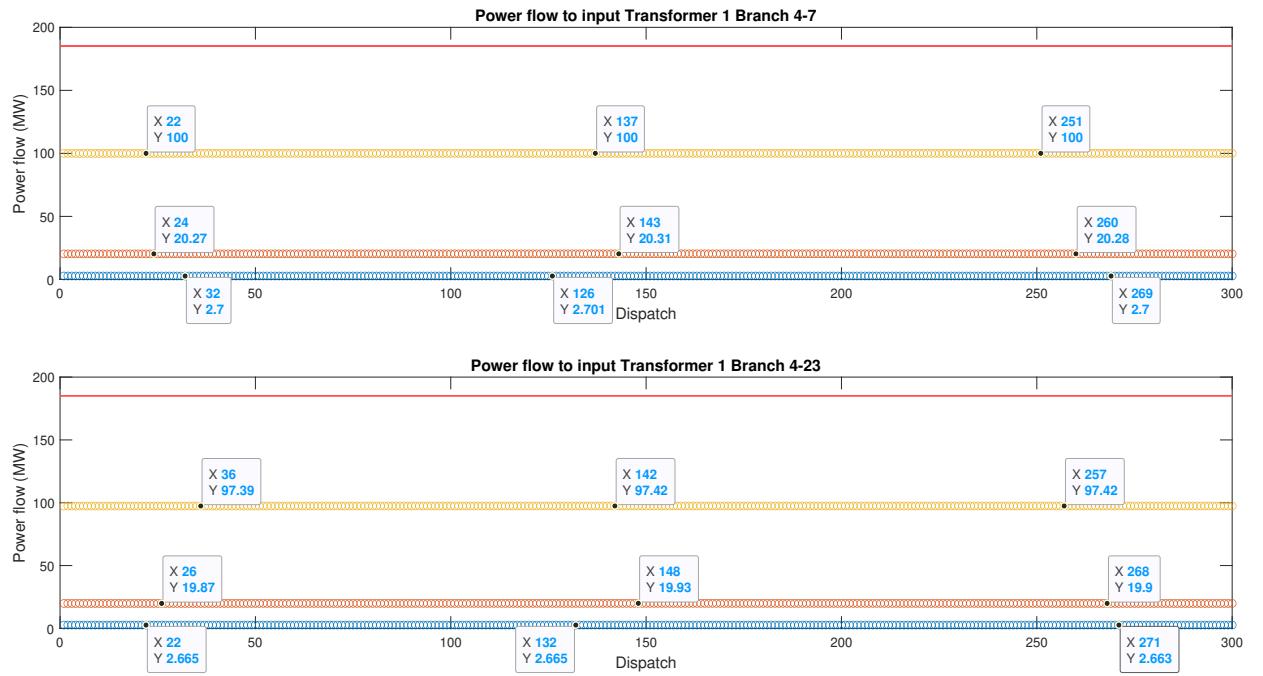
Figure A.46: Power flow through branches 4-7 and 4-23 for the hybrid farm. From down to up, active power generation: low; normal; high. The red line visualizes the apparent power limit for this branch
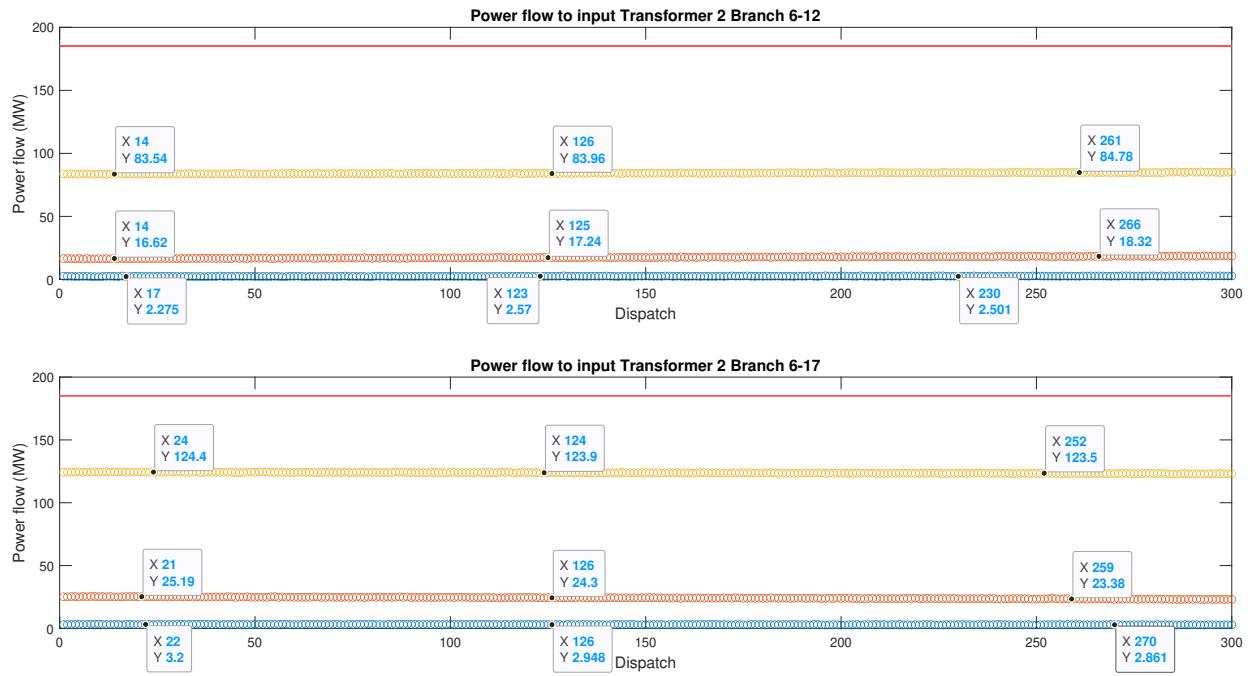
Figure A.47: Power flow through branches 6-12 and 6-17 for the hybrid farm. From down to up, active power generation: low; normal; high. The red line visualizes the apparent power limit for this branch

A.7.14. String level wind farm plots
A.7.15. Power losses
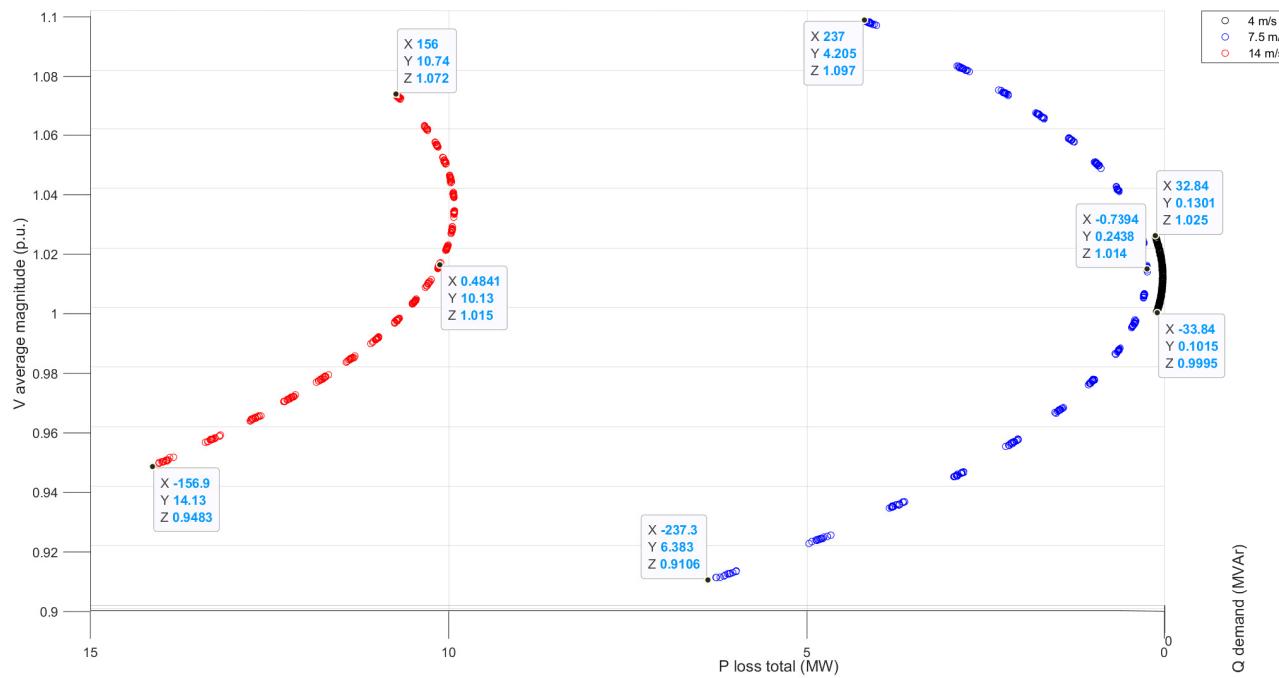
Figure A.48: 3-D plot of the relation of the average voltage magnitude (p.u.), active power losses and random Q demands for the wind farm on string level. This plot is generated in order to show the relations in a clear and visualizable manner.
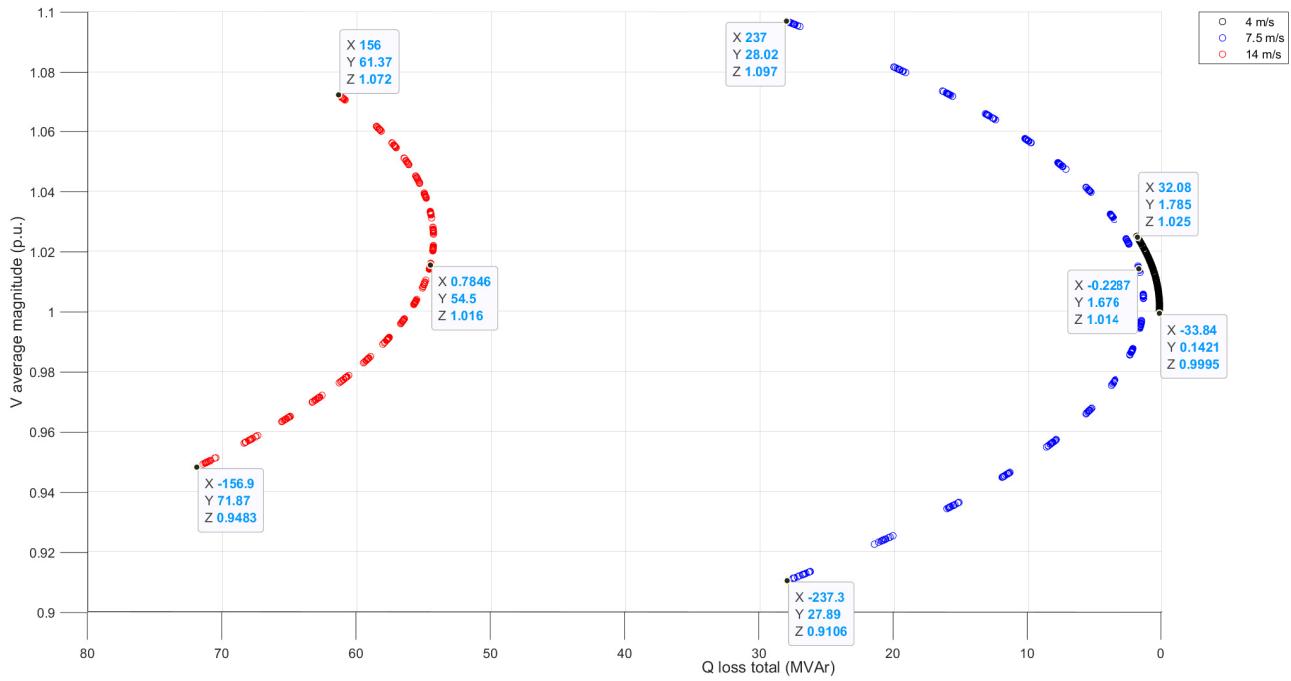
Figure A.49: 3-D plot of the relation of the average voltage magnitude (p.u.), reactive power losses and random Q demands for the wind farm on string level. This plot is generated in order to show the relations in a clear and visualizable manner.
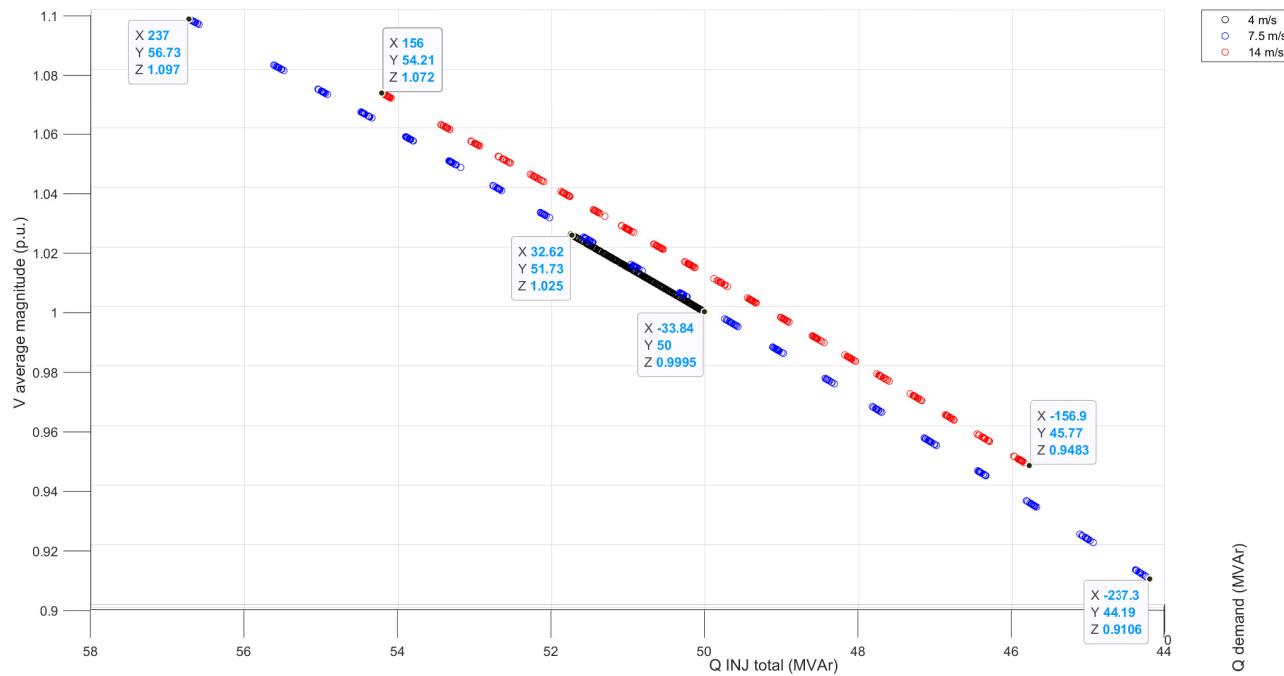
Figure A.50: 3-D plot of the relation of the average voltage magnitude (p.u.), sum of reactive power injections and random Q demands for the wind farm on string level. This plot is generated in order to show the relations in a clear and visualizable manner.

A.7.16. Voltage profiles
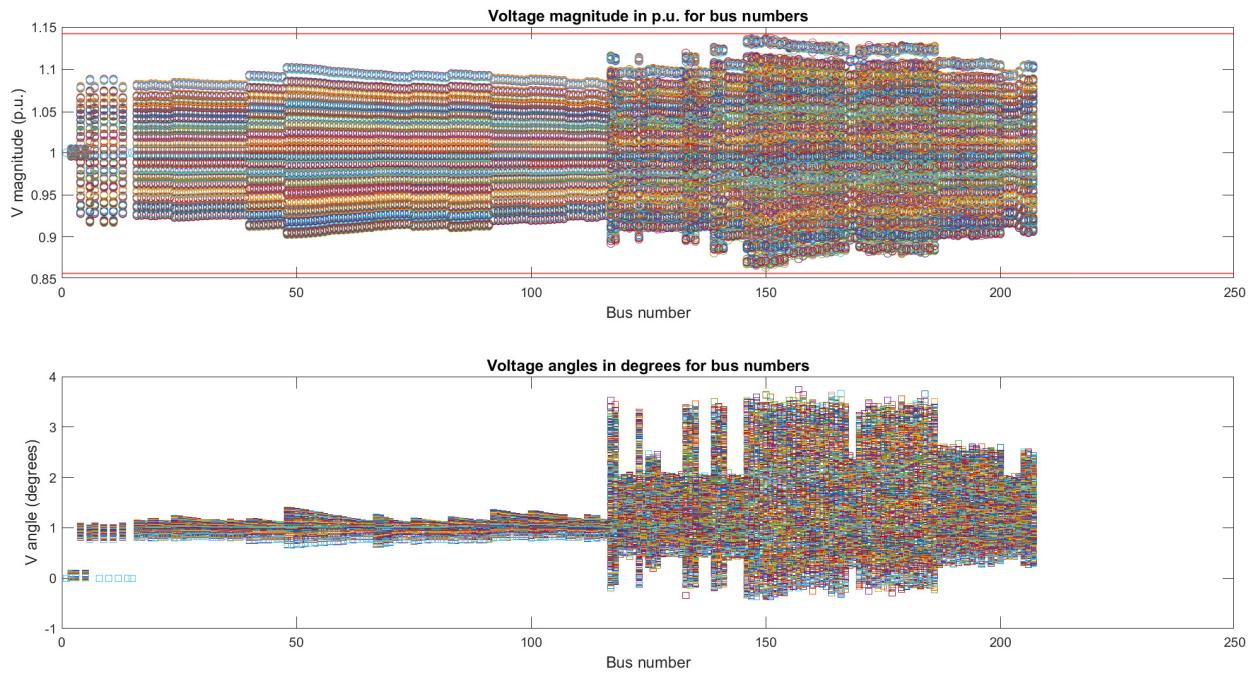
Figure A.51: Voltage magnitude and angle for each bus number of App. A.3 after running power flows for the wind farm on string level at 7.5 m/s. Most busses deviate from 1 p.u., except for the slack bus, i.e. bus 1.

A.7.17. Power flows through transformer and PCC branch
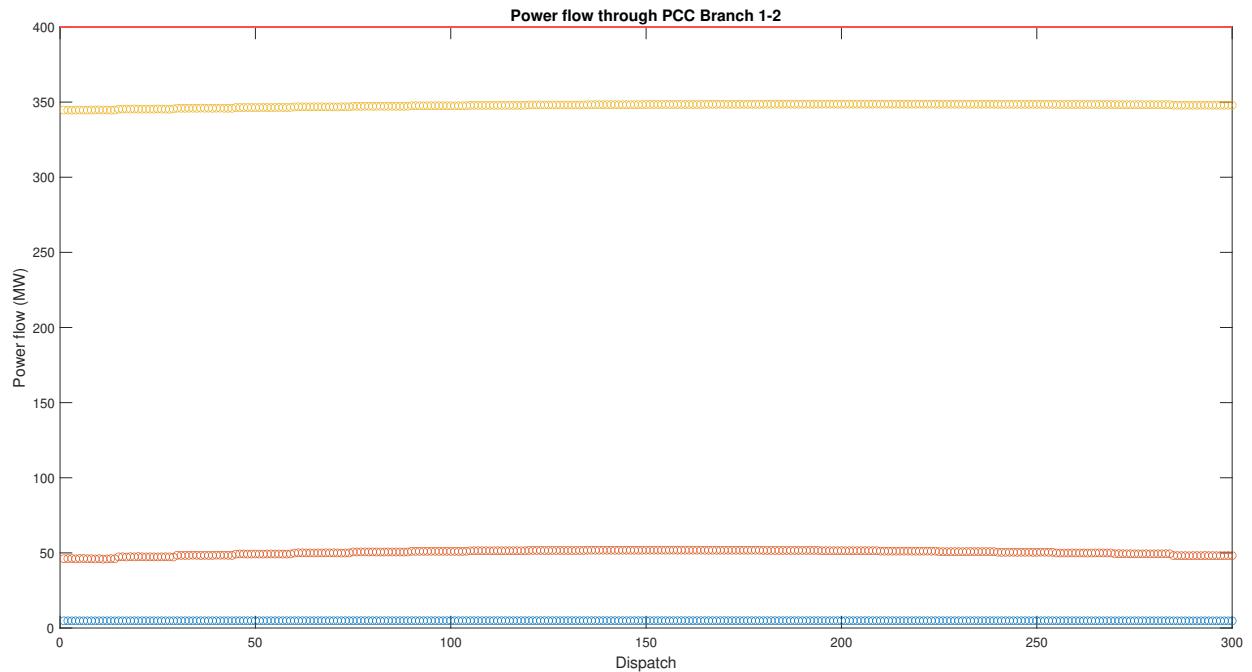
Figure A.52: Power flow through branche 1-2 for the wind farm modeled on string level. From down to up, wind speeds = 4;7.5;14 m/s. The red line visualizes the apparent power limit for this branch.
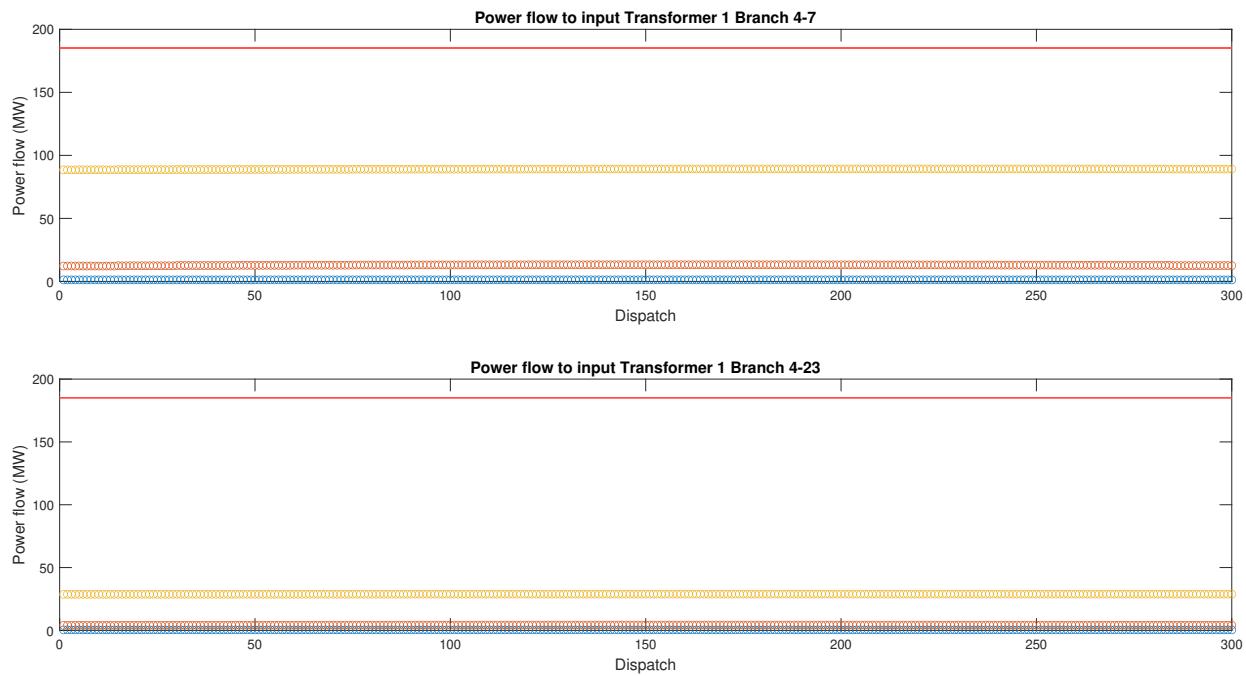
Figure A.53: Power flow through branches 4-7 and 4-23 for the wind farm modeled on string level. From down to up, wind speeds = 4;7.5;14 m/s. The red line visualizes the apparent power limit for this branch.
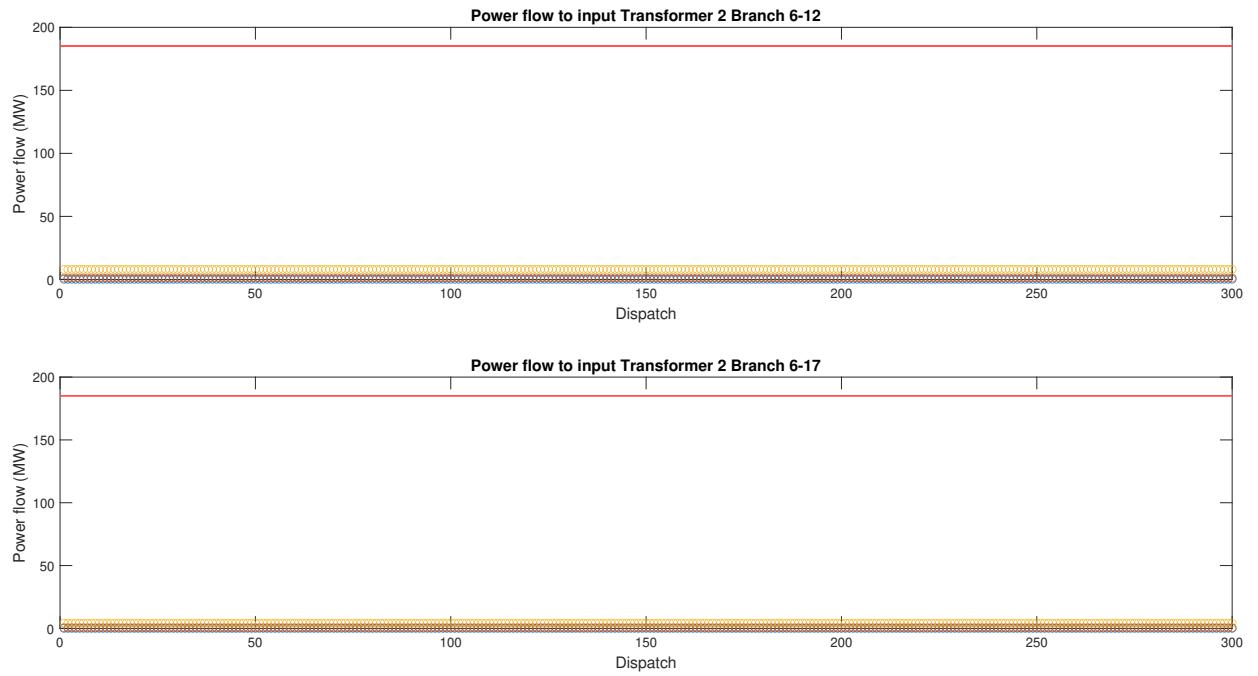
Figure A.54: Power flow through branches 6-12 and 6-17 for the wind farm modeled on string level. From down to up, wind speeds = 4;7.5;14 m/s. The red line visualizes the apparent power limit for this branch.
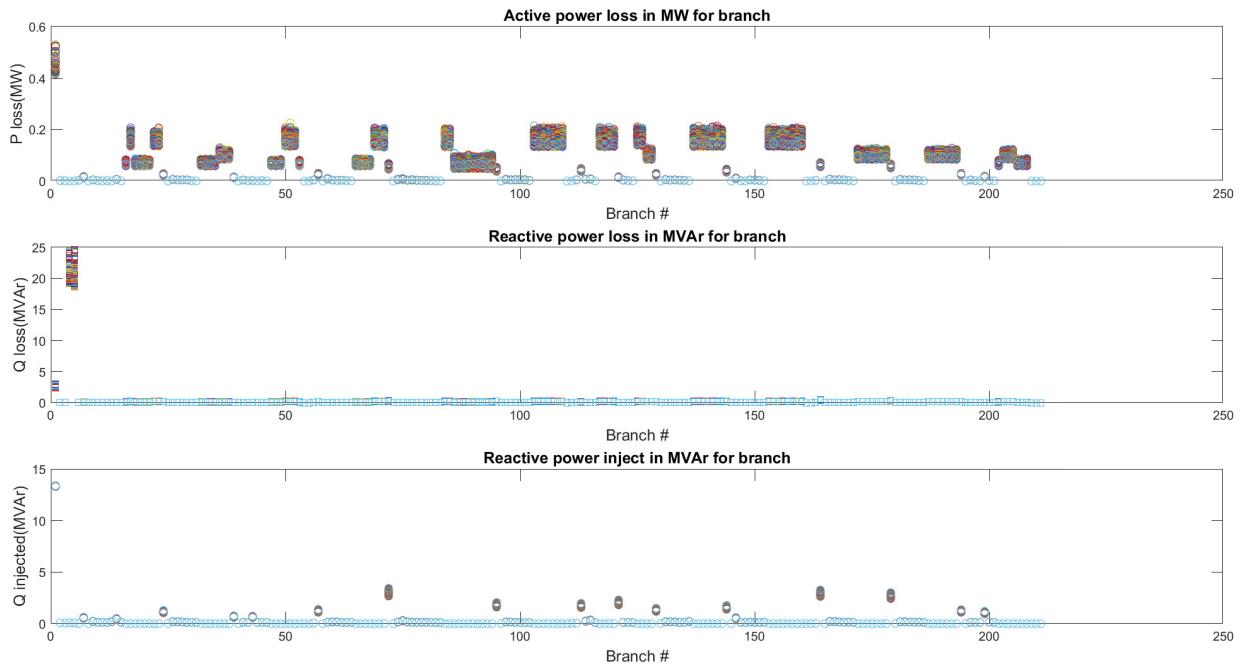
Figure A.55: Active, reactive, injective losses in the each branch of the wind farm on string level system with a wind speed of 14 m/s. The 2 busses connected to the specified branch are shown in App. A.16.

A.8. Prototype
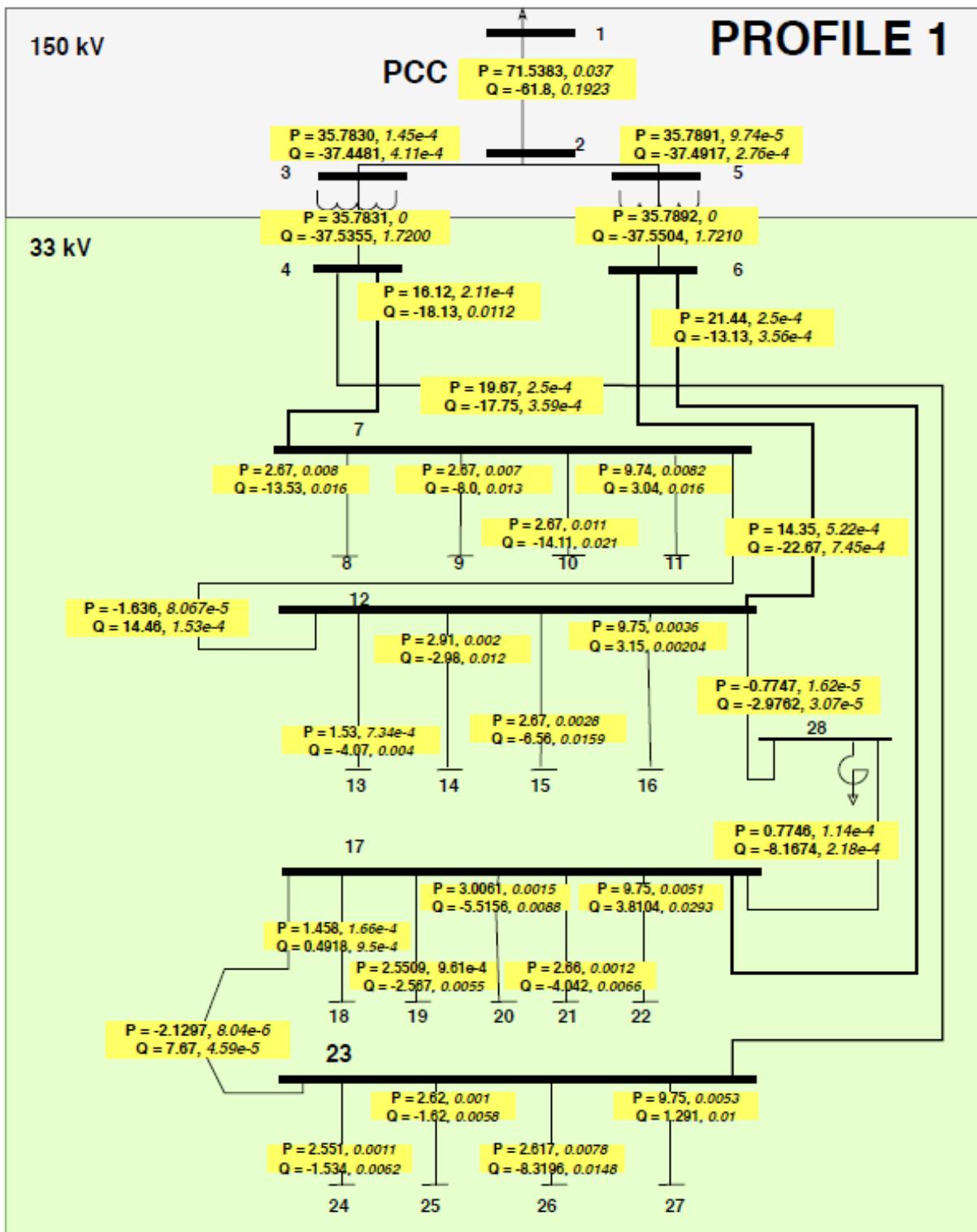
Figure A.56: Power flows through system for test profile 1. The profile description is specified in Tab. 4.5. The first column of the power flows is for the P/Q power injection in the branch, written in bold. The second column of the power flows is for the P/Q losses in the branch, written in cursive and bold. Values are in **MW** and **MVAr**.
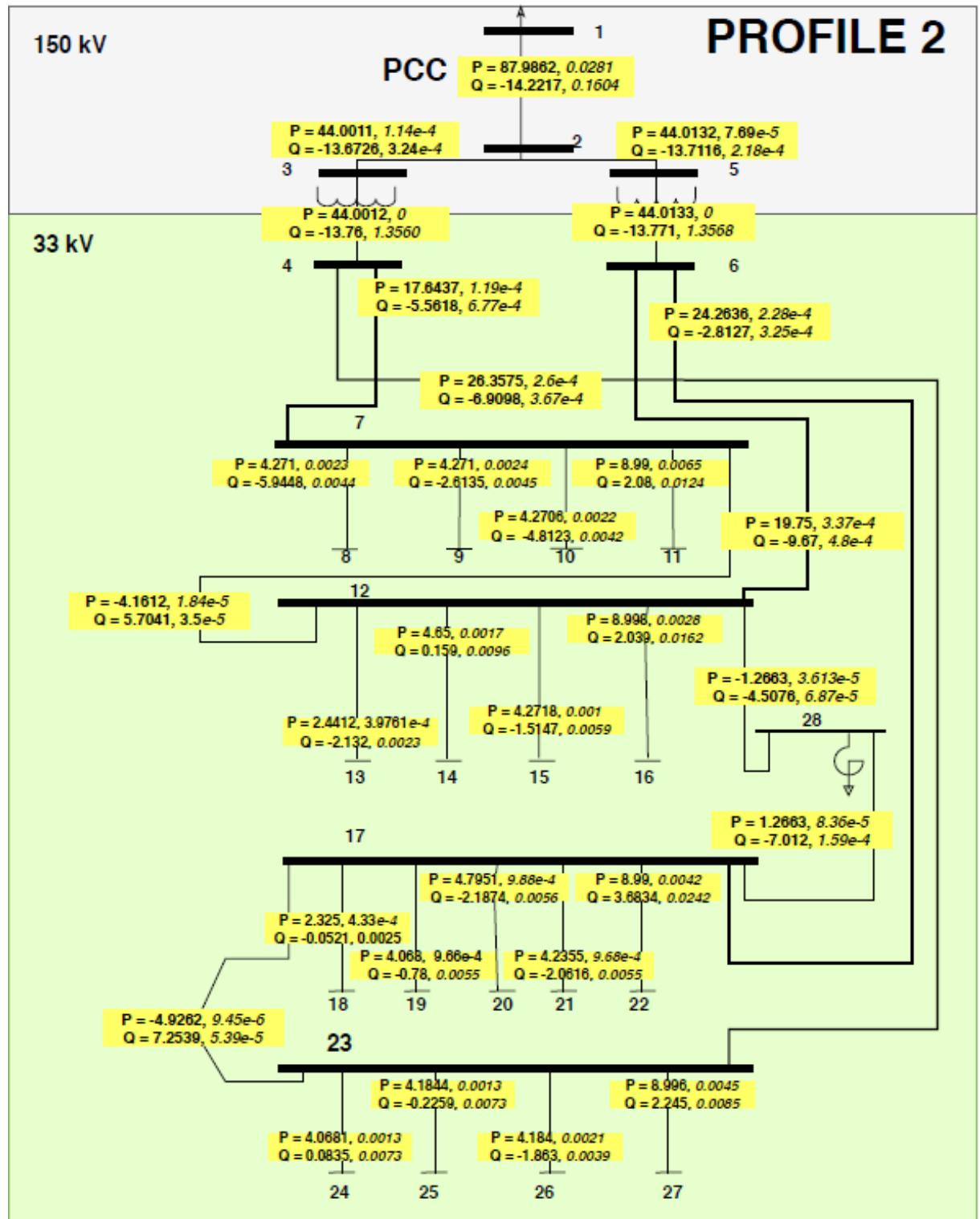
Figure A.57: Power flows through system for test profile 2. The profile description is specified in Tab. 4.5. The first column of the power flows is for the P/Q power injection in the branch, written in bold. The second column of the power flows is for the P/Q losses in the branch, written in cursive and bold. Values are in **MW** and **MVAr**.
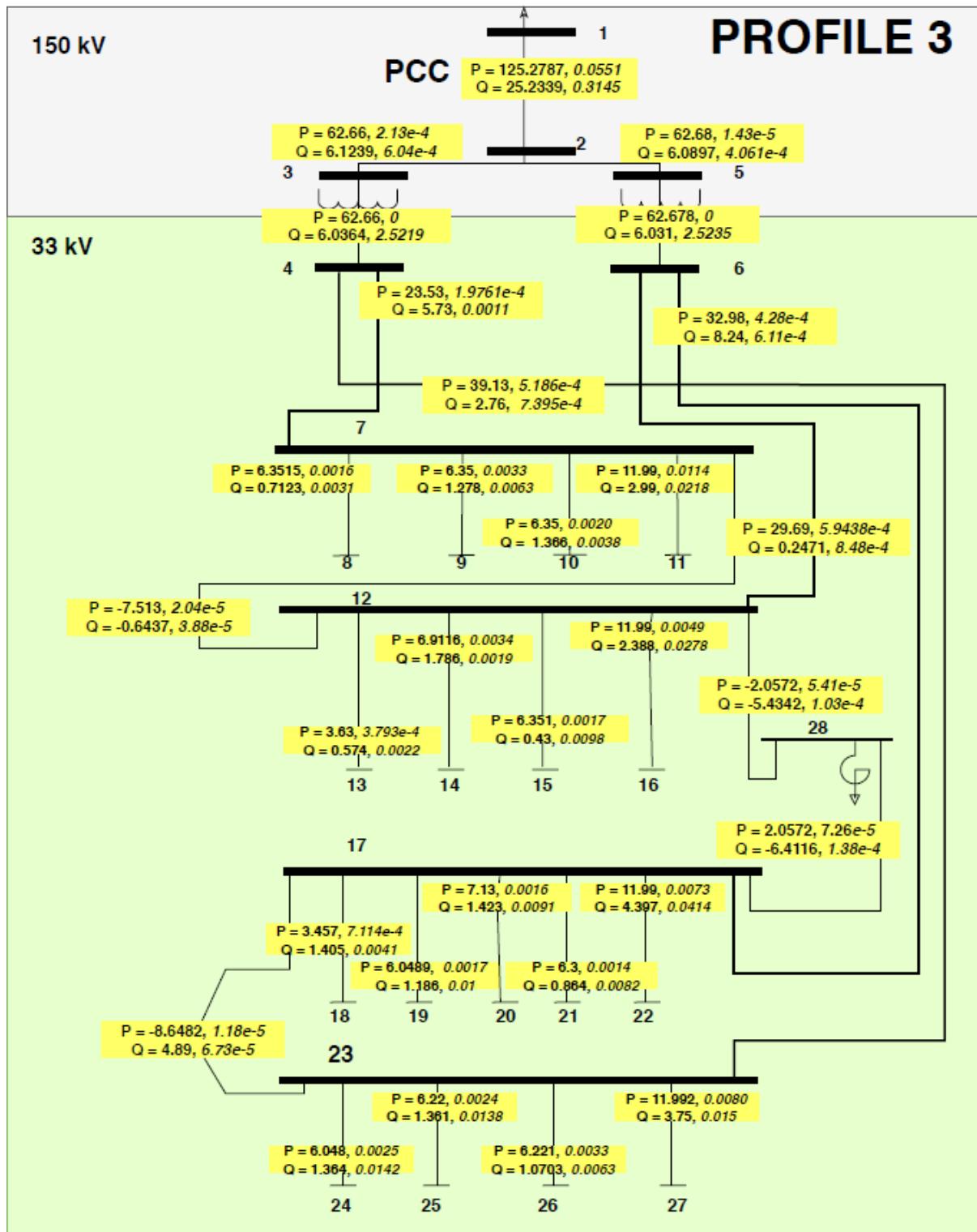
Figure A.58: Power flows through system for test profile 3. The profile description is specified in Tab. 4.5. The first column of the power flows is for the P/Q power injection in the branch, written in bold. The second column of the power flows is for the P/Q losses in the branch, written in cursive and bold. Values are in **MW** and **MVAr**.
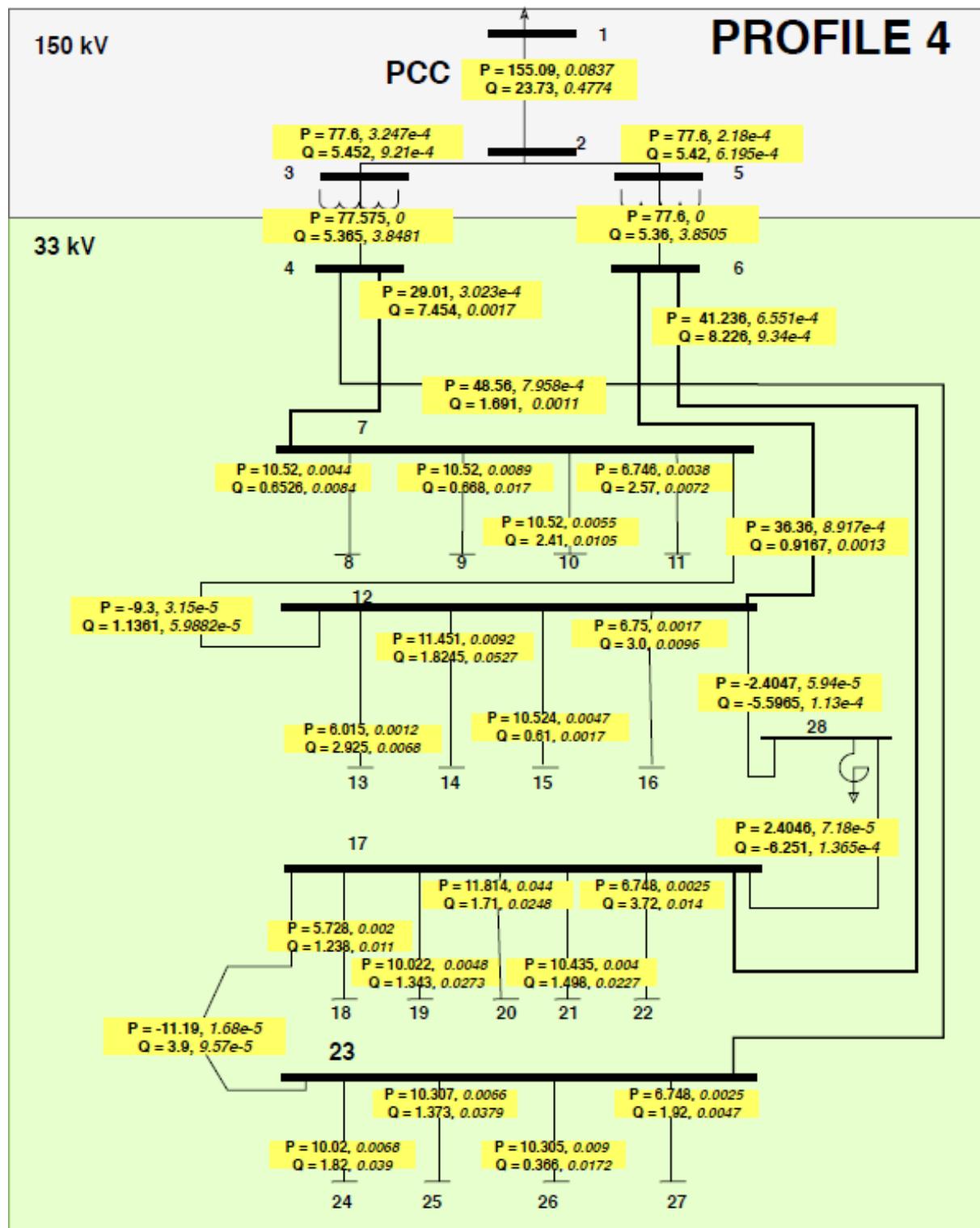
Figure A.59: Power flows through system for test profile 4. The profile description is specified in Tab. 4.5. The first column of the power flows is for the P/Q power injection in the branch, written in bold. The second column of the power flows is for the P/Q losses in the branch, written in cursive and bold. Values are in **MW** and **MVAr**.

A.9. MatLab codes
A.9.1. Newton Raphson method

```
%%Authors: F. Rimon and M. Mastouri
%Last edited: 05/06/2020

%This is a method that simulates the hand calculations done to solve a
%Newton Raphson Power flow

%The case study used is a branch of the case study of the Bachelor
    Thesis
%Project of Group 09.01
close all;
clear all;
clc
%% Power flow for Node 1(Bus 24) of Branch 23-24 with Q from samples_Q
    data #Dispatch 1000
% %Workspace needs to be included

done = 0;
iter = 1; %count iterations needed
while(done == 0 )

mag = 1;
angle = 0;
P_1 = 0.294;
Q_1 = 0.0169;

P1  =(mag*7.1621*cosd(angle-118.6)+7.326*cosd(-80)*(mag^2));
Q1 = (mag*7.1621*sind(angle-118.6)-7.326*sind(-80)*(mag^2));

Calculate derivatives
diff_P1_angle = -7.1621*mag*sind(angle-118.6);
diff_P1_mag = 7.1621*cosd(angle-118.6)+7.326*cosd(-80)*2*mag;

diff_Q1_angle = 7.1621*mag*cosd(angle-118.6);
diff_Q1_mag = 7.1621*sind(angle-118.6)-7.326*sind(-80)*2*mag;

equation to be solved
new_P = P_1-P1;
new_Q = Q_1-Q1;
delta_flow = [new_P;new_Q];

Put derivatives in Jacobian
jacob = [diff_P1_angle diff_P1_mag; diff_Q1_angle diff_Q1_mag];

Solve linear equation
x = linsolve(jacob,delta_flow);
delta_angle_degree = (x(1,:)./(2*pi))*360; %convert radian angle to
    degree angle

specify new angle and magnitude
new_angle = angle - delta_angle_degree;
new_mag = mag - x(2,:);
```

```
determine if result is below threshold

if(new_P <= 0.1)
    done = 1;
    iter = iter;

else
    done = 0;
    mag = new_mag;
    angle = new_angle;
    iter = iter + 1;
end
end

%After the final answers are determined, insert them manually into
    these
%equations to determine the losses in the system.
new_angle = 19.4;
new_mag = 1.0;
Z_l = 0.02356859504 + 0.134446281*i;
new_mag_phasor = new_mag*(cosd(new_angle)+sind(new_angle)*i);
old_mag_phasor = 0.9776*(cosd(18.5814)+sind(18.5814)*i);
I_23_24 = (new_mag_phasor - old_mag_phasor)/Z_l;
P_loss = (abs(I_23_24))^2*real(Z_l);
Q_loss = (abs(I_23_24))^2*imag(Z_l);

Base = 100;

P_loss_real = P_loss *Base;
Q_loss_real = Q_loss *Base;
%% Power flow for Node 2 (Bus 23) of Branch 23-24 with Q from samples_Q
    data #Dispatch 1000
%Workspace needs to be included
%
% done_2 = 0;
% iter_2 = 1; %count iterations needed
% while(done_2 == 0 )
%
% mag = 1;
% angle = 18;
% P_2 = -0.294;
% Q_2 = -0.0169;
% % solution = nr_method(0.9776,18.5814,0.294,0.000169)
%
% P2  =(mag*7.18*cosd(angle -119.25)+7.326*cosd(-80)*(mag^2));
% Q2 = (mag*7.18*sind(angle -119.25)-7.326*sind(-80)*(mag^2));
%
% %Calculate derivatives
% diff_P2_angle = -7.18*mag*sind(angle -119.25);
% diff_P2_mag = 7.18*cosd(angle -119.25)+7.326*cosd(-80)*2*mag;
%
% diff_Q2_angle = 7.18*mag*cosd(angle -119.25);
% diff_Q2_mag = 7.18*sind(angle -119.25)-7.326*sind(-80)*2*mag;
%
% %equation to be solved
% new_P_2 = P_2-P2;
```

```matlab
% new_Q_2 = Q_2-Q2;
% delta_flow = [new_P_2;new_Q_2];
%
% %Put derivatives in Jacobian
% jacob = [diff_P2_angle diff_P2_mag; diff_Q2_angle diff_Q2_mag];
%
% %Solve linear equation
% x = linsolve(jacob,delta_flow);
% delta_angle_degree = (x(1,:)./(2*pi))*360; %convert radian angle to
%    degree angle
%
% %specify new angle and magnitude
% new_angle = angle - delta_angle_degree;
% new_mag = mag - x(2,:);
%
% %determine if result is below threshold
%
% if(new_P_2 <= 0.00001)
%     done_2 = 1;
%     iter_2 = iter_2;
%
% else
%     done_2 = 0;
%     mag = new_mag;
%     angle = new_angle;
%     iter_2 = iter_2 + 1;
% end
% end
%% Power flow for Node 2 of Branch 23-24 with Q from generator pf data
%    #Dispatch 1000
% % %Workspace needs to be included
%
% % done = 0;
% % iter = 1; %count iterations needed
% % while(done == 0 )
% %
% % mag = 1.01;
% % angle = 20.7;
% % P_1 = 0.294;
% % Q_1 = 0.000256;
% %
% % P1  =(mag*7.1621*cosd(angle-118.6)+7.326*cosd(-80)*(mag^2));
% % Q1 = (mag*7.1621*sind(angle-118.6)-7.326*sind(-80)*(mag^2));
% %
% % Calculate derivatives
% % diff_P1_angle = -7.1621*mag*sind(angle-118.6);
% % diff_P1_mag = 7.1621*cosd(angle-118.6)+7.326*cosd(-80)*2*mag;
% %
% % diff_Q1_angle = 7.1621*mag*cosd(angle-118.6);
% % diff_Q1_mag = 7.1621*sind(angle-118.6)-7.326*sind(-80)*2*mag;
% %
% % equation to be solved
% % new_P = P_1-P1;
% % new_Q = Q_1-Q1;
% % delta_flow = [new_P;new_Q];
% %
```

```
% % Put derivatives in Jacobian
% % jacob = [diff_P1_angle diff_P1_mag; diff_Q1_angle diff_Q1_mag];
% %
% % Solve linear equation
% % x = linsolve(jacob,delta_flow);
% % delta_angle_degree = (x(1,:)./(2*pi))*360; %convert radian angle to
        degree angle
% %
% % specify new angle and magnitude
% % new_angle = angle - delta_angle_degree;
% % new_mag = mag - x(2,:);
% %
% % determine if result is below threshold
% %
% % if(new_P <= 0.001)
% %      done = 1;
% %      iter = iter;
% %
% % else
% %      done = 0;
% %      mag = new_mag;
% %      angle = new_angle;
% %      iter = iter + 1;
% % end
% % end

% new_angle = 19.7;
% new_mag = 0.9801;
% Z_l = 0.02356859504 + 0.134446281*i;
% new_mag_phasor = new_mag*(cosd(new_angle)+sind(new_angle)*i);
% old_mag_phasor = 0.9776*(cosd(18.5814)+sind(18.5814)*i);
% I_23_24 = (new_mag_phasor - old_mag_phasor)/Z_l;
% P_loss = (abs(I_23_24))^2*real(Z_l);
% Q_loss = (abs(I_23_24))^2*imag(Z_l);
%
% Base = 100;
%
% P_loss_real = P_loss *Base;
% Q_loss_real = Q_loss *Base;
```

A.9.2. Wind farm modeling

```
%Authors: Farley Rimon & Marouane Mastouri
%Last updated: 12/06/2020 (dd-mm-yyyy)

%Modeling PF for a Substation with a Wind-and Solar Park
%A case study is loaded with 13 strings of Wind Turbine Generators and
    3
%strings from a PV-module.
%Step 2 involves the modeling of the power flow in situations. These
    are
%useful to determine limiting constraints in the substation's power
    flow

%For the test of low generation:
% v=4m/s
```

```matlab
%Q_mean = ddddd

%For the test of nominal generation:

clear

tic

%% Step 1: Load data of the case
mpc_substation_system13 = loadcase('system_13_V1');
P_idx = find(mpc_substation_system13.gen(:,2)~=0); %Find indexes of
    generating strings in generator data
P_wt_idx = P_idx(5:end);
P_pv_idx = P_idx(1:4);

%Indicate branch limits for components that cause the constraints
B_limit_1_2 = 400;
B_limit_4_7 = 185.19;
B_limit_4_23 = 185.19;
B_limit_6_12 = 185.19;
B_limit_6_17 = 185.19;

%disconnect PV to run only WTG test

for(i=1:length(P_pv_idx))

mpc_substation_system13.gen(P_pv_idx(i),8) = 0; %disconnect PV to run
    only WTG test

end

%Initialize active power generation

mpc_substation_system13.bus(8,2) = 4;
mpc_substation_system13.bus(10,2) = 4;
mpc_substation_system13.bus(12,2) = 4;
mpc_substation_system13.bus(14,2) = 4;

mpc_substation_system13.branch(54,11) = 0;
mpc_substation_system13.branch(110,11) = 0;
mpc_substation_system13.branch(161,11) = 0;
mpc_substation_system13.branch(209,11) = 0;


%Branch status disconnect/connect
%branch_r_status_idx = find(mpc_substation_system13.branch(:,11)==0); %
    Find indexes of generating strings in generator data


%define all constants
%WTG Farm
% type_wtg= 4; %total types of WTG
  N_daily_dispatch = 300; %total available wind dispatch profiles
  N_strings = 13'; %total Wind Turbine Generators strings
  v_c_in = 3 ; %general cut in speed in m/s
  v_r = 14 ; %general rated speed in m/s, fixed for step 2a
```

```matlab
v_c_off = 25 ; %general cut off speed in m/s
for (i=1:N_daily_dispatch)
   v_w(i,:) = 14 ; %nominal wind speed in m/s
end

for(j=1:length(P_wt_idx))
P_wt_max(1,j) = mpc_substation_system13.gen(P_wt_idx(j),2); %Rated
   power in MW for each string
end

for(j=1:length(P_wt_idx))
Q_wt_max(1,j) = mpc_substation_system13.gen(P_wt_idx(j),3); %Rated
   power in MW for each string
end

 %% Step 2: Generate random variables

%%Generate a random wind distribution

% a= 2.54; %shape parameter in p.u., the lower the more uniformly
   spread, 1.2 is best
% b= 7.86;%scale parameter in m/s, the higher the more the probability
   is spread, 12 is best
% rand('twister',5489); % Fix seeds of the random number generator
% rng( 'default'); %specifies seed for the random number generator,
   seed = 0
% v_w = wblrnd(b,a, [N_daily_dispatch, 1]); %Initialise matrix for
   random wind speeds

%Convert generated power at rated wind speed

P_wt = zeros(N_daily_dispatch, length(P_wt_max)); %Make matrix for
   generated nominal wind speed


for(i=1: length(P_wt_max)) %makes a 1x13
    for(j=1: N_daily_dispatch) %makes a 96x1
    %%apply boundary conditions to determine which equation is valid
     if(v_w(j) <= v_c_in)
         P_wt(j,i) =0;

    elseif ( (v_w(j) > v_c_in) &&  (v_w(j) <= v_r) )

         P_wt(j,i)=P_wt_max(i)*(v_w(j)^3-v_c_in^3)/(v_r^3-v_c_in^3);

    elseif ((v_w(j) > v_r) && (v_w(j) <= v_c_off))
         P_wt(j,i) = P_wt_max(i); %assigns every power to every
            dispatch

     elseif (v_w(j) > v_c_off)
         P_wt(j,i) = 0;
    end
    end
end

%Initialize active power generation
```

```matlab
P_wt_total = sum(P_wt, 2);
mpc_substation_system13.gen(6:end,2) = P_wt(1,:);
mpc_substation_system13.bus(1,3) = P_wt_total(1,:);
%mpc_substation_system13.gen(1,9) = P_wt_total(1,:);
mpc_substation_system13.gen(2:5,2) = 0;

%% %% Random Qs for WTG strings

rc_string_in = zeros(1,length(P_wt_max));

for(i=1:length(P_wt_max))
if (mpc_substation_system13.gen(P_wt_idx(i),3) <= 0.85) %% Type D
    rc_string_in(i) = 4.25;
elseif(mpc_substation_system13.gen(P_wt_idx(i),3) > 0.85 &&
    mpc_substation_system13.gen(P_wt_idx(i),3) <= 2.65) %% Type A
    rc_string_in(i) = 6.625;
elseif (mpc_substation_system13.gen(P_wt_idx(i),3) > 2.65)
    if((mpc_substation_system13.gen(P_wt_idx(i),9) <= 4))        %% Type
        B
        rc_string_in(i) = 6.22222;
    elseif((mpc_substation_system13.gen(P_wt_idx(i),9) > 4))    %% Type
        C
        rc_string_in(i) = 7;
    end
end
end

rc_string_end = zeros(1,length(P_wt_max));

for(i=1:length(P_wt_max))
if (mpc_substation_system13.gen(P_wt_idx(i),3) <= 0.85) %% Type D
    rc_string_end(i) = 4.3;
elseif(mpc_substation_system13.gen(P_wt_idx(i),3) > 0.85 &&
    mpc_substation_system13.gen(P_wt_idx(i),3) <= 2.65) %% Type A
    rc_string_end(i) = 2.095;
elseif (mpc_substation_system13.gen(P_wt_idx(i),3) > 2.65)
    if((mpc_substation_system13.gen(P_wt_idx(i),9) <= 4))   %% Type B
        rc_string_end(i) = 1.7037;
    elseif((mpc_substation_system13.gen(P_wt_idx(i),9) > 4)) %% Type C
        rc_string_end(i) = 1.357;
    end
end
end

P_reg_in = zeros(1,length(P_wt_max));

for(i=1:length(P_wt_max))
if (mpc_substation_system13.gen(P_wt_idx(i),3) <= 0.85) %% Type D
    P_reg_in(i) = 0.2;
elseif(mpc_substation_system13.gen(P_wt_idx(i),3) > 0.85 &&
    mpc_substation_system13.gen(P_wt_idx(i),3) <= 2.65) %% Type A
    P_reg_in(i) = 0.4;
elseif (mpc_substation_system13.gen(P_wt_idx(i),3) > 2.65)
    if((mpc_substation_system13.gen(P_wt_idx(i),9) <= 4))   %% Type B
        P_reg_in(i) = 0.4;
    elseif((mpc_substation_system13.gen(P_wt_idx(i),9) > 4)) %% Type C
```

```matlab
            P_reg_in(i) = 0.4;
        end
    end
end

P_reg_end = zeros(1,length(P_wt_max));

for(i=1:length(P_wt_max))
if (mpc_substation_system13.gen(P_wt_idx(i),3) <= 0.85) %% Type D
    P_reg_end(i) = 2.25;
elseif(mpc_substation_system13.gen(P_wt_idx(i),3) > 0.85 &&
    mpc_substation_system13.gen(P_wt_idx(i),3) <= 2.65) %% Type A
    P_reg_end(i) = 3.675;
elseif (mpc_substation_system13.gen(P_wt_idx(i),3) > 2.65)
    if((mpc_substation_system13.gen(P_wt_idx(i),9) <= 4))   %% Type B
        P_reg_end(i) = 3.325;
    elseif((mpc_substation_system13.gen(P_wt_idx(i),9) > 4)) %% Type C
        P_reg_end(i) = 3.85;
    end
end
end




% rc_string_in = [6.625  6.625    11.969  13.625  6.22      11.969  6.22
        6.22     11.2    7.36     6.22     12.25 10.64]; %specifies slope
    MVAr/MW at beginning for each WTG string
% P_reg_in = [0.1 0.1 0.0544  0.047619    0.1 0.0544  0.1 0.1 0.0606
    0.061    0.1 0.0556  0.0556]; %Percentage of total power to reach Q
    max in capability curve
% rc_string_end = [1.5     1.5      0.507   3.143   1.48    0.507   1.8519
        1.48    0.4408   0.4047   1.48     0.531   0.531]; %specifies slope
    MVAr/MW at end for each WTG string
% %new_Q_max = [0.72     0.72     0.5117   0.596   0.65     0.5117   0.59
        0.643    0.547    0.302    0.643 0.4898   0.4898]' * Q_wt_max; %
    Calculates new available MVAr at P_wt_max
% P_reg_end = [0.88     0.88     0.372   0.917   0.83125   0.372   0.83125
        0.83125   0.3023 0.225   0.83125   0.346    0.346]; %Percentage of
    total power to reach final Q in capability curve
a = 0.04;                      %Percentage of standard deviation, from
    papers around from 8% till 2%

Q_wt = zeros (N_daily_dispatch, length(P_wt_max));


    for i=1:length(P_wt_max)
        for j=1:N_daily_dispatch
            if (P_wt(j,i) < (P_reg_in(i)*P_wt_max(i)))
                Q_wt(j,i) = rc_string_in(i)*P_wt(j,i);
                if (Q_wt(j,i) >= Q_wt_max(i))
                    Q_wt(j,i) = Q_wt_max(i);
                end
            elseif ((P_wt(j,i) >= (P_reg_in(i)*P_wt_max(i))) && (P_wt(j
```

```matlab
                    ,i) < (P_reg_end(i)*P_wt_max(i))))
                        Q_wt(j,i) = Q_wt_max(i);
                elseif ((P_wt(j,i) >= (P_reg_end(i)*P_wt_max(i))))
                        Q_wt(j,i) = Q_wt_max(i) - rc_string_end(i).*(P_wt(j,i)-
                            P_reg_end(i)*P_wt_max(i));
                        if (Q_wt(j,i) < 0)
                            Q_wt(j,i) = 0;
                        end
                end
            end
        end
    end

Q_dem_tot = sum(Q_wt(1,:));
Q_mean_wt = zeros(1, length(P_wt_max));%matrix with mu for each string


for(i=1:N_daily_dispatch)
    Q_wt_max_matrix(i,:) = Q_wt_max;
end

for(i=1:N_daily_dispatch)
    Q_std_wt(i,:) = unifrnd(1,Q_wt_max_matrix(i,:));
end

for(j=1:length(P_wt_max))
for(i=1:(N_daily_dispatch))
    if(i <= (N_daily_dispatch/20))
        Q_mean_wt1(i,j) = -20*(Q_dem_tot/ length(P_wt_max))/20 ;
    elseif ((i > (1*N_daily_dispatch/20)) && (i <=(2*N_daily_dispatch
        /20)))
    for(i=1:(N_daily_dispatch/20))
        Q_mean_wt2(i,j) = -18*(Q_dem_tot/ length(P_wt_max))/20;
    end
    elseif ((i > (2*N_daily_dispatch/20)) && (i <=(3*N_daily_dispatch
        /20)))
    for(i=1:(N_daily_dispatch/20))
        Q_mean_wt3(i,j) = -16*(Q_dem_tot/ length(P_wt_max))/20;
    end
    elseif ((i > (3*N_daily_dispatch/20)) && (i <=(4*N_daily_dispatch
        /20)))
    for(i=1:(N_daily_dispatch/20))
        Q_mean_wt4(i,j) = -14*(Q_dem_tot/ length(P_wt_max))/20;
    end
    elseif ((i > (4*N_daily_dispatch/20)) && (i <=(5*N_daily_dispatch
        /20)))
    for(i=1:(N_daily_dispatch/20))
        Q_mean_wt5(i,j) = -12*(Q_dem_tot/ length(P_wt_max))/20;
    end
    elseif ((i > (5*N_daily_dispatch/20)) && (i <=(6*N_daily_dispatch
        /20)))
    for(i=1:(N_daily_dispatch/20))
        Q_mean_wt6(i,j) = -10*(Q_dem_tot/ length(P_wt_max))/20;
    end
    elseif ((i > (6*N_daily_dispatch/20)) && (i <=(7*N_daily_dispatch
        /20)))
    for(i=1:(N_daily_dispatch/20))
```

```
      Q_mean_wt7(i,j) = -8*(Q_dem_tot/ length(P_wt_max))/20;
  end
  elseif ((i > (7*N_daily_dispatch/20)) && (i <=(8*N_daily_dispatch
      /20)))
  for(i=1:(N_daily_dispatch/20))
      Q_mean_wt8(i,j) = -6*(Q_dem_tot/ length(P_wt_max))/20;
  end
  elseif ((i > (8*N_daily_dispatch/20)) && (i <=(9*N_daily_dispatch
      /20)))
  for(i=1:(N_daily_dispatch/20))
      Q_mean_wt9(i,j) = -4*(Q_dem_tot/ length(P_wt_max))/20;
  end
  elseif ((i > (9*N_daily_dispatch/20)) && (i <=(10*N_daily_dispatch
      /20)))
  for(i=1:(N_daily_dispatch/20))
      Q_mean_wt10(i,j) = -2*(Q_dem_tot/ length(P_wt_max))/20;
  end
  elseif ((i > (10*N_daily_dispatch/20)) && (i <=(11*N_daily_dispatch
      /20)))
  for(i=1:(N_daily_dispatch/20))
      Q_mean_wt11(i,j) = 0;
  end
  elseif ((i > (11*N_daily_dispatch/20)) && (i <=(12*N_daily_dispatch
      /20)))
  for(i=1:(N_daily_dispatch/20))
      Q_mean_wt12(i,j) = 2*(Q_dem_tot/ length(P_wt_max))/20;
  end
      elseif ((i > (12*N_daily_dispatch/20)) && (i <=(13*
          N_daily_dispatch/20)))
  for(i=1:(N_daily_dispatch/20))
      Q_mean_wt13(i,j) = 4*(Q_dem_tot/ length(P_wt_max))/20;
  end
      elseif ((i > (13*N_daily_dispatch/20)) && (i <=(14*
          N_daily_dispatch/20)))
  for(i=1:(N_daily_dispatch/20))
      Q_mean_wt14(i,j) = 6*(Q_dem_tot/ length(P_wt_max))/20;
  end
      elseif ((i > (14*N_daily_dispatch/20)) && (i <=(15*
          N_daily_dispatch/20)))
  for(i=1:(N_daily_dispatch/20))
      Q_mean_wt15(i,j) = 8*(Q_dem_tot/ length(P_wt_max))/20;
  end
      elseif ((i > (15*N_daily_dispatch/20)) && (i <=(16*
          N_daily_dispatch/20)))
  for(i=1:(N_daily_dispatch/20))
      Q_mean_wt16(i,j) = 10*(Q_dem_tot/ length(P_wt_max))/20;
  end

      elseif ((i > (16*N_daily_dispatch/20)) && (i <=(17*
          N_daily_dispatch/20)))
  for(i=1:(N_daily_dispatch/20))
      Q_mean_wt17(i,j) = 12*(Q_dem_tot/ length(P_wt_max))/20;
  end

      elseif ((i > (17*N_daily_dispatch/20)) && (i <=(18*
          N_daily_dispatch/20)))
```

```matlab
    for(i=1:(N_daily_dispatch/20))
        Q_mean_wt18(i,j) = 14*(Q_dem_tot/ length(P_wt_max))/20;
    end

        elseif ((i > (18*N_daily_dispatch/20)) && (i <=(19*
            N_daily_dispatch/20)))
    for(i=1:(N_daily_dispatch/20))
        Q_mean_wt19(i,j) = 16*(Q_dem_tot/ length(P_wt_max))/20;
    end

        elseif ((i > (19*N_daily_dispatch/20)) && (i <=(20*
            N_daily_dispatch/20)))
    for(i=1:(N_daily_dispatch/20))
        Q_mean_wt20(i,j) = 20*(Q_dem_tot/ length(P_wt_max))/20;
    end
end
end
end

for(i=1:length(P_wt_max)) %makes a 1x13
  for(j=1:(N_daily_dispatch/20)) %makes a 96x1
    samples_Q_wt(j,i)= normrnd(Q_mean_wt1(i), a*Q_std_wt(i), [1, 1]); %
        Creates random samples for Q in 96x13, some values violating
        the constraints
  end
  for(j=(1*N_daily_dispatch/20):(2*N_daily_dispatch/20))
      samples_Q_wt(j,i)= normrnd(Q_mean_wt2(i), a*Q_std_wt(i), [1, 1])
          ; %Creates random samples for Q
  end
  for(j=(2*N_daily_dispatch/20):(3*N_daily_dispatch/20))
      samples_Q_wt(j,i)= normrnd(Q_mean_wt3(i), a*Q_std_wt(i), [1, 1])
          ; %Creates random samples for Q
  end
  for(j=(3*N_daily_dispatch/20):(4*N_daily_dispatch/20))
      samples_Q_wt(j,i)= normrnd(Q_mean_wt4(i), a*Q_std_wt(i), [1, 1])
          ; %Creates random samples for Q
  end
  for(j=(4*N_daily_dispatch/20):(5*N_daily_dispatch/20))
      samples_Q_wt(j,i)= normrnd(Q_mean_wt5(i), a*Q_std_wt(i), [1, 1])
          ; %Creates random samples for Q
  end
  for(j=(5*N_daily_dispatch/20):(6*N_daily_dispatch/20))
      samples_Q_wt(j,i)= normrnd(Q_mean_wt6(i), a*Q_std_wt(i), [1, 1])
          ; %Creates random samples for Q
  end
  for(j=(6*N_daily_dispatch/20):(7*N_daily_dispatch/20))
      samples_Q_wt(j,i)= normrnd(Q_mean_wt7(i), a*Q_std_wt(i), [1, 1])
          ; %Creates random samples for Q
  end
  for(j=(7*N_daily_dispatch/20):(8*N_daily_dispatch/20))
      samples_Q_wt(j,i)= normrnd(Q_mean_wt8(i), a*Q_std_wt(i), [1, 1])
          ; %Creates random samples for Q
  end
  for(j=(8*N_daily_dispatch/20):(9*N_daily_dispatch/20))
      samples_Q_wt(j,i)= normrnd(Q_mean_wt9(i), a*Q_std_wt(i), [1, 1])
          ; %Creates random samples for Q
```

```matlab
    end
    for(j=(9*N_daily_dispatch/20):(10*N_daily_dispatch/20))
        samples_Q_wt(j,i)= normrnd(Q_mean_wt10(i), a*Q_std_wt(i), [1,
            1]); %Creates random samples for Q
    end
    for(j=(10*N_daily_dispatch/20):(11*N_daily_dispatch/20))
        samples_Q_wt(j,i)= normrnd(Q_mean_wt11(i), a*Q_std_wt(i), [1,
            1]); %Creates random samples for Q
    end
    for(j=(11*N_daily_dispatch/20):(12*N_daily_dispatch/20))
        samples_Q_wt(j,i)= normrnd(Q_mean_wt12(i), a*Q_std_wt(i), [1,
            1]); %Creates random samples for Q
    end
        for(j=(12*N_daily_dispatch/20):(13*N_daily_dispatch/20))
        samples_Q_wt(j,i)= normrnd(Q_mean_wt13(i), a*Q_std_wt(i), [1,
            1]); %Creates random samples for Q
        end
        for(j=(13*N_daily_dispatch/20):(14*N_daily_dispatch/20))
        samples_Q_wt(j,i)= normrnd(Q_mean_wt14(i), a*Q_std_wt(i), [1,
            1]); %Creates random samples for Q
        end
        for(j=(14*N_daily_dispatch/20):(15*N_daily_dispatch/20))
        samples_Q_wt(j,i)= normrnd(Q_mean_wt15(i), a*Q_std_wt(i), [1,
            1]); %Creates random samples for Q
        end
        for(j=(15*N_daily_dispatch/20):(16*N_daily_dispatch/20))
        samples_Q_wt(j,i)= normrnd(Q_mean_wt16(i), a*Q_std_wt(i), [1,
            1]); %Creates random samples for Q
        end
        for(j=(16*N_daily_dispatch/20):(17*N_daily_dispatch/20))
        samples_Q_wt(j,i)= normrnd(Q_mean_wt17(i), a*Q_std_wt(i), [1,
            1]); %Creates random samples for Q
        end
        for(j=(17*N_daily_dispatch/20):(18*N_daily_dispatch/20))
        samples_Q_wt(j,i)= normrnd(Q_mean_wt18(i), a*Q_std_wt(i), [1,
            1]); %Creates random samples for Q
        end
        for(j=(18*N_daily_dispatch/20):(19*N_daily_dispatch/20))
        samples_Q_wt(j,i)= normrnd(Q_mean_wt19(i), a*Q_std_wt(i), [1,
            1]); %Creates random samples for Q
        end
        for(j=(19*N_daily_dispatch/20):(20*N_daily_dispatch/20))
        samples_Q_wt(j,i)= normrnd(Q_mean_wt20(i), a*Q_std_wt(i), [1,
            1]); %Creates random samples for Q
        end
end

%% Step 3: Update case file and run Power Flow

stop =0;


while(stop == 0)
    for(i=1:N_daily_dispatch)
    for (j=1:length(P_wt_max))
    %for (k=1:N_branches_shunt)
```

```matlab
        if(i < N_daily_dispatch)
mpc_substation_system13.gen(P_wt_idx(j),3) = samples_Q_wt(i,j);
mpc_substation_system13.bus(1,4) = sum(samples_Q_wt(i,j));

%run power flow for each dispatch
tStart = cputime;
results_pf = runpf(mpc_substation_system13); %run power flow
    once Q is loaded per dispatch
[results_loss results_inject] = get_losses(results_pf); %losses

%Make matrix to specify branch losses and reactive power
    injection
results_loss_matrix = zeros(31, 50); %first row is bus "from",
    second row bus "to", third row is loss

bus_from = mpc_substation_system13.branch(:,1);
bus_to = mpc_substation_system13.branch(:,2);

%Perform operation only if system converges
    if (results_pf.success == 1)

%Save data for each power flow
Vmag(:,i) = results_pf.bus(:,8); %Saves voltage magnitude for
    every bus
Vangle(:,i) = results_pf.bus(:,9); %Saves angle magnitude for
    every bus
P_flow_1_2(:,i) = results_pf.branch(1,16); %Saves Power flow in
    MW for Branch to PCC
P_flow_4_23(:,i) = results_pf.branch(25,16); %Saves Power flow
    in MW for Branch to Input transformer 1
P_flow_4_7(:,i) = results_pf.branch(6,16); %Saves Power flow in
    MW for Branch to Input transformer 1
P_flow_6_12(:,i) = results_pf.branch(12,16); %Saves Power flow
    in MW for Branch to Input transformer 2
P_flow_6_17(:,i) = results_pf.branch(18,16); %Saves Power flow
    in MW for Branch to Input transformer 2

results_loss_real(:,i) = real(results_loss);
results_loss_im(:,i) = imag(results_loss);
results_inject_t(:,i) = results_inject;
results_loss_matrix = [bus_from bus_to results_loss_real
    results_loss_im    results_inject_t];

    end

    elseif(i == N_daily_dispatch)
        mpc_substation_system13.gen(P_wt_idx(j),3) = samples_Q_wt(i
            ,j);
        mpc_substation_system13.bus(1,4) = sum(samples_Q_wt(i,j));

  if (results_pf.success == 1)

%Save data for each power flow
Vmag(:,i) = results_pf.bus(:,8);
Vangle(:,i) = results_pf.bus(:,9);
```

```matlab
        P_flow_1_2(:,i) = results_pf.branch(1,16); %Saves Power flow in
            MW for Branch to PCC
        P_flow_4_23(:,i) = results_pf.branch(25,16); %Saves Power flow
            in MW for Branch to Input transformer 1
        P_flow_4_7(:,i) = results_pf.branch(6,16); %Saves Power flow in
            MW for Branch to Input transformer 1
        P_flow_6_12(:,i) = results_pf.branch(12,16); %Saves Power flow
            in MW for Branch to Input transformer 2
        P_flow_6_17(:,i) = results_pf.branch(18,16); %Saves Power flow
            in MW for Branch to Input transformer 2

        %Save all the losses generated in each bus/branch for all
        %dispatches
        results_loss_real(:,i) = real(results_loss);
        results_loss_im(:,i) = imag(results_loss);
        results_inject_t(:,i) = results_inject;
        results_loss_matrix = [bus_from bus_to results_loss_real
            results_loss_im    results_inject_t];

        %Computes location and value of maximum loss

        constraints_v_low = Vmag(Vmag < 0.8567); %Note values greater
            than minimum p.u.
        constraints_v_high = Vmag(Vmag > 1.1424);  %Note values greater
            than maximum p.u.

        idx_constraints_v_low = zeros(207, N_daily_dispatch); %28 is
            amount of busses in the circuit
for (a=1:N_daily_dispatch)


        idx_constraints_v_low(:,a) = (Vmag(:,a) < 0.8567);
        idx_constraints_v_high(:,a) = (Vmag(:,a) > 1.1424);
        [idx_r_Q_v_low idx_c_Q_v_low] = find(idx_constraints_v_low~=0);
            %find location in matrix where there is v low
        [idx_r_Q_v_high idx_c_Q_v_high] = find(idx_constraints_v_high
            ~=0);
end
        %Calculate lowest voltage magnitude value on the dispatches
            where a
        %violation has occured
        unique_idx_c_Q_v_low = unique(idx_c_Q_v_low);
        unique_idx_r_Q_v_low = unique(idx_r_Q_v_low);
            V_lowest = Vmag(:,unique_idx_c_Q_v_low);

        for(b=1:length(unique_idx_c_Q_v_low))
            constraints_v_lowest(:,b) =  min(V_lowest(:,b));
        end

        %Calculate lowest voltage magnitude value on the dispatches
            where a
        %violation has occured

        unique_idx_c_Q_v_high = unique(idx_c_Q_v_high);
        unique_idx_r_Q_v_high = unique(idx_r_Q_v_high);
            V_highest = Vmag(:,unique_idx_c_Q_v_high);
```

```matlab
        for(c=1:length(unique_idx_c_Q_v_high))
            constraints_v_highest(:,c) =  max(V_highest(:,c));
        end

    Q_dem_constraints_v_low = samples_Q_wt(idx_c_Q_v_low,:); %Find
        the Q demands for that specific dispatch
    Q_dem_constraints_v_high = samples_Q_wt(idx_c_Q_v_high,:); %
        Find the Q demands for that specific dispatch

    P_loss_v_low = results_loss_real(:, idx_c_Q_v_low);
    P_loss_v_high = results_loss_real(:, idx_c_Q_v_high);

    Q_loss_v_low = results_loss_im(:, idx_c_Q_v_low);
    Q_loss_v_high = results_loss_im(:, idx_c_Q_v_high);

    Q_inj_v_low = results_inject_t(:, idx_c_Q_v_low);
    Q_inj_v_high = results_inject_t(:, idx_c_Q_v_high);

     end
  end
  end
    stop = 1; %stop while loop
  end
  end
%end


    %% Step 4: Plot results in a visable manner

    %Print  voltage data
    figure(1)
    subplot(2,1,1)
    plot(Vmag,'o');
    yline(0.8567,'r','LineWidth',1);
    yline(1.1424,'r','LineWidth',1);
    xlabel('Bus number','FontSize',12);
    ylabel('V magnitude (p.u.)','FontSize',12);
    title('Voltage magnitude in p.u. for bus numbers','FontSize'
        ,12)
    hold on;

    subplot(2,1,2)
    plot(Vangle,'s');
    xlabel('Bus number','FontSize',12);
    ylabel('V angle (degrees)','FontSize',12);
    title('Voltage angles in degrees for bus numbers','FontSize'
        ,12)
    hold on;

    %Print losses data
    figure(2)
    subplot(3,1,1)
    plot(results_loss_real,'o');
    xlabel('Branch #','FontSize',12);
    ylabel('P loss(MW)','FontSize',12);
```

```matlab
title('Active power loss in MW for branch','FontSize',12)
hold on;


subplot(3,1,2)
plot(results_loss_im,'s');
xlabel('Branch #','FontSize',12);
ylabel('Q loss(MVAr)','FontSize',12);
title('Reactive power loss in MVAr for branch','FontSize',12)
hold on;

subplot(3,1,3)
plot(results_inject_t,'o');
xlabel('Branch #','FontSize',12);
ylabel('Q injected(MVAr)','FontSize',12);
title('Reactive power inject in MVAr for branch','FontSize',12)
hold on;

figure(6)

plot(P_flow_1_2,'o');
xlabel('Dispatch','FontSize',12);
ylabel('Power flow (MW)','FontSize',12);
yline(B_limit_1_2 ,'r','LineWidth',1);
title('Power flow through PCC Branch 1-2','FontSize',12);
hold on;

figure(7)
subplot(2,1,1)

plot(P_flow_4_7,'o');
xlabel('Dispatch','FontSize',12);
ylabel('Power flow (MW)','FontSize',12);
yline(B_limit_4_7 ,'r','LineWidth',1);
title('Power flow to input Transformer 1 Branch 4-7','FontSize'
    ,12);
hold on;

subplot(2,1,2)

plot(P_flow_4_23,'o');
xlabel('Dispatch','FontSize',12);
ylabel('Power flow (MW)','FontSize',12);
yline(B_limit_4_23 ,'r','LineWidth',1);
title('Power flow to input Transformer 1 Branch 4-23','FontSize
    ',12)
hold on;

figure(8)
subplot(2,1,1)

plot(P_flow_6_12,'o');
xlabel('Dispatch','FontSize',12);
ylabel('Power flow (MW)','FontSize',12);
yline(B_limit_6_12 ,'r','LineWidth',1);
title('Power flow to input Transformer 2 Branch 6-12','FontSize
```

```matlab
      ',12)
hold on;

subplot (2 ,1 ,2)

plot(P_flow_6_17 ,'o');
xlabel('Dispatch','FontSize',12);
ylabel('Power flow (MW)','FontSize',12);
yline(B_limit_6_17 ,'r','LineWidth',1);
title('Power flow to input Transformer 2 Branch 6-17','FontSize
    ',12)
hold on;


 %Print relation between demand , total system losses and
     voltage

%Calculate average voltage for specific Q_demand
 v_avg = mean(Vmag);

%Calculate average minimum voltage for specific Q_demand
%this is equal to constraints_v_low

%Calculate total losses for average voltage of each dispatch
P_loss_tot = sum(results_loss_real);
Q_loss_tot = sum(results_loss_im);
Q_inj_tot = sum(results_inject_t);

%Calculate total losses for voltage constraints
P_loss_tot_v_low = sum(P_loss_v_low);
Q_loss_tot_v_low = sum(Q_loss_v_low);
Q_inj_tot_v_low = sum(Q_inj_v_low);

P_loss_tot_v_low = unique(P_loss_tot_v_low);
Q_loss_tot_v_low = unique(Q_loss_tot_v_low);
Q_inj_tot_v_low = unique(Q_inj_tot_v_low);

P_loss_tot_v_high = sum(P_loss_v_high);
Q_loss_tot_v_high = sum(Q_loss_v_high);
Q_inj_tot_v_high = sum(Q_inj_v_high);


P_loss_tot_v_high = unique(P_loss_tot_v_high);
Q_loss_tot_v_high = unique(Q_loss_tot_v_high);
Q_inj_tot_v_high = unique(Q_inj_tot_v_high);

%Calculate total Q_demand

Q_tot = sum(samples_Q_wt ,2);

%Calculate total Q_demand for dispatches causing violation

Q_tot_constraints_v_low = sum(Q_dem_constraints_v_low ,2);
Q_tot_constraints_v_high = sum(Q_dem_constraints_v_high ,2);

Q_tot_constraints_v_low = unique(Q_tot_constraints_v_low);
```

```matlab
Q_tot_constraints_v_high = unique(Q_tot_constraints_v_high);

%add zeros in order to plot

P_loss_tot_v_low(numel(Q_tot_constraints_v_low)) = 0;
Q_loss_tot_v_low(numel(Q_tot_constraints_v_low)) = 0;
Q_inj_tot_v_low(numel(Q_tot_constraints_v_low)) = 0;

P_loss_tot_v_high(numel(Q_tot_constraints_v_high)) = 0;
Q_loss_tot_v_high(numel(Q_tot_constraints_v_high)) = 0;
Q_inj_tot_v_high(numel(Q_tot_constraints_v_high)) = 0;

%Plot 3D plot Q demand, P loss and (minimum and maximum)
    average voltage
figure(3)

plot3(Q_tot, P_loss_tot, v_avg,'o','Color', 'c', 'MarkerSize'
    ,5); %plot for avg
hold on;
plot3(Q_tot_constraints_v_low, P_loss_tot_v_low,
    constraints_v_lowest,'o','Color', 'r', 'MarkerSize',5); %
    plot for v constraints low
hold on;
plot3(Q_tot_constraints_v_high, P_loss_tot_v_high,
    constraints_v_highest,'o','Color', 'r', 'MarkerSize',5); %
    plot for v constraints low
hold on;

grid on;

xlabel('Q demand (MVAr)','FontSize',12);
ylabel('P loss total (MW)','FontSize',12);
zlabel('V average magnitude (p.u.)','FontSize',12);

legend('4 m/s','7.5 m/s', '14 m/s');
%Plot 3D plot Q loss for minimum and average voltage
figure(4)

plot3(Q_tot, Q_loss_tot, v_avg,'o','Color', 'c', 'MarkerSize'
    ,5); %plot for avg
hold on;
plot3(Q_tot_constraints_v_low, Q_loss_tot_v_low,
    constraints_v_lowest,'o','Color', 'r', 'MarkerSize',5); %
    plot for v constraints low
hold on;
plot3(Q_tot_constraints_v_high, Q_loss_tot_v_high',
    constraints_v_highest,'o','Color', 'r', 'MarkerSize',5); %
    plot for v constraints low
hold on;

grid on;

xlabel('Q demand (MVAr)','FontSize',12);
ylabel('Q loss total (MVAr)','FontSize',12);
zlabel('V average magnitude (p.u.)','FontSize',12);
```

```matlab
        legend('4 m/s','7.5 m/s', '14 m/s');
        %Plot 3D plot for minimum and average
        figure(5)

        plot3(Q_tot, Q_inj_tot,v_avg,'o','Color', 'c', 'MarkerSize',5);
            %plot for avg
        hold on;
        plot3(Q_tot_constraints_v_low,Q_inj_tot_v_low,
            constraints_v_lowest,'o','Color', 'r', 'MarkerSize',5); %
            plot for v constraints low
        hold on;
        plot3(Q_tot_constraints_v_high, Q_inj_tot_v_high',
            constraints_v_highest,'o','Color', 'r', 'MarkerSize',5); %
            plot for v constraints low
        hold on;

        grid on;

        xlabel('Q demand (MVAr)','FontSize',12);
        ylabel('Q INJ total (MVAr)','FontSize',12);
        zlabel('V average magnitude (p.u.)','FontSize',12);

        legend('4 m/s','7.5 m/s', '14 m/s');

        toc
```

A.9.3. Hybrid farm modeling

```matlab
%Authors: Farley Rimon & Marouane Mastouri
%Last updated: 09/06/2020 (dd-mm-yyyy)

%Modeling PF for a Substation with a Wind-and Solar Park
%A case study is loaded with 13 strings of Wind Turbine Generators and
    4
%strings from a PV-module.


clear;
%% Step 1: Load data of the case
mpc_substation_system13 = loadcase('system_13');
P_idx = find(mpc_substation_system13.gen(:,2)~=0); %Find indexes of
    generating strings in generator data
P_wt_idx = P_idx(5:end);
P_pv_idx = P_idx(1:4);

%Indicate branch limits for components that cause the constraints
B_limit_1_2 = 400;
B_limit_4_7 = 185.19;
B_limit_4_23 = 185.19;
B_limit_6_12 = 185.19;
B_limit_6_17 = 185.19;


%define all constants
%WTG Farm
% type_wtg= 4; %total types of WTG
```

```matlab
  N_daily_dispatch = 300; %total available wind dispatch profiles
  N_strings = 13'; %total Wind Turbine Generators strings
  v_c_in = 3 ; %general cut in speed in m/s
  v_r = 14 ; %general rated speed in m/s, fixed for step 2a
  %v_w = 14 ; %nominal wind speed in m/s
  v_c_off = 25 ; %general cut off speed in m/s
  for (i=1:N_daily_dispatch)
    v_w(i,:) = 14; %nominal wind speed in m/s
  end
  P_wt_max = [29.4 29.4 29.4 16.8 32 29.4 16 28 33 29.15 28 28.8 28.8];
       %Rated power in MW for each string
  Q_wt_max = [21.2 18.55 19.15 10.9 22.4 19.15 12.2 19.6 22.4 13.248
     19.6 19.6 19.6] ; %Max positive/negative reactive power in MVAr
     generated for eacht string 1-13

  %PV farm
  N_strings_pv = 4; %total strings
  P_pv_max = [12  12  12  12];  %Max active power in MW generated per
     PV string 1-4
  Q_pv_max = (1/3)*P_pv_max; %Max reactive power in MVAr per PV string
     1-4

  A_pv = 114441.8056; %Area in m2 of each PV system , a total of 4 PV
  t_sun_h = 11; % Sun hours per day
  t_increase_h = 24/N_daily_dispatch; % 15minutes increase per day
     needed to go from 0 to max solar irradiance in W/m2
  t_steps = [1:t_increase_h:(6+t_increase_h)];

  %Insert season
  solar_irr_max= 800;                            %max solar irradiance in
     W/m2
  P_module_max = 288;                            %output per module for
     800 W/m2
  rc_g_solar_power = (P_module_max)/((10-4)); %rc in W/m2 * 15min from
     0 solar irradiance to max in, linear increase
  N_modules = 41667;                             %number of modules

  P_module_solar = rc_g_solar_power * t_steps;

  %Hybrid wind and solar
  P_total_max = [P_pv_max P_wt_max];
  N_tot_strings = N_strings + N_strings_pv;

  %% Step 2: Generate random variables

%%Generate a random wind distribution

%a= 2.54; %shape parameter in p.u., the lower the more uniformly spread
   , 1.2 is best
%b= 7.86;%scale parameter in m/s, the higher the more the probability
   is spread, 12 is best
%rand('twister',5489); % Fix seeds of the random number generator
%rng( 'default'); %specifies seed for the random number generator, seed
   = 0
%v_w = wblrnd(b,a, [N_daily_dispatch, 1]); %Initialise matrix for
   random wind speeds
```

```matlab
%Convert generated power at rated wind speed

% P_wt = zeros(N_daily_dispatch , N_strings); %Make matrix for generated
     nominal wind speed
%
%
% for(i=1: length(P_wt_max)) %makes a 1x13
%      for(j=1: N_daily_dispatch) %makes a 96x1
%      %%apply boundary conditions to determine which equation is valid
%        if(v_w(j) <= v_c_in)
%            P_wt(j,i) = 0;
%
%      elseif ( (v_w(j) > v_c_in) && (v_w(j) <= v_r) )
%
%            P_wt(j,i)=P_wt_max(i)*(v_w(j)^3-v_c_in^3)/(v_r^3-v_c_in^3);
%
%      elseif ((v_w(j) > v_r) && (v_w(j) <= v_c_off))
%            P_wt(j,i) = P_wt_max(i); %assigns every power to every
   dispatch
%
%        elseif (v_w(j) > v_c_off)
%            P_wt(j,i) = 0;
%        end
%      end
% end


%Summer model for solar
%    for(j=1: length(P_pv_max)) %makes a 1x4
%        k=1;
%          for(i=1: N_daily_dispatch) %makes a 1000x1
%
%            if (i < (4/24)*N_daily_dispatch ) %Assume before 4 am ,
   no PV energy generated
%                P_pv(i,j) = 0;
%
%            elseif( (i >= ((4/24)*N_daily_dispatch)) && (i < ((10/24)
   *N_daily_dispatch)) )%Assume 4 - 10 am , PV power increasing
   linearly
%                P_pv(i,j) = (P_module_solar(k)*N_modules)*10^-6; %
   Output active power in MW
%                if (P_pv(i,j) > P_pv_max(:,j))
%                    P_pv(i,j) = P_pv_max(:,j);
%                end
%                if (k<length(t_steps))
%                    k=k+1;
%                end
%            elseif( (i >= ((10/24)*N_daily_dispatch)) && (i <
   ((21/24)*N_daily_dispatch)) ) %Assume 10 am - 9pm , PV max energy
   generated
%                P_pv(i,j) = P_pv_max(1,j);
%
%            elseif( (i >= ((21/24)*N_daily_dispatch))  ) %Assume 9 pm
    -12 am, no PV energy generated
%                P_pv(i,j) = 0;
```

```matlab
%         end
%      end
%    end

  P_pv_max = [12  12  12  12];  %Avg active power in MW generated per
      PV string 1-4
  P_pv_min = [1.5    1.5    1.5    1.5];
  P_pv_nom = [7.5    7.5    7.5    7.5];

  P_pv = zeros(N_daily_dispatch, length(P_pv_min));

  for(i=1:N_daily_dispatch)
      P_pv(i,:) = P_pv_max;
  end
   %Initialize active power generation for wind
    P_wt_total = sum(P_wt, 2);
    mpc_substation_system13.gen(6:18,2) = P_wt(1,:);
    mpc_substation_system13.bus(1,3) = P_wt_total(1,:) + sum(P_pv(1,:)
        ,2);

    %initialize normal active power generation for solar
    mpc_substation_system13.gen(2:5,2) = P_pv(1,:);


    %Initialize active power generation


%Hybrid wind and solar
P_total = [P_pv P_wt];


%% Step 2c: Generate random Qs with wind speeds and solar irradiance (
    fixed tap positions)

%% Random Qs for WTG strings

% rc_string_in = [6.625  6.625   11.969  13.625  6.22     11.969  6.22
      6.22     11.2    7.36     6.22     12.25 10.64]; %specifies slope
   MVAr/MW at beginning for each WTG string
% P_reg_in = [0.1 0.1 0.0544  0.047619    0.1 0.0544  0.1 0.1 0.0606
    0.061    0.1 0.0556  0.0556]; %Percentage of total power to reach Q
    max in capability curve
% rc_string_end = [1.5     1.5      0.507   3.143   1.48    0.507    1.8519
      1.48     0.4408  0.4047   1.48     0.531    0.531]; %specifies slope
    MVAr/MW at end for each WTG string
% %new_Q_max = [0.72    0.72     0.5117  0.596   0.65     0.5117   0.59
       0.643    0.547    0.302    0.643 0.4898    0.4898]' * Q_wt_max; %
    Calculates new available MVAr at P_wt_max
% P_reg_end = [0.88    0.88     0.372   0.917   0.83125   0.372    0.83125
       0.83125   0.3023 0.225   0.83125   0.346    0.346]; %Percentage of
    total power to reach final Q in capability curve
% a = 0.08;                         %Percentage of standard deviation, from
    papers around from 8% till 2%
%
% Q_wt = zeros (N_daily_dispatch, N_strings);
%
```

```
%
%     for i=1:N_strings
%         for j=1:N_daily_dispatch
%             if (P_wt(j,i) < (P_reg_in(i)*P_wt_max(i)))
%                 Q_wt(j,i) = rc_string_in(i)*P_wt(j,i);
%                 if (Q_wt(j,i) >= Q_wt_max(i))
%                     Q_wt(j,i) = Q_wt_max(i);
%                 end
%             elseif ((P_wt(j,i) >= (P_reg_in(i)*P_wt_max(i))) && (P_wt
   (j,i) < (P_reg_end(i)*P_wt_max(i))))
%                 Q_wt(j,i) = Q_wt_max(i);
%             elseif ((P_wt(j,i) >= (P_reg_end(i)*P_wt_max(i))))
%                 Q_wt(j,i) = Q_wt_max(i) - rc_string_end(i).*(P_wt(j,i
   )-P_reg_end(i)*P_wt_max(i));
%                 if (Q_wt(j,i) < 0)
%                     Q_wt(j,i) = 0;
%                 end
%             end
%         end
%     end
%
% Q_mean_wt = zeros(1, N_strings);%matrix with mu for each string
% Q_dem_tot = sum(Q_wt(1,:)) ;


%
% for (i=1:N_daily_dispatch)
%     Q_pv_max_matrix(i,:) = Q_pv_max;
% end
%
%
% for(i=1:N_daily_dispatch)
%     Q_wt_max_matrix(i,:) = Q_wt_max;
% end
%
% for(i=1:N_daily_dispatch)
%     Q_std_wt(i,:) = unifrnd(1,Q_wt_max_matrix(i,:));
% end
%
% for(j=1:N_strings)
% for(i=1:(N_daily_dispatch))
%     if(i <= (N_daily_dispatch/20))
%         Q_mean_wt1(i,j) = -20*(Q_dem_tot/ N_strings)/20 ;
%     elseif ((i > (1*N_daily_dispatch/20)) && (i <=(2*N_daily_dispatch
   /20)))
%     for(i=1:(N_daily_dispatch/20))
%         Q_mean_wt2(i,j) = -18*(Q_dem_tot/ N_strings)/20;
%     end
%     elseif ((i > (2*N_daily_dispatch/20)) && (i <=(3*N_daily_dispatch
   /20)))
%     for(i=1:(N_daily_dispatch/20))
%         Q_mean_wt3(i,j) = -16*(Q_dem_tot/ N_strings)/20;
%     end
%     elseif ((i > (3*N_daily_dispatch/20)) && (i <=(4*N_daily_dispatch
   /20)))
%     for(i=1:(N_daily_dispatch/20))
%         Q_mean_wt4(i,j) = -14*(Q_dem_tot/ N_strings)/20;
```

```matlab
%       end
%       elseif ((i > (4*N_daily_dispatch/20)) && (i <=(5*N_daily_dispatch
    /20)))
%       for(i=1:(N_daily_dispatch/20))
%           Q_mean_wt5(i,j) = -12*(Q_dem_tot/ N_strings)/20;
%       end
%       elseif ((i > (5*N_daily_dispatch/20)) && (i <=(6*N_daily_dispatch
    /20)))
%       for(i=1:(N_daily_dispatch/20))
%           Q_mean_wt6(i,j) = -10*(Q_dem_tot/ N_strings)/20;
%       end
%       elseif ((i > (6*N_daily_dispatch/20)) && (i <=(7*N_daily_dispatch
    /20)))
%       for(i=1:(N_daily_dispatch/20))
%           Q_mean_wt7(i,j) = -8*(Q_dem_tot/ N_strings)/20;
%       end
%       elseif ((i > (7*N_daily_dispatch/20)) && (i <=(8*N_daily_dispatch
    /20)))
%       for(i=1:(N_daily_dispatch/20))
%           Q_mean_wt8(i,j) = -6*(Q_dem_tot/ N_strings)/20;
%       end
%       elseif ((i > (8*N_daily_dispatch/20)) && (i <=(9*N_daily_dispatch
    /20)))
%       for(i=1:(N_daily_dispatch/20))
%           Q_mean_wt9(i,j) = -4*(Q_dem_tot/ N_strings)/20;
%       end
%       elseif ((i > (9*N_daily_dispatch/20)) && (i <=(10*
    N_daily_dispatch/20)))
%       for(i=1:(N_daily_dispatch/20))
%           Q_mean_wt10(i,j) = -2*(Q_dem_tot/ N_strings)/20;
%       end
%       elseif ((i > (10*N_daily_dispatch/20)) && (i <=(11*
    N_daily_dispatch/20)))
%       for(i=1:(N_daily_dispatch/20))
%           Q_mean_wt11(i,j) = 0;
%       end
%       elseif ((i > (11*N_daily_dispatch/20)) && (i <=(12*
    N_daily_dispatch/20)))
%       for(i=1:(N_daily_dispatch/20))
%           Q_mean_wt12(i,j) = 2*(Q_dem_tot/ N_strings)/20;
%       end
%           elseif ((i > (12*N_daily_dispatch/20)) && (i <=(13*
    N_daily_dispatch/20)))
%       for(i=1:(N_daily_dispatch/20))
%           Q_mean_wt13(i,j) = 4*(Q_dem_tot/ N_strings)/20;
%       end
%           elseif ((i > (13*N_daily_dispatch/20)) && (i <=(14*
    N_daily_dispatch/20)))
%       for(i=1:(N_daily_dispatch/20))
%           Q_mean_wt14(i,j) = 6*(Q_dem_tot/ N_strings)/20;
%       end
%           elseif ((i > (14*N_daily_dispatch/20)) && (i <=(15*
    N_daily_dispatch/20)))
%       for(i=1:(N_daily_dispatch/20))
%           Q_mean_wt15(i,j) = 8*(Q_dem_tot/ N_strings)/20;
%       end
```

```
%            elseif ((i > (15*N_daily_dispatch/20)) && (i <=(16*
   N_daily_dispatch/20)))
%      for(i=1:(N_daily_dispatch/20))
%            Q_mean_wt16(i,j) = 10*(Q_dem_tot/ N_strings)/20;
%        end
%
%            elseif ((i > (16*N_daily_dispatch/20)) && (i <=(17*
   N_daily_dispatch/20)))
%      for(i=1:(N_daily_dispatch/20))
%            Q_mean_wt17(i,j) = 12*(Q_dem_tot/ N_strings)/20;
%        end
%
%            elseif ((i > (17*N_daily_dispatch/20)) && (i <=(18*
   N_daily_dispatch/20)))
%      for(i=1:(N_daily_dispatch/20))
%            Q_mean_wt18(i,j) = 14*(Q_dem_tot/ N_strings)/20;
%        end
%
%            elseif ((i > (18*N_daily_dispatch/20)) && (i <=(19*
   N_daily_dispatch/20)))
%      for(i=1:(N_daily_dispatch/20))
%            Q_mean_wt19(i,j) = 16*(Q_dem_tot/ N_strings)/20;
%        end
%
%            elseif ((i > (19*N_daily_dispatch/20)) && (i <=(20*
   N_daily_dispatch/20)))
%      for(i=1:(N_daily_dispatch/20))
%            Q_mean_wt20(i,j) = 20*(Q_dem_tot/ N_strings)/20;
%        end
% end
% end
% end
%
% for(i=1:N_strings) %makes a 1x13
%   for(j=1:(N_daily_dispatch/20)) %makes a 96x1
%     samples_Q_wt(j,i)= normrnd(Q_mean_wt1(i), a*Q_std_wt(i), [1, 1]);
   %Creates random samples for Q in 96x13, some values violating the
   constraints
%    end
%   for(j=(1*N_daily_dispatch/20):(2*N_daily_dispatch/20))
%        samples_Q_wt(j,i)= normrnd(Q_mean_wt2(i), a*Q_std_wt(i), [1,
   1]); %Creates random samples for Q
%    end
%   for(j=(2*N_daily_dispatch/20):(3*N_daily_dispatch/20))
%        samples_Q_wt(j,i)= normrnd(Q_mean_wt3(i), a*Q_std_wt(i), [1,
   1]); %Creates random samples for Q
%    end
%   for(j=(3*N_daily_dispatch/20):(4*N_daily_dispatch/20))
%        samples_Q_wt(j,i)= normrnd(Q_mean_wt4(i), a*Q_std_wt(i), [1,
   1]); %Creates random samples for Q
%    end
%   for(j=(4*N_daily_dispatch/20):(5*N_daily_dispatch/20))
%        samples_Q_wt(j,i)= normrnd(Q_mean_wt5(i), a*Q_std_wt(i), [1,
   1]); %Creates random samples for Q
%    end
%   for(j=(5*N_daily_dispatch/20):(6*N_daily_dispatch/20))
```

```
%          samples_Q_wt(j,i)= normrnd(Q_mean_wt6(i), a*Q_std_wt(i), [1,
    1]); %Creates random samples for Q
%     end
%   for(j=(6*N_daily_dispatch/20):(7*N_daily_dispatch/20))
%          samples_Q_wt(j,i)= normrnd(Q_mean_wt7(i), a*Q_std_wt(i), [1,
    1]); %Creates random samples for Q
%     end
%   for(j=(7*N_daily_dispatch/20):(8*N_daily_dispatch/20))
%          samples_Q_wt(j,i)= normrnd(Q_mean_wt8(i), a*Q_std_wt(i), [1,
    1]); %Creates random samples for Q
%     end
%   for(j=(8*N_daily_dispatch/20):(9*N_daily_dispatch/20))
%          samples_Q_wt(j,i)= normrnd(Q_mean_wt9(i), a*Q_std_wt(i), [1,
    1]); %Creates random samples for Q
%     end
%   for(j=(9*N_daily_dispatch/20):(10*N_daily_dispatch/20))
%          samples_Q_wt(j,i)= normrnd(Q_mean_wt10(i), a*Q_std_wt(i), [1,
    1]); %Creates random samples for Q
%       end
%   for(j=(10*N_daily_dispatch/20):(11*N_daily_dispatch/20))
%          samples_Q_wt(j,i)= normrnd(Q_mean_wt11(i), a*Q_std_wt(i), [1,
    1]); %Creates random samples for Q
%     end
%   for(j=(11*N_daily_dispatch/20):(12*N_daily_dispatch/20))
%          samples_Q_wt(j,i)= normrnd(Q_mean_wt12(i), a*Q_std_wt(i), [1,
    1]); %Creates random samples for Q
%     end
%     for(j=(12*N_daily_dispatch/20):(13*N_daily_dispatch/20))
%          samples_Q_wt(j,i)= normrnd(Q_mean_wt13(i), a*Q_std_wt(i), [1,
    1]); %Creates random samples for Q
%       end
%     for(j=(13*N_daily_dispatch/20):(14*N_daily_dispatch/20))
%          samples_Q_wt(j,i)= normrnd(Q_mean_wt14(i), a*Q_std_wt(i), [1,
    1]); %Creates random samples for Q
%       end
%     for(j=(14*N_daily_dispatch/20):(15*N_daily_dispatch/20))
%          samples_Q_wt(j,i)= normrnd(Q_mean_wt15(i), a*Q_std_wt(i), [1,
    1]); %Creates random samples for Q
%       end
%     for(j=(15*N_daily_dispatch/20):(16*N_daily_dispatch/20))
%          samples_Q_wt(j,i)= normrnd(Q_mean_wt16(i), a*Q_std_wt(i), [1,
    1]); %Creates random samples for Q
%       end
%     for(j=(16*N_daily_dispatch/20):(17*N_daily_dispatch/20))
%          samples_Q_wt(j,i)= normrnd(Q_mean_wt17(i), a*Q_std_wt(i), [1,
    1]); %Creates random samples for Q
%       end
%     for(j=(17*N_daily_dispatch/20):(18*N_daily_dispatch/20))
%          samples_Q_wt(j,i)= normrnd(Q_mean_wt18(i), a*Q_std_wt(i), [1,
    1]); %Creates random samples for Q
%       end
%     for(j=(18*N_daily_dispatch/20):(19*N_daily_dispatch/20))
%          samples_Q_wt(j,i)= normrnd(Q_mean_wt19(i), a*Q_std_wt(i), [1,
    1]); %Creates random samples for Q
%       end
%     for(j=(19*N_daily_dispatch/20):(20*N_daily_dispatch/20))
```

```matlab
%          samples_Q_wt(j,i)= normrnd(Q_mean_wt20(i), a*Q_std_wt(i), [1,
%   1]); %Creates random samples for Q
%      end
% end
%
%
%
%
%% Random Q's for PV strings

%1 Assume +-Qmax is 1/3 Pmax

%2 Assume Pmax, Q=0 & P=0, Qmax, extra task)

% for(j=1: length(P_pv_max)) %makes a 1x4
%      k=1;
%        for(i=1: N_daily_dispatch) %makes a 1000x1
%
%            if (i < (4/24)*N_daily_dispatch ) %Assume before 4 am ,
%   no PV energy generated
%                P_pv(i,j) = 0;
%
%            elseif( (i >= ((4/24)*N_daily_dispatch)) && (i < ((10/24)
%   *N_daily_dispatch)) )%Assume 4 - 10 am , PV power increasing
%   linearly
%                P_pv(i,j) = (P_module_solar(k)*N_modules)*10^-6; %
%   Output active power in MW
%                if (P_pv(i,j) > P_pv_max(:,j))
%                    P_pv(i,j) = P_pv_max(:,j);
%                end
%                if (k<length(t_steps))
%                    k=k+1;
%                end
%            elseif( (i >= ((10/24)*N_daily_dispatch)) && (i <
%   ((21/24)*N_daily_dispatch)) ) %Assume 10 am - 9pm , PV max energy
%   generated
%                P_pv(i,j) = P_pv_max(1,j);
%
%            elseif( (i >= ((21/24)*N_daily_dispatch))  ) %Assume 9 pm
%    -12 am, no PV energy generated
%                P_pv(i,j) = 0;
%            end
%      end
% end

for(i=1:N_daily_dispatch)
    for(j=1:length(P_pv_max))
        Q_pv(i,j) = (1/3)*P_pv(i,j);
    end
end

Q_dem_tot_pv = sum(Q_pv(1,:));
Q_mean_pv = zeros(1, N_strings_pv);%matrix with mu for each string 1-1


for(j=1:N_strings_pv)
```

```matlab
for(i=1:(N_daily_dispatch))
    if(i <= (N_daily_dispatch/10))
        Q_mean_pv1(i,j) = -10*(Q_dem_tot_pv/ N_strings_pv)/10 ;
    elseif ((i > (1*N_daily_dispatch/10)) && (i <=(2*N_daily_dispatch
        /10)))
    for(i=1:(N_daily_dispatch/10))
        Q_mean_pv2(i,j) = -8*(Q_dem_tot_pv/ N_strings_pv)/10;
    end
    elseif ((i > (2*N_daily_dispatch/10)) && (i <=(3*N_daily_dispatch
        /10)))
    for(i=1:(N_daily_dispatch/10))
        Q_mean_pv3(i,j) = -6*(Q_dem_tot_pv/ N_strings_pv)/10;
    end
    elseif ((i > (3*N_daily_dispatch/10)) && (i <=(4*N_daily_dispatch
        /10)))
    for(i=1:(N_daily_dispatch/10))
        Q_mean_pv4(i,j) = -4*(Q_dem_tot_pv/ N_strings_pv)/10;
    end
    elseif ((i > (4*N_daily_dispatch/10)) && (i <=(5*N_daily_dispatch
        /10)))
    for(i=1:(N_daily_dispatch/10))
        Q_mean_pv5(i,j) = -2*(Q_dem_tot_pv/ N_strings_pv)/10;
    end
    elseif ((i > (5*N_daily_dispatch/10)) && (i <=(6*N_daily_dispatch
        /10)))
    for(i=1:(N_daily_dispatch/10))
        Q_mean_pv6(i,j) = 0;
    end
    elseif ((i > (6*N_daily_dispatch/10)) && (i <=(7*N_daily_dispatch
        /10)))
    for(i=1:(N_daily_dispatch/10))
        Q_mean_pv7(i,j) = 2*(Q_dem_tot_pv/ N_strings_pv)/10;
    end
    elseif ((i > (7*N_daily_dispatch/10)) && (i <=(8*N_daily_dispatch
        /10)))
    for(i=1:(N_daily_dispatch/10))
        Q_mean_pv8(i,j) = 4*(Q_dem_tot_pv/ N_strings_pv)/10;
    end
    elseif ((i > (8*N_daily_dispatch/10)) && (i <=(9*N_daily_dispatch
        /10)))
    for(i=1:(N_daily_dispatch/10))
        Q_mean_pv9(i,j) = 6*(Q_dem_tot_pv/ N_strings_pv)/10;
    end
    elseif ((i > (9*N_daily_dispatch/10)) && (i <=(10*N_daily_dispatch
        /10)))
    for(i=1:(N_daily_dispatch/10))
        Q_mean_pv10(i,j) = 10*(Q_dem_tot_pv/ N_strings_pv)/10;
    end
end
end
end

for i=1:length(Q_mean_pv)
    Q_std_pv(i)=unifrnd(1,Q_pv_max(i)); %make a uniform distribution
        for the standard deviation string 1-13
end
```

```matlab
for(i=1:N_strings_pv) %makes a 1x13
  for(j=1:(N_daily_dispatch/10)) %makes a 96x1
    samples_Q_pv(j,i)= normrnd(Q_mean_pv1(i), a*Q_std_pv(i), [1, 1]); %
      Creates random samples for Q in 96x13, some values violating
      the constraints
  end
  for(j=(1*N_daily_dispatch/10):(2*N_daily_dispatch/10))
    samples_Q_pv(j,i)= normrnd(Q_mean_pv2(i), a*Q_std_pv(i), [1, 1])
      ; %Creates random samples for Q
  end
  for(j=(2*N_daily_dispatch/10):(3*N_daily_dispatch/10))
    samples_Q_pv(j,i)= normrnd(Q_mean_pv3(i), a*Q_std_pv(i), [1, 1])
      ; %Creates random samples for Q
  end
  for(j=(3*N_daily_dispatch/10):(4*N_daily_dispatch/10))
    samples_Q_pv(j,i)= normrnd(Q_mean_pv4(i), a*Q_std_pv(i), [1, 1])
      ; %Creates random samples for Q
  end
  for(j=(4*N_daily_dispatch/10):(5*N_daily_dispatch/10))
    samples_Q_pv(j,i)= normrnd(Q_mean_pv5(i), a*Q_std_pv(i), [1, 1])
      ; %Creates random samples for Q
  end
  for(j=(5*N_daily_dispatch/10):(6*N_daily_dispatch/10))
    samples_Q_pv(j,i)= normrnd(Q_mean_pv6(i), a*Q_std_pv(i), [1, 1])
      ; %Creates random samples for Q
  end
  for(j=(6*N_daily_dispatch/10):(7*N_daily_dispatch/10))
    samples_Q_pv(j,i)= normrnd(Q_mean_pv7(i), a*Q_std_pv(i), [1, 1])
      ; %Creates random samples for Q
  end
  for(j=(7*N_daily_dispatch/10):(8*N_daily_dispatch/10))
    samples_Q_pv(j,i)= normrnd(Q_mean_pv8(i), a*Q_std_pv(i), [1, 1])
      ; %Creates random samples for Q
  end
  for(j=(8*N_daily_dispatch/10):(9*N_daily_dispatch/10))
    samples_Q_pv(j,i)= normrnd(Q_mean_pv9(i), a*Q_std_pv(i), [1, 1])
      ; %Creates random samples for Q
  end
  for(j=(9*N_daily_dispatch/10):(N_daily_dispatch))
    samples_Q_pv(j,i)= normrnd(Q_mean_pv10(i), a*Q_std_pv(i), [1,
      1]); %Creates random samples for Q
  end
end

%% Combining PV and Wind

samples_Q_tot = [samples_Q_pv];
Q_total_max = [Q_pv];

constraints_neg_tot = zeros(N_daily_dispatch,N_tot_strings);
constraints_pos_tot = zeros(N_daily_dispatch,N_tot_strings);
  for(k=1: N_tot_strings)
   constraints_neg_tot = samples_Q_tot(samples_Q_tot < -Q_total_max(k))
     ; %Note values greater than positive max reactive
```

```matlab
    constraints_pos_tot = samples_Q_tot(samples_Q_tot > Q_total_max(k));
        %Note values greater than negative max reactive

  idx_constraints_neg_tot(:,k) = (samples_Q_tot(:,k) < -Q_total_max(k
      )); %Note values greater than max reactive
  idx_constraints_pos_tot(:,k) = (samples_Q_tot(:,k) >  Q_total_max(k
      ));

    end

%% Step 3: Update case file and run Power Flow

stop =0;


while(stop == 0)
    for(i=1:N_daily_dispatch)
    for (j=1:N_strings)
    %for (k=1:N_branches_shunt)

        if(i < N_daily_dispatch)
        mpc_substation_system13.gen(P_wt_idx(j),3) = samples_Q_wt(i,j);
        for(a=1:4)
        mpc_substation_system13.gen(P_pv_idx(a),3) = samples_Q_pv(i,a);
        end
        %mpc_substation_system13.bus(1,4) = sum(samples_Q_tot(i,:));
        %initialize active power generation
        mpc_substation_system13.bus(1,4) = sum(samples_Q_tot(i,j));

        %run power flow for each dispatch
        tStart = cputime;
        results_pf = runpf(mpc_substation_system13); %run power flow
            once Q is loaded per dispatch
        [results_loss results_inject] = get_losses(results_pf); %losses

        %Make matrix to specify branch losses and reactive power
            injection
        results_loss_matrix = zeros(31, 50); %first row is bus "from",
            second row bus "to", third row is loss

        bus_from = mpc_substation_system13.branch(:,1);
        bus_to = mpc_substation_system13.branch(:,2);

        %Perform operation only if system converges
          if (results_pf.success == 1)

        %Save data for each power flow
        Vmag(:,i) = results_pf.bus(:,8); %Saves voltage magnitude for
            every bus
        Vangle(:,i) = results_pf.bus(:,9); %Saves angle magnitude for
            every bus
        P_flow_1_2(:,i) = results_pf.branch(1,16); %Saves Power flow in
            MW for Branch to PCC
        P_flow_4_23(:,i) = results_pf.branch(25,16); %Saves Power flow
            in MW for Branch to Input transformer 1
        P_flow_4_7(:,i) = results_pf.branch(6,16); %Saves Power flow in
```

```matlab
         MW for Branch to Input transformer 1
    P_flow_6_12(:,i) = results_pf.branch(12,16); %Saves Power flow
       in MW for Branch to Input transformer 2
    P_flow_6_17(:,i) = results_pf.branch(18,16); %Saves Power flow
       in MW for Branch to Input transformer 2

    results_loss_real(:,i) = real(results_loss);
    results_loss_im(:,i) = imag(results_loss);
    results_inject_t(:,i) = results_inject;
    results_loss_matrix = [bus_from bus_to results_loss_real
       results_loss_im    results_inject_t];

      end

      elseif(i == N_daily_dispatch)
    mpc_substation_system13.gen(P_wt_idx(j),3) = samples_Q_wt(i,j);
    for(a=1:4)
    mpc_substation_system13.gen(P_pv_idx(a),3) = samples_Q_pv(i,a);
    end
       mpc_substation_system13.bus(1,4) = sum(samples_Q_tot(i,j));

     if (results_pf.success == 1)

    %Save data for each power flow
    Vmag(:,i) = results_pf.bus(:,8);
    Vangle(:,i) = results_pf.bus(:,9);
    P_flow_1_2(:,i) = results_pf.branch(1,16); %Saves Power flow in
        MW for Branch to PCC
    P_flow_4_23(:,i) = results_pf.branch(25,16); %Saves Power flow
       in MW for Branch to Input transformer 1
    P_flow_4_7(:,i) = results_pf.branch(6,16); %Saves Power flow in
        MW for Branch to Input transformer 1
    P_flow_6_12(:,i) = results_pf.branch(12,16); %Saves Power flow
       in MW for Branch to Input transformer 2
    P_flow_6_17(:,i) = results_pf.branch(18,16); %Saves Power flow
       in MW for Branch to Input transformer 2

    %Save all the losses generated in each bus/branch for all
    %dispatches
    results_loss_real(:,i) = real(results_loss);
    results_loss_im(:,i) = imag(results_loss);
    results_inject_t(:,i) = results_inject;
    results_loss_matrix = [bus_from bus_to results_loss_real
       results_loss_im    results_inject_t];

    %Computes location and value of maximum loss

    constraints_v_low = Vmag(Vmag < 0.8567); %Note values greater
       than minimum p.u.
    constraints_v_high = Vmag(Vmag > 1.1424);  %Note values greater
        than maximum p.u.

    idx_constraints_v_low = zeros(28, N_daily_dispatch); %28 is
       amount of busses in the circuit
for (a=1:N_daily_dispatch)
    %Vlow is ..... for shunt connected
```

```matlab
        %Vlow is ..... for shunt disconnected
        %Vhigh is ..... for shunt connected
        %Vhigh is ..... for shunt disconnected

        idx_constraints_v_low(:,a) = (Vmag(:,a) < 0.8567);
        idx_constraints_v_high(:,a) = (Vmag(:,a) > 1.1424);
        [idx_r_Q_v_low idx_c_Q_v_low] = find(idx_constraints_v_low~=0);
            %find location in matrix where there is v low
        [idx_r_Q_v_high idx_c_Q_v_high] = find(idx_constraints_v_high
            ~=0);
end
        %Calculate lowest voltage magnitude value on the dispatches
            where a
        %violation has occured
        unique_idx_c_Q_v_low = unique(idx_c_Q_v_low);
        unique_idx_r_Q_v_low = unique(idx_r_Q_v_low);
            V_lowest = Vmag(:,unique_idx_c_Q_v_low);

        for(b=1:length(unique_idx_c_Q_v_low))
            constraints_v_lowest(:,b) =  min(V_lowest(:,b));
        end

        %Calculate lowest voltage magnitude value on the dispatches
            where a
        %violation has occured

        unique_idx_c_Q_v_high = unique(idx_c_Q_v_high);
        unique_idx_r_Q_v_high = unique(idx_r_Q_v_high);
            V_highest = Vmag(:,unique_idx_c_Q_v_high);

          for(c=1:length(unique_idx_c_Q_v_high))
            constraints_v_highest(:,c) =  max(V_highest(:,c));
          end
%       constraints_v_lowest_repeat = repelem(constraints_v_lowest,
    length(constraints_v_low));
%       constraints_v_highest_repeat = repelem(constraints_v_highest,
    length(constraints_v_high));


        Q_dem_constraints_v_low = samples_Q_tot(idx_c_Q_v_low,:); %Find
            the Q demands for that specific dispatch
        Q_dem_constraints_v_high = samples_Q_tot(idx_c_Q_v_high,:); %
            Find the Q demands for that specific dispatch

        P_loss_v_low = results_loss_real(:, idx_c_Q_v_low);
        P_loss_v_high = results_loss_real(:, idx_c_Q_v_high);

        Q_loss_v_low = results_loss_im(:, idx_c_Q_v_low);
        Q_loss_v_high = results_loss_im(:, idx_c_Q_v_high);

        Q_inj_v_low = results_inject_t(:, idx_c_Q_v_low);
        Q_inj_v_high = results_inject_t(:, idx_c_Q_v_high);

         end
```

```matlab
end
end
     stop = 1; %stop while loop
end
end

    %% Step 4: Plot results in a visable manner

    %Print  voltage data
    figure(1)
    subplot(2,1,1)
    plot(Vmag,'o');
    yline(0.8567,'r','LineWidth',1);
    yline(1.1424,'r','LineWidth',1);
    xlabel('Bus number','FontSize',12);
    ylabel('V magnitude (p.u.)','FontSize',12);
    title('Voltage magnitude in p.u. for bus numbers','FontSize'
        ,12)
    hold on;

    subplot(2,1,2)
    plot(Vangle,'s');
    xlabel('Bus number','FontSize',12);
    ylabel('V angle (degrees)','FontSize',12);
    title('Voltage angles in degrees for bus numbers','FontSize'
        ,12)
    hold on;

    %Print losses data
    figure(2)
    subplot(3,1,1)
    plot(results_loss_real,'o');
    xlabel('Branch #','FontSize',12);
    ylabel('P loss(MW)','FontSize',12);
    title('Active power loss in MW for branch','FontSize',12)
    hold on;


    subplot(3,1,2)
    plot(results_loss_im,'s');
    xlabel('Branch #','FontSize',12);
    ylabel('Q loss(MVAr)','FontSize',12);
    title('Reactive power inject in MVAr for branch','FontSize',12)
    hold on;

    subplot(3,1,3)
    plot(results_inject_t,'o');
    xlabel('Branch #');
    ylabel('Q injected(MVAr)','FontSize',12);
    title('Reactive power inject in MVAr for branch','FontSize',12)
    hold on;

    figure(6)

    plot(P_flow_1_2,'o');
    xlabel('Dispatch','FontSize',12);
```

```matlab
        ylabel('Power flow (MW)','FontSize',12);
        yline(B_limit_4_7 ,'r','LineWidth',1);
        title('Power flow to input Transformer 1 Branch 4-7','FontSize'
            ,12);
        hold on;

        figure(7)
        subplot(2,1,1)

        plot(P_flow_4_7 ,'o');
        xlabel('Dispatch','FontSize',12);
        ylabel('Power flow (MW)','FontSize',12);
        yline(B_limit_4_7 ,'r','LineWidth',1);
        title('Power flow to input Transformer 1 Branch 4-7','FontSize'
            ,12);;
        hold on;

        subplot(2,1,2)

        plot(P_flow_4_23 ,'o');
        xlabel('Dispatch','FontSize',12);
        ylabel('Power flow (MW)','FontSize',12);
        yline(B_limit_4_23 ,'r','LineWidth',1);
        title('Power flow to input Transformer 1 Branch 4-23','FontSize
            ',12)
        hold on;

        figure(8)
        subplot(2,1,1)

        plot(P_flow_6_12 ,'o');
        xlabel('Dispatch','FontSize',12);
        ylabel('Power flow (MW)','FontSize',12);
        yline(B_limit_6_12 ,'r','LineWidth',1);
        title('Power flow to input Transformer 2 Branch 6-12','FontSize
            ',12)
        hold on;

        subplot(2,1,2)

        plot(P_flow_6_17 ,'o');
        xlabel('Dispatch','FontSize',12);
        ylabel('Power flow (MW)','FontSize',12);
        yline(B_limit_6_17 ,'r','LineWidth',1);
        title('Power flow to input Transformer 2 Branch 6-17','FontSize
            ',12)
        hold on;

        %Print relation between demand , total system losses and voltage

        %Calculate average voltage for specific Q_demand
        v_avg = mean(Vmag);

    %Calculate average minimum voltage for specific Q_demand
        %this is equal to constraints_v_low
```

```matlab
        %Calculate total losses for average voltage of each dispatch
        P_loss_tot = sum(results_loss_real);
        Q_loss_tot = sum(results_loss_im);
        Q_inj_tot = sum(results_inject_t);

        %Calculate total losses for voltage constraints
        P_loss_tot_v_low = sum(P_loss_v_low);
        Q_loss_tot_v_low = sum(Q_loss_v_low);
        Q_inj_tot_v_low = sum(Q_inj_v_low);

        P_loss_tot_v_low = unique(P_loss_tot_v_low);
        Q_loss_tot_v_low = unique(Q_loss_tot_v_low);
        Q_inj_tot_v_low = unique(Q_inj_tot_v_low);

        P_loss_tot_v_high = sum(P_loss_v_high);
        Q_loss_tot_v_high = sum(Q_loss_v_high);
        Q_inj_tot_v_high = sum(Q_inj_v_high);


        P_loss_tot_v_high = unique(P_loss_tot_v_high);
        Q_loss_tot_v_high = unique(Q_loss_tot_v_high);
        Q_inj_tot_v_high = unique(Q_inj_tot_v_high);

        %Calculate total Q_demand

        Q_tot = sum(samples_Q_tot,2);

        %Calculate total Q_demand for dispatches causing violation

        Q_tot_constraints_v_low = sum(Q_dem_constraints_v_low,2);
        Q_tot_constraints_v_high = sum(Q_dem_constraints_v_high,2);

        Q_tot_constraints_v_low = unique(Q_tot_constraints_v_low);
        Q_tot_constraints_v_high = unique(Q_tot_constraints_v_high);

        %add zeros in order to plot
%
%          P_loss_tot_v_low(numel(Q_tot_constraints_v_low)) = 0;
%          Q_loss_tot_v_low(numel(Q_tot_constraints_v_low)) = 0;
%          Q_inj_tot_v_low(numel(Q_tot_constraints_v_low)) = 0;
%
%          P_loss_tot_v_high(numel(Q_tot_constraints_v_high)) = 0;
%          Q_loss_tot_v_high(numel(Q_tot_constraints_v_high)) = 0;
%          Q_inj_tot_v_high(numel(Q_tot_constraints_v_high)) = 0;


        %Plot 3D plot Q demand, P loss and (minimum and maximum)
            average voltage
        figure(3)

        plot3(Q_tot, P_loss_tot, v_avg,'o','Color', 'r', 'MarkerSize'
            ,5); %plot for avg
        hold on;
%        plot3(Q_tot_constraints_v_low, P_loss_tot_v_low,
    constraints_v_lowest,'o','Color', 'r', 'MarkerSize',5); %plot for v
     constraints low
```

```matlab
%         hold on;
%         plot3(Q_tot_constraints_v_high, P_loss_tot_v_high,
    constraints_v_highest,'o','Color', 'r', 'MarkerSize',5); %plot for
    v constraints low
%         hold on;

        grid on;

        xlabel('Q demand (MVAr)','FontSize',12);
        ylabel('P loss total (MW)','FontSize',12);
        zlabel('V average magnitude (p.u.)','FontSize',12);

        legend('Low generation','Nominal generation', 'High generation'
            );
        %Plot 3D plot Q loss for minimum and average voltage
        figure(4)

        plot3(Q_tot, Q_loss_tot, v_avg,'o','Color', 'r', 'MarkerSize'
            ,5); %plot for avg
        hold on;
%         plot3(Q_tot_constraints_v_low, Q_loss_tot_v_low,
    constraints_v_lowest,'o','Color', 'r', 'MarkerSize',5); %plot for v
     constraints low
%         hold on;
%         plot3(Q_tot_constraints_v_high, Q_loss_tot_v_high',
    constraints_v_highest,'o','Color', 'r', 'MarkerSize',5); %plot for
    v constraints low
%         hold on;

        grid on;

        xlabel('Q demand (MVAr)','FontSize',12);
        ylabel('Q loss total (MVAr)','FontSize',12);
        zlabel('V average magnitude (p.u.)','FontSize',12);

        legend('Low generation','Nominal generation', 'High generation'
            );
        %Plot 3D plot for minimum and average
        figure(5)

        plot3(Q_tot, Q_inj_tot,v_avg,'o','Color', 'r', 'MarkerSize',5);
             %plot for avg
        hold on;
%         plot3(Q_tot_constraints_v_low,Q_inj_tot_v_low,
    constraints_v_lowest,'o','Color', 'r', 'MarkerSize',5); %plot for v
     constraints low
%         hold on;
%         plot3(Q_tot_constraints_v_high, Q_inj_tot_v_high',
    constraints_v_highest,'o','Color', 'r', 'MarkerSize',5); %plot for
    v constraints low
%         hold on;

        grid on;

        xlabel('Q demand (MVAr)','FontSize',12);
        ylabel('Q INJ total (MVAr)','FontSize',12);
```

```matlab
zlabel('V average magnitude (p.u.)','FontSize',12);

legend('Low generation','Nominal generation', 'High generation'
    );
```